REDUCED ORDER MODELING OF HEAT EXCHANGERS USING HIGH ORDER FINITE CONTROL VOLUME MODELS

A Record of Study

by

ABHISHEK GUPTA

Submitted to the Office of Graduate Studies of
Texas A&M University
in partial fulfillment of the requirements for the degree of

MASTERS OF SCIENCE

December 2007

Major Subject: Mechanical Engineering

REDUCED ORDER MODELING OF HEAT EXCHANGERS USING HIGH ORDER FINITE CONTROL VOLUME MODELS

A Record of Study

by

ABHISHEK GUPTA

Submitted to the Office of Graduate Studies of
Texas A&M University
in partial fulfillment of the requirements for the degree of

MASTERS OF SCIENCE

Approved by:

Chair of Committee,	Dr. Bryan P. Rasmussen
Committee Members,	Dr. Won-jong Kim
	Dr. Theofanis Strouboulis
Head of Department,	Dr. S.C. Lau

December 2007

Major Subject: Mechanical Engineering

ABSTRACT

Reduced Order Modeling of Heat Exchangers Using

High Order Finite Control Volume Models. (December 2007)

Abhishek Gupta, B.Tech., Amity School of Engineering & Technology, New Delhi

Chair of Advisory Committee: Dr. Bryan P. Rasmussen

A distributed parameter approach for dynamic modeling of heat exchangers and using it to obtain low order models have been presented in this report. The finite control volume (FCV) approach accurately captures the distributed nature of the system parameters but the models obtained are complex and have a high order. This report presents a FCV approach to multi-phase flow heat exchanger dynamics as a set of Ordinary Differential Equations (ODEs), rather than a set of Differential-Algebraic-Equations (DAEs) that are typically used in this paradigm. It also presents an approach to apply model reduction techniques to FCV models to obtain low order models. A key advantage of these approaches is retention of the physical nature of the system states which are lost when using standard model reduction procedures. The low order models obtained are control oriented and can be utilized for analysis and improvement of the efficiency of heating, ventilation and air-conditioning devices.

In the loving memory of my mother

ACKNOWLEDGEMENTS

I would like to thank my committee chair, Dr. Bryan P. Rasmussen, and my committee members, Dr. Kim and Dr. Strouboulis for their guidance and support throughout the course of this research. Thanks to Matt Elliott for providing with the necessary experimental data and being a wonderful mentor. Thanks to all my colleagues at Thermo-Fluids Control Laboratory for collaborative research and holding enlightening conversations. I am also grateful to everybody who directly or indirectly helped me during the course of this research. Thanks to Dr. Rasmussen for providing much needed insight, encouragement, support and understanding. This research would not have been possible without his counsel and direction. Last but not the least, I would like to thank my parents for their love, support and understanding.

NOMENCLATURE

FCV	Finite Control Volume
MB	Moving Boundary
n	Number of Control Regions
P	Pressure
T	Temperature
V	Volume
h	Enthalpy
m	Mass of fluid
u	Internal Energy
ρ	Density
A	Area
α	Heat Transfer Coefficient
S	Slip
C	Specific Heat

Subscripts

o	Outer
i	Inner
k	k^{th} control volume

out	Outlet
in	Inlet
e	Evaporator
c	Condenser
r	Refrigerant
w	Wall
a, air	Secondary Fluid (Air/Water)
f	Liquid
g	Vapor
cs	Cross-sectional
total	Total

TABLE OF CONTENTS

Page

LIST OF FIGURES

Page

LIST OF TABLES

Page

Chapter 1

INTRODUCTION

A distributed parameter approach for dynamic modeling of heat exchangers and using it to obtain low order models have been presented in this report. The presented approach also ensures that the physical nature of the states of the low order system is also retained. The low order models obtained are control oriented and can be utilized for analysis and improvement of the efficiency of heating, ventilation and air-conditioning devices.

The total world consumption of marketed energy is projected to increase by 57 percent from 2004 to 2030. The non-renewable share of total world energy use was about 93 percent in 2004 [1]. Besides, combustion of fossil fuels produces CO_2 which is by far the largest contributor to global warming. The Inter-governmental Panel on Climate Change (IPCC) indicates the need for an immediate 50-70% reduction in global CO_2 emissions in order to stabilize global CO_2 concentrations at the 1990 level by 2100 [2]. With the oil prices soaring to a record high of over $90 per barrel [3] and an impending need to reduce the consumption of fossil fuels, improving the efficiency of heating, ventilation and air-conditioning devices is a basal requirement. Availability of control-oriented dynamic models is essential to enable prediction, analysis, and control design for these complex energy systems.

Two modeling paradigms have been shown to be effective in modeling the dynamics of multi-phase heat exchangers. The more complex finite control volume (FCV) approach accurately captures the distributed nature of the system parameters; while the simpler moving boundary (MB) lumped parameter approach uses effective parameter values to create a more control-oriented model. This report presents a FCV approach to multi-phase flow heat exchanger dynamics as a set of Ordinary Differential Equations (ODEs), rather than a set of Differential-Algebraic-Equations (DAEs) that are typically used in this paradigm. It also presents an approach to apply model reduction techniques to FCV models to extract an optimal choice of effective parameters for use in the simpler control oriented models. A key advantage of these approaches is retention of the physical nature of the system states which are lost when using standard model reduction procedures.

1.1 Vapor Compression System

A vapor compression system uses a circulating compressible refrigerant as the medium which absorbs and removes heat from one component and subsequently rejects that heat in another component. Figure 1.1 depicts a typical single-stage vapor compression system. All such systems have four components: compressor, condenser, evaporator and an expansion valve. Circulating refrigerant enters the compressor as saturated vapor and is compressed to a higher pressure, resulting in a higher temperature as well. The superheated vapor is routed through a condenser where it is condensed into

a liquid by flowing through tubes with secondary fluid (such as air or water) flowing across them. The heat rejected by the circulating refrigerant is carried away by the secondary fluid in the condenser. Then the saturated liquid is passed through an expansion valve. At the exit of the valve, the refrigerant is usually two-phase and at a lower pressure. Next, the two-phase refrigerant is routed through an evaporator where it is converted into superheated vapor by flowing through tubes with secondary fluid flowing across them. Thus, heat is absorbed by the circulating refrigerant from the secondary fluid in the evaporator. The superheated refrigerant is routed back into the compressor thus, completing the vapor compression cycle. The vapor compression cycle described in this section is represented on ph-diagram in Figure 1.2. To model a vapor compression system, a few standard assumptions are made. First, the compression of the fluid is assumed to be adiabatic. Second, isobaric conditions in the condenser and evaporator are assumed. Third, expansion through the valve is assumed to be isenthalpic.

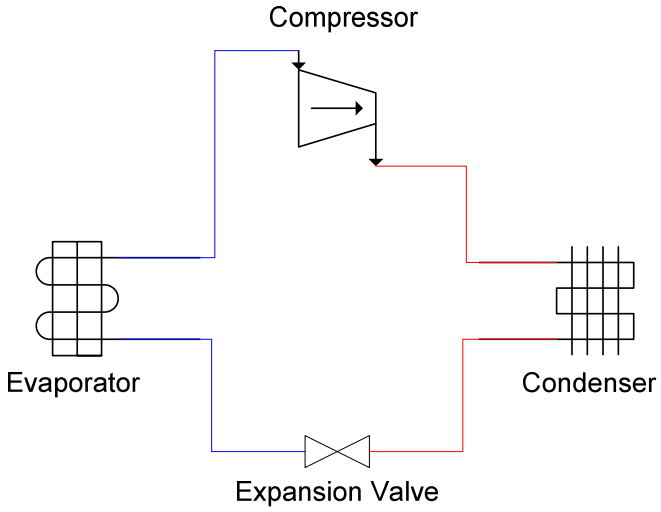

Figure 1.1: Simple Vapor Compression Cycle System

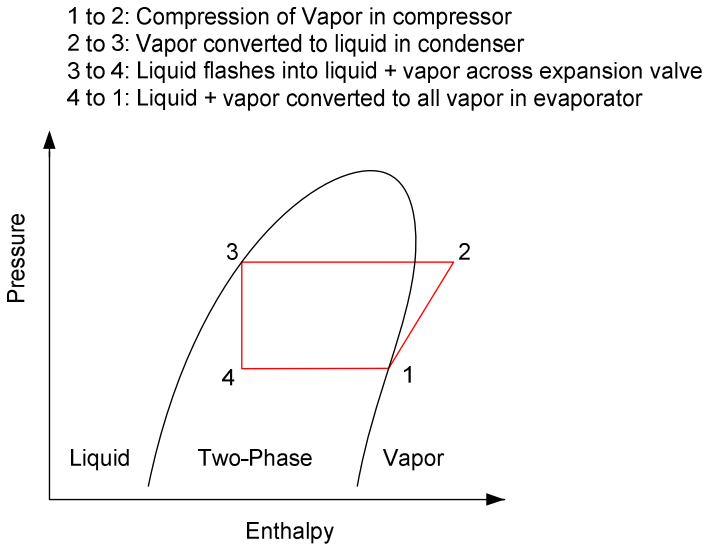

Figure 1.2: Simple Vapor Compression Cycle System

Modern heat exchangers employ a variety of techniques to maximize heat transfer. In particular, the heat exchanger may use multiple fluid paths, which may branch into additional paths as the fluid evaporates to accommodate the increasing volume of fluid. Even the simplest variation in geometry (such as shown in Figure 1.3) will affect several key physical parameters such as surface areas and fluid flow cross-sectional areas.

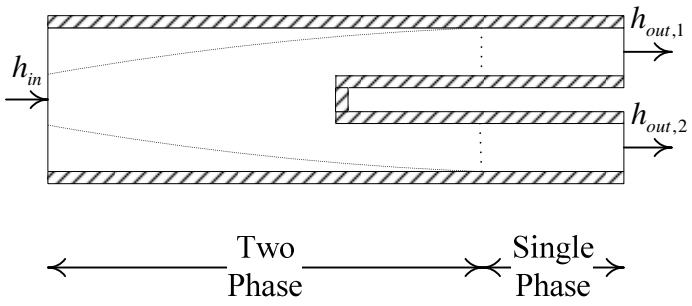

Figure 1.3: Simple Variation in Geometry of Heat Exchanger

There are extensive and ongoing research attempts to develop empirical correlations for the rate of heat transfer as a function of temperature, pressure, fluid phase, heat flux, passage geometry, etc. For example, Wattelet [27] has presented a comprehensive literature review for heat transfer flow regimes in a horizontal-tube evaporator. The Wattlet-Chato correlation for evaporating flows, and the Dobson-Chato correlation for condensing flows are shown in Figure 1.4. The figure shows that the heat transfer coefficient can change by an order of magnitude as the fluid changes phases (fluid quality is a relative measure of vapor and liquid content in a two-phase flow). Using high-level of discretization, the FCV model is capable of capturing the large variations is system parameters, such as heat transfer coefficients, that vary widely throughout the two-phase and single-phase fluid regions and significantly impact the dynamic response of the system. Some of the attempts to model these complex components of a vapor compression system have been discussed in the next section.

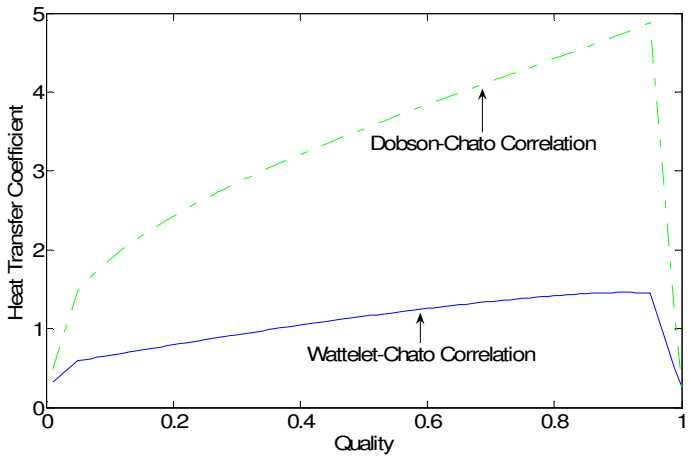

Figure 1.4: Plot of Heat Transfer Coefficient for Evaporating/Condensing Flows

1.2 Literature Review

Several authors have made significant contributions to this field of research. In 1955, Paynter [20] presented a model based on transfer function of a heat exchanger to predict the transient response of parallel-flow and counter-flow heat exchangers. To estimate the transient response, he suggested design parameters to be considered and compared his models with experimental data.

Gruhle and Isermann [13] suggested the distributed parameter approach for modeling of heat exchangers in 1984. The distributed parameter process was approximated by several lumped parameter models. MacArthur and Grald [16] utilized distributed parameter approach for predicting the performance of a cyclic heat pump and compared their results with experimental data. Later in 1992, they presented a moving boundary approach to model heat exchangers [12].

In 1996, He [14,15] utilized lumped parameter approach to describe the dynamics of vapor compression cycle. Later in 1997, Willatzen [28] used the moving boundary approach for dynamic simulation of heat exchangers. In 1997, Narayanan et al. [18] presented a lumped parameter formulation of a vertical evaporator. They also accounted for pressure drop and axial variation of heat flux in their model.

Mithraratne et al. [17] presented a distributed parameter model of simulating the dynamics of an evaporator controlled by a thermostatic expansion valve (TEV) in a vapor compression refrigeration system in 1998. They also included the axial conduction

of heat in the pipe wall as it affects the TEV. In 1998, Tummescheit and Eborn [26] presented the lumped parameter as well as distributed parameter models as a commercially available software package known as Modelica™. Bendapudi [8] compared and validated the moving boundary as well as finite control volume approaches. He also provided a literature review of notable prior efforts in this field of research [7].

Many authors have contributed in developing low order models as well as high order discretized models for modeling of heat exchangers. The low order models require significant amount of tuning of the parameters for effective prediction of transients. The high order models resulting from using the distributed parameter approach are not suitable for controller design. Low order models obtained by applying standard model reduction techniques to the higher order models, lose the significance of the system states. The effort detailed in this report utilizes the high order models to characterize the heat exchanger and use it to determine low order models with system states having physical significance.

Most of the modeling approaches used by the authors above apply the assumption of mean void fraction to characterize the two-phase region in the heat exchangers. The void fraction model has been discussed in the next section.

1.2.1 Void Fraction

Void fraction is defined as the ratio of vapor volume to total volume in a two-phase fluid flow. It has long been used to describe certain characteristics of two-phase flows. Many experimental correlations have been proposed for predicting void fraction for various conditions and fluids. Rice [24] has presented the well known void fraction correlations in his reviews for ASHRAE. The void fraction is generally represented as function of mass quality, x and combinations of various types of property indices (which remain constant for a given average evaporator or condenser saturation temperature). Quality of a two-phase fluid is defined as the ratio of vapor mass to total mass of the fluid. Rice has categorized the correlations into four divisions: Homogeneous, Slip Ratio, Lockhart-Martinelli, and Mass Flux Dependent. The former two types are relatively much simpler than the latter two. In a two-phase flow, slip ratio is defined as the ratio of vapor velocity to liquid velocity. The slip ratio correlation defines void fraction as Equation 1.1, where x is the fluid quality and S is the slip ratio.

$$\gamma = \frac{1}{1+\left(\frac{1-x}{x}\right)\left(\frac{\rho_g}{\rho_f}\right)S} \qquad (1.1)$$

The slip ratio may be varied from unity to a large number. The homogenous correlation is simply a special case with the slip ratio equal to unity. Zivi developed a void fraction equation similar in form to Equation 1.1 where S is given by Equation 1.2.

For the purpose of this research, slip ratio is assumed to be a number between unity and S obtained by Equation 1.2.

$$S = \left(\frac{\rho_g}{\rho_f} \right)^{-1/3} \qquad (1.2)$$

1.3 Organization of Report

The remainder of this report is organized as follows. Chapter 2 describes the modeling procedure for each of the evaporator and condenser models using MB and FCV approach. Chapter 3 describes the procedure for obtaining linearized models of the heat exchangers. Chapter 4 details the experimental setup and explains the experiments conducted. Chapter 5 presents the simulation environment developed for simulation, model validation, and controller design. Model validation results are given in Chapter 6. Chapter 7 presents the general approach used to derive reduced order models using the higher order FCV models. Conclusions and suggestions for future work are given in Chapter 8.

CHAPTER 2

DYNAMIC MODELING

This chapter discusses the modeling of heat exchangers (including evaporator and condenser). Modeling of two phase fluid flow to capture the detailed dynamics is not only difficult and mathematically complex but it requires a considerable amount of time and effort to complete the task. Several methods to model two-phase fluid flow have been reviewed by D.A. Drew for Annual Review of Fluid Mechanics [10]. Fluid flow through an evaporator or a condenser involves one or more transition of fluid phase from vapor to single-phase and vice versa. The modeling of heat exchangers begins with governing equations. Some basic assumptions have been postulated without significantly compromising the physics of interest.

2.1 Modeling Assumptions

Several assumptions are made to approximate and simplify the subsequent development of the model. These assumptions have been commonly used in the past efforts as well. Firstly, the heat exchanger is assumed to be a long, thin and horizontal tube such that the refrigerant flow inside it can be modeled as a one-dimensional fluid flow. The refrigerant flow inside the tube is truly three-dimensional because of turbulence. The major impact of turbulence affects convective heat transfer coefficient from the refrigerant to the tube. The use of an appropriate heat transfer coefficient

correlation should be able to capture the effects of turbulence and the refrigerant can be safely assumed to have a one-dimensional flow.

Secondly, the pressure drop along the length of the heat exchanger due to change in momentum of refrigerant or due to viscous friction is assumed to be negligible. Thus, the refrigerant pressure along the heat exchanger tube is uniform. This eliminates the need for the equation for conservation of momentum.

The third assumption is that the axial conduction of heat in the refrigerant as well as the tube material is much less as compared to the heat transfer between refrigerant and tube material on one side and tube material and secondary fluid on the other side. Lastly, the cross-sectional area of the flow-stream within each control region is assumed to be constant.

2.2 Moving Boundary Model

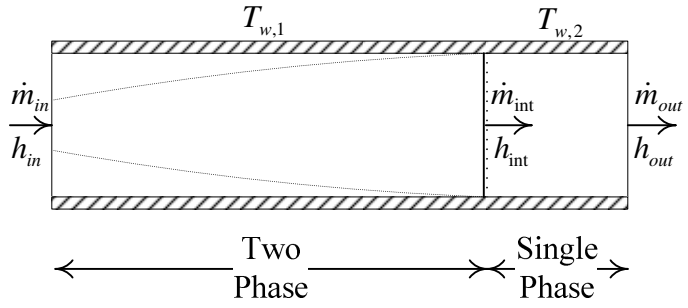

Figure 2.1: MB Evaporator Model Diagram

The moving boundary (MB) approach to multi-phase heat exchanger modeling relies on several fundamental assumptions as described in the previous section. Despite the complexity of typical heat exchanger geometries, the MB approach assumes the heat exchanger can be modeled as one-dimensional fluid flow through a horizontal tube, with equivalent mass, surface areas, length, and volume as shown in Figure 2.1. The standard derivation procedure requires the integration of the governing PDEs given in Equations 2.1-2.3 along the length of the heat exchanger to remove spatial dependence. The integration rule given in Equation 2.4, commonly known as Leibniz's equation, is used to handle the time-varying boundary between the fluid regions. This approach can be tedious and require a significant amount of algebraic manipulation. With some minor differences many authors use some form of this approach to model an evaporator in a sub-critical cycle [8,12,14,26]. In this case, the fluid is assumed to enter as a two-phase mixture, and leave as a superheated vapor, and thus the model is divided into two regions. The model assumes a time-invariant mean void fraction in the two-phase region.

$$\frac{\partial \rho A}{\partial t} + \frac{\partial \dot{m}}{\partial z} = 0 \qquad (2.1)$$

$$\frac{\partial (\rho A h - AP)}{\partial t} + \frac{\partial (\dot{m} h)}{\partial z} = p_i \alpha_i (T_w - T_r) \qquad (2.2)$$

$$(C_p \rho A)_w \frac{\partial T_w}{\partial t} = p_i \alpha_i (T_r - T_w) + p_o \alpha_o (T_a - T_w) \qquad (2.3)$$

$$\int_{z_1(t)}^{z_2(t)} \frac{\partial f(z,t)}{\partial t} dz = \frac{d}{dt}\left[\int_{z_1(t)}^{z_2(t)} f(z,t) dz\right] - f(z_2(t),t)\frac{d(z_2(t))}{dt} + f(z_1(t),t)\frac{d(z_1(t))}{dt} \quad (2.4)$$

The conservation of refrigerant mass as applied to the two-phase and superheat regions is given in Equations 2.5 and 2.6. Similarly the conservation of refrigerant energy is shown in Equations 2.7 and 2.8, and the conservation of heat exchanger wall energy is shown in Equations 2.9 and 2.10.

$$\left(\frac{d\rho_f}{dP_e}(1-\bar{\gamma}) + \frac{d\rho_g}{dP_e}(\bar{\gamma})\right) A_{cs} L_1 \dot{P}_e + \left(\rho_f - \rho_g\right)(1-\bar{\gamma}) A_{cs} \dot{L}_1 + \left(\rho_g - \rho_f\right) A_{cs} L_1 \dot{\bar{\gamma}} + \dot{m}_{\text{int}} - \dot{m}_{in} = 0 \quad (2.5)$$

$$\left[\left(\left.\frac{\partial \rho_2}{\partial P_e}\right|_{h_2}\right) + \frac{1}{2}\left(\left.\frac{\partial \rho_2}{\partial h_2}\right|_{P_e}\right)\left(\frac{dh_g}{dP_e}\right)\right] A L_2 \dot{P}_e + \frac{1}{2}\left(\left.\frac{\partial \rho_2}{\partial h_2}\right|_{P_e}\right) A L_2 \dot{h}_{out} + (\rho_g - \rho_2) A \dot{L}_1 + \dot{m}_{out} - \dot{m}_{\text{int}} = 0 \quad (2.6)$$

$$\left(\frac{d(\rho_f h_f)}{dP_e}(1-\bar{\gamma}) + \frac{d(\rho_g h_g)}{dP_e}(\bar{\gamma}) - 1\right) A_{cs} L_1 \dot{P}_e + \left(\rho_g h_g - \rho_f h_f\right) A_{cs} L_1 \dot{\bar{\gamma}} + \left(\rho_f h_f - \rho_g h_g\right)(1-\bar{\gamma}) A_{cs} \dot{L}_1 + \dot{m}_{\text{int}} h_{\text{int}} - \dot{m}_{in} h_{in} = \alpha_i A_i \left(\frac{L_1}{L_{Total}}\right)(T_{w1} - T_{r1}) \quad (2.7)$$

$$\left[\left(\left(\left.\frac{\partial\rho_2}{\partial P_e}\right|_{h_2}\right)+\left(\frac{1}{2}\right)\left(\frac{dh_g}{dP_e}\right)\left(\left.\frac{\partial\rho_2}{\partial h_2}\right|_{P_e}\right)\right)h_2+\left(\frac{1}{2}\right)\left(\frac{dh_g}{dP_e}\right)\rho_2-1\right]A_{cs}L_2\dot{P}_e$$
$$+\left[\left(\left.\frac{\partial\rho_2}{\partial h_2}\right|_{P_e}\right)h_2+\rho_2\right]\left(\frac{1}{2}\right)A_{cs}L_2\dot{h}_{out}+\left(\rho_g h_g-\rho_2 h_2\right)A_{cs}\dot{L}_1 \qquad (2.8)$$
$$+\dot{m}_{out}h_{out}-\dot{m}_{\text{int}}h_{\text{int}}=\alpha_i A_i\left(\frac{L_2}{L_{Total}}\right)\left(T_{w2}-T_{r2}\right)$$

$$\left(C_p\rho V\right)_w\dot{T}_{w1}=\alpha_i A_i\left(T_r-T_w\right)+\alpha_o A_o\left(T_a-T_w\right) \qquad (2.9)$$

$$\left(C_p\rho V\right)_w\left[\dot{T}_{w2}-\left(\frac{T_{w2}-T_{w1}}{L_2}\right)\dot{L}_1\right]=\alpha_i A_i\left(T_r-T_w\right)+\alpha_o A_o\left(T_a-T_w\right) \qquad (2.10)$$

The resulting six ordinary differential equations can be algebraically combined to yield five ODEs and eliminate the term for mass flow rate at the interface boundary, $\dot{m}_{\text{int}}$. This results in Equation 2.11, which is of the $Z(x,u)\cdot\dot{x}=f(x,u)$ form with the states and input vectors defined in Equations 2.12 and 2.13 respectively. The elements of the $Z(x,u)$ matrix are given in Equations 2.14-2.22. A complete derivation, as well as the linearization, can be found in [22,23].

$$\begin{bmatrix} z_{11} & z_{12} & 0 & 0 & 0 \\ z_{21} & z_{22} & z_{23} & 0 & 0 \\ z_{31} & z_{32} & z_{33} & 0 & 0 \\ 0 & 0 & 0 & z_{44} & 0 \\ z_{51} & 0 & 0 & 0 & z_{55} \end{bmatrix}\begin{bmatrix} \dot{L}_1 \\ \dot{P}_e \\ \dot{h}_{out} \\ \dot{T}_{w1} \\ \dot{T}_{w2} \end{bmatrix}=\begin{bmatrix} \dot{m}_{in}\left(h_{in}-h_g\right)+\alpha_{i1}A_i\left(\frac{L_1}{L_{Total}}\right)\left(T_{w1}-T_{r1}\right) \\ \dot{m}_{out}\left(h_g-h_{out}\right)+\alpha_{i2}A_i\left(\frac{L_2}{L_{Total}}\right)\left(T_{w2}-T_{r2}\right) \\ \dot{m}_{in}-\dot{m}_{out} \\ \alpha_o A_o\left(T_a-T_{w1}\right)-\alpha_{i1}A_i\left(T_{w1}-T_{r1}\right) \\ \alpha_o A_o\left(T_a-T_{w2}\right)-\alpha_{i2}A_i\left(T_{w2}-T_{r2}\right) \end{bmatrix} \qquad (2.11)$$

$$x = \begin{bmatrix} L_1 & P_e & h_{out} & T_{w1} & T_{w2} \end{bmatrix}^T \quad (2.12)$$

$$u = \begin{bmatrix} \dot{m}_{in} & \dot{m}_{out} & h_{in} & T_{air,in} & \dot{m}_{air} \end{bmatrix}^T \quad (2.13)$$

$$z_{11} = \left[\rho_f \left(h_f - h_g\right)\right]\left(1-\bar{\gamma}\right)A_{cs} \quad (2.14)$$

$$z_{12} = \left[\left(\frac{d\left(\rho_f h_f\right)}{dP_e} - \frac{d\rho_f}{dP_e}h_g\right)\left(1-\bar{\gamma}\right) + \left(\frac{d\left(\rho_g h_g\right)}{dP_e} - \frac{d\rho_g}{dP_e}h_g\right)\left(\bar{\gamma}\right) - 1\right]A_{cs}L_1 \quad (2.15)$$

$$z_{22} = \left[\left(\left(\frac{\partial\rho_2}{\partial P_e}\bigg|_{h_2}\right) + \left(\frac{1}{2}\right)\left(\frac{\partial\rho_2}{\partial h_2}\bigg|_{P_e}\right)\left(\frac{dh_g}{dP_e}\right)\right)\left(h_2 - h_g\right) + \left(\frac{\rho_2}{2}\right)\left(\frac{dh_g}{dP_e}\right) - 1\right]A_{cs}L_2 \quad (2.16)$$

$$z_{31} = \left[\left(\rho_g - \rho_2\right) + \left(\rho_f - \rho_g\right)\left(1-\bar{\gamma}\right)\right]A_{cs} \quad (2.17)$$

$$z_{32} = \left[\left[\left(\frac{\partial\rho_2}{\partial P_e}\bigg|_{h_2}\right) + \frac{1}{2}\left(\frac{\partial\rho_2}{\partial h_2}\bigg|_{P_e}\right)\left(\frac{dh_g}{dP_e}\right)\right]L_2 + \left[\left(\frac{d\rho_f}{dP_e}\right)\left(1-\bar{\gamma}\right) + \left(\frac{d\rho_g}{dP_e}\right)\left(\bar{\gamma}\right)\right]L_1\right]A_{cs} \quad (2.18)$$

$$z_{33} = \frac{1}{2}\left(\frac{\partial\rho_2}{\partial h_2}\bigg|_{P_e}\right)A_{cs}L_2 \quad (2.19)$$

$$z_{44} = \left(C_p\rho V\right)_w \quad (2.20)$$

$$z_{51} = \left(C_p\rho V\right)_w\left(\frac{T_{w1} - T_{w2}}{L_2}\right) \quad (2.21)$$

$$z_{55} = \left(C_p\rho V\right)_w \quad (2.22)$$

2.3 Finite Control Volume Evaporator Model

For developing the finite control volume (FCV) approach, we begin with discretizing the evaporator model into n control volumes. Depending on the geometry of the heat exchanger, the k^{th} control region will have an internal surface area, $A_{i,k}$, external surface area, $A_{o,k}$, and volume of the control region, $V_{e,k}$. The governing ordinary differential equations are obtained by applying the basic assumptions enlisted in the previous section to the fundamental conservation equations for each control region. Lumped parameters are associated with each control region. Although the resulting equations use lumped parameters for each assumed control region, by increasing the number of control volumes (i.e. increasing the level of discretization), the model approximates the distributed parametric nature of a real heat exchanger (Figure 2.2).

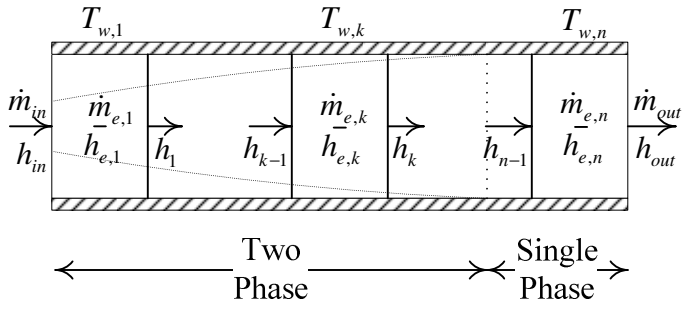

Figure 2.2: FCV Evaporator Model Diagram

If the fluid entering the evaporator is two-phase and the fluid exiting the evaporator is single-phase, the evaporator broadly consists of two regions: two-phase region and a superheated region. For modeling purpose, it has been assumed that the

fluid gradually transitions from two-phase to single-phase fluid inside the heat exchanger (shown in Figure 2.2). The outlet enthalpy of the fluid in a control region determines the state of the fluid in that region. If the outlet enthalpy of the fluid in a region is less than or equal to the vapor saturation enthalpy (at the evaporator pressure), the state of the fluid in that region is two-phase. If the outlet enthalpy of the fluid in a region is greater than the vapor saturation enthalpy, the state of the fluid in that region is single-phase. The control region in which the final transition of fluid from two-phase to single-phase occurs has been termed by the author as the 'transition region'. The state of the fluid in the transition region is assumed to be single-phase. In an evaporator shown in Figure 2.2, if the transition line is closer to the left boundary of the transition region, the better is our assumption of guessing the state of the fluid in that region. The modeling error due to the assumption of the state of fluid in the transition region can be minimized by increasing the number of control volumes. In the Figure 2.2, h_{k-1}, $\dot{m}_{k-1}$ and h_k, $\dot{m}_k$ are the enthalpy and mass flow rate of the refrigerant at the inlet and outlet of the k^{th} control region. h_{in}, $\dot{m}_{in}$ and h_{out}, $\dot{m}_{out}$ are the enthalpy and mass flow rate of the refrigerant at the inlet and outlet of the heat exchanger. $\dot{m}_{e,k}$ gives the rate of change of refrigerant mass in the k^{th} control region and $h_{e,k}$ is assumed to be the average enthalpy in the k^{th} control region of the heat exchanger. The conservation equations for refrigerant energy, mass and tube-wall energy are considered for obtaining the governing ordinary differential equations.

2.3.1 Conservation of Refrigerant Energy

We begin with consideration of refrigerant energy for each control region. The rate of change of internal energy in a control region, $\dot{U}$ is given by Equation 2.23, where $\dot{H}_{in}$ is the rate of energy entering the region by means of refrigerant mass, $\dot{H}_{out}$ is the rate of energy leaving the region by means of refrigerant mass and $\dot{Q}_w$ is the rate of energy leaving the region through heat transfer to the heat exchanger wall. The fluid flow energy at a point is given by $\dot{H} = \dot{m} \cdot h$ where $\dot{m}$ is the mass flow rate of the fluid and h is the enthalpy of the fluid at that point. The wall heat transfer term for a region is defined as $\dot{Q}_w = \alpha_i A_i \left(T_w - T_r\right)$ where α_i is the lumped heat transfer coefficient between refrigerant and wall material, A_i is the internal surface area of the heat exchanger wall in that region, T_w and T_r are the lumped wall temperature and refrigerant temperature in that region. Substituting the defined terms in Equation 2.23, the equations for conservation of refrigerant energy for all the control regions of the heat exchanger are presented in Equation 2.24.

$$\dot{U} = H_{in} - H_{out} + \dot{Q}_w \qquad (2.23)$$

$$\begin{bmatrix} \dot{U}_1 \\ \vdots \\ \dot{U}_k \\ \vdots \\ \dot{U}_n \end{bmatrix} = \begin{bmatrix} \dot{m}_{in} h_{in} - \dot{m}_1 h_1 + \alpha_{i,1} A_{i,1} \left(T_{w,1} - T_{r,1}\right) \\ \vdots \\ \dot{m}_{k-1} h_{k-1} - \dot{m}_k h_k + \alpha_{i,k} A_{i,k} \left(T_{w,k} - T_{r,k}\right) \\ \vdots \\ \dot{m}_{n-1} h_{n-1} - \dot{m}_{out} h_{out} + \alpha_{i,n} A_{i,n} \left(T_{w,n} - T_{r,n}\right) \end{bmatrix} \qquad (2.24)$$

2.3.2 Conservation of Refrigerant Mass

The conservation of refrigerant mass in each control volume is given by Equation 2.25, which is equal to the difference of the refrigerant mass entering and leaving that control volume. All the equations in Equation 2.25 can be combined together by adding them and are presented in Equation 2.26 where $\dot{m}_e$ gives the rate of change of total refrigerant mass in the heat exchanger.

$$\begin{bmatrix} \dot{m}_{e,1} \\ \vdots \\ \dot{m}_{e,k} \\ \vdots \\ \dot{m}_{e,n} \end{bmatrix} = \begin{bmatrix} \dot{m}_{in} - \dot{m}_1 \\ \vdots \\ \dot{m}_{k-1} - \dot{m}_k \\ \vdots \\ \dot{m}_{n-1} - \dot{m}_{out} \end{bmatrix} \quad (2.25)$$

$$\dot{m}_e = \dot{m}_{in} - \dot{m}_{out} \quad (2.26)$$

2.3.3 Conservation of Tube Wall Energy

The conservation of wall energy in a control region is given in Equation 2.27 where $\dot{E}_w$ is the rate of change of total energy of the heat exchanger wall in the control region considered and $\dot{Q}_a$ is the rate of energy entering the heat exchanger wall through heat transfer from the external fluid. Substituting the defined terms in Equation 2.27, the equations for conservation of tube wall energy for all the control regions of the heat exchanger are presented in Equation 2.28.

$$\dot{E}_w = \dot{Q}_a - \dot{Q}_w \tag{2.27}$$

$$\begin{bmatrix} \dot{E}_{w,1} \\ \vdots \\ \dot{E}_{w,k} \\ \vdots \\ \dot{E}_{w,n} \end{bmatrix} = \begin{bmatrix} \alpha_{o,1} A_{o,1} \left(T_{a,1} - T_{w,1}\right) - \alpha_{i,1} A_{i,1} \left(T_{w,1} - T_{r,1}\right) \\ \vdots \\ \alpha_{o,k} A_{o,k} \left(T_{a,k} - T_{w,k}\right) - \alpha_{i,k} A_{i,k} \left(T_{w,k} - T_{r,k}\right) \\ \vdots \\ \alpha_{o,n} A_{o,n} \left(T_{a,n} - T_{w,n}\right) - \alpha_{i,n} A_{i,n} \left(T_{w,n} - T_{r,n}\right) \end{bmatrix} \tag{2.28}$$

2.3.4 Governing Differential Equations

The combined results presented in Equations 2.24, 2.26 and 2.28 are given in Equation 2.29. Defining internal energy in terms of refrigerant mass and average specific internal energy $U_{e,k} = m_{e,k} \cdot u_{e,k}$, the time derivative of this term can be expanded as in Equation 2.30 for the k^{th} control region. Defining refrigerant mass in terms of average density, $\rho_{e,k}$ and internal volume $V_{e,k}$ as $m_{e,k} = V_{e,k} \cdot \rho_{e,k}$, yields Equation 2.31 for the k^{th} control region. Since density and internal energy can be given as functions of pressure, P_e, and enthalpy, $h_{\mathrm{e,k}}$, of the region being considered, the time derivative of these variables can be written in terms of the desired state (Equation 2.32). Simplifying this expression and substituting the formal definition of enthalpy $h_{e,k} = u_{e,k} + \dfrac{P_e}{\rho_{e,k}}$, and its partial derivatives of $\left.\dfrac{\partial u_{e,k}}{\partial P_e}\right|_{h_{e,k}} = \dfrac{-1}{\rho_{e,k}} + \dfrac{P_e}{{\rho_{e,k}}^2} \left.\dfrac{\partial \rho_{e,k}}{\partial P_e}\right|_{h_{e,k}}$ and $\left.\dfrac{\partial u_{e,k}}{\partial h_{e,k}}\right|_{P_e} = 1 + \dfrac{P_e}{{\rho_{e,k}}^2} \left.\dfrac{\partial \rho_{e,k}}{\partial h_{e,k}}\right|_{P_e}$ results in Equations 2.33, 2.34 and 2.35. Likewise, expanding the time derivative of

mass inventory results in Equations 2.36 and 2.37. Finally, defining the total wall energy as the product of thermal capacitance and temperature $E_{w,k} = \left(C_p \rho V\right)_w T_{w,k}$, the time derivative of this term can be written as in Equation 2.38.

$$\begin{bmatrix} \dot{U}_1 \\ \vdots \\ \dot{U}_k \\ \vdots \\ \dot{U}_n \\ \dot{m}_e \\ \dot{E}_{w,1} \\ \vdots \\ \dot{E}_{w,k} \\ \vdots \\ \dot{E}_{w,n} \end{bmatrix} = \begin{bmatrix} \dot{m}_{in} h_{in} - \dot{m}_1 h_1 + \alpha_{i,1} A_{i,1} \left(T_{w,1} - T_{r,1}\right) \\ \vdots \\ \dot{m}_{k-1} h_{k-1} - \dot{m}_k h_k + \alpha_{i,k} A_{i,k} \left(T_{w,k} - T_{r,k}\right) \\ \vdots \\ \dot{m}_{n-1} h_{n-1} - \dot{m}_{out} h_{out} + \alpha_{i,n} A_{i,n} \left(T_{w,n} - T_{r,n}\right) \\ \dot{m}_{in} - \dot{m}_{out} \\ \alpha_{o,1} A_{o,1} \left(T_{a,1} - T_{w,1}\right) - \alpha_{i,1} A_{i,1} \left(T_{w,1} - T_{r,1}\right) \\ \vdots \\ \alpha_{o,k} A_{o,k} \left(T_{a,k} - T_{w,k}\right) - \alpha_{i,k} A_{i,k} \left(T_{w,k} - T_{r,k}\right) \\ \vdots \\ \alpha_{o,n} A_{o,n} \left(T_{a,n} - T_{w,n}\right) - \alpha_{i,n} A_{i,n} \left(T_{w,n} - T_{r,n}\right) \end{bmatrix} \quad (2.29)$$

$$\dot{U}_{e,k} = \dot{m}_{e,k} \cdot u_{e,k} + m_{e,k} \cdot \dot{u}_{e,k} \quad (2.30)$$

$$\dot{U}_{\mathrm{e,k}} = V_{\mathrm{e,k}} \left(\dot{\rho}_{\mathrm{e,k}} \cdot u_{\mathrm{e,k}} + \rho_{\mathrm{e,k}} \cdot \dot{u}_{\mathrm{e,k}}\right) \quad (2.31)$$

$$\begin{aligned} \dot{U}_{\mathrm{e,k}} = V_{\mathrm{e,k}} \Bigg[& \left(\left(\frac{\partial \rho_{e,k}}{\partial P_e} \bigg|_{h_{e,k}} \right) \dot{P}_e + \left(\frac{\partial \rho_{e,k}}{\partial h_{e,k}} \bigg|_{P_e} \right) \dot{h}_{e,k} \right) u_{e,k} \\ & + \left(\left(\frac{\partial u_{e,k}}{\partial P_e} \bigg|_{h_{e,k}} \right) \dot{P}_e + \left(\frac{\partial u_{e,k}}{\partial h_{e,k}} \bigg|_{P_e} \right) \dot{h}_{e,k} \right) \rho_{e,k} \Bigg] \end{aligned} \quad (2.32)$$

$$\dot{U}_{e,k} = V_{e,k}\left[\left(\left.\frac{\partial \rho_{e,k}}{\partial P_e}\right|_{h_{e,k}}\right)u_{e,k} + \left(\left.\frac{\partial u_{e,k}}{\partial P_e}\right|_{h_{e,k}}\right)\rho_{e,k}\right]\dot{P}_e + V_{e,k}\left[\left(\left.\frac{\partial \rho_{e,k}}{\partial h_{e,k}}\right|_{P_e}\right)u_{e,k} + \left(\left.\frac{\partial u_{e,k}}{\partial h_{e,k}}\right|_{P_e}\right)\rho_{e,k}\right]\dot{h}_{e,k} \quad (2.33)$$

$$\dot{U}_{e,k} = V_{e,k}\left[\left(\left.\frac{\partial \rho_{e,k}}{\partial P_e}\right|_{h_{e,k}}\right)\left(u_{e,k} + \frac{P_e}{\rho_{e,k}}\right) - 1\right]\dot{P}_e + V_{e,k}\left[\left(\left.\frac{\partial \rho_{e,k}}{\partial h_{e,k}}\right|_{P_e}\right)\left(u_{e,k} + \frac{P_e}{\rho_{e,k}}\right) + \rho_{e,k}\right]\dot{h}_{e,k} \quad (2.34)$$

$$\dot{U}_{e,k} = V_{e,k}\left[\left(\left.\frac{\partial \rho_{e,k}}{\partial P_e}\right|_{h_{e,k}}\right)h_{e,k} - 1\right]\dot{P}_e + V_{e,k}\left[\left(\left.\frac{\partial \rho_{e,k}}{\partial h_{e,k}}\right|_{P_e}\right)h_{e,k} + \rho_{e,k}\right]\dot{h}_{e,k} \quad (2.35)$$

$$\dot{m}_{e,k} = \dot{\rho}_{e,k} \cdot V_{e,k} \quad (2.36)$$

$$\dot{m}_{e,k} = \left[\left(\left.\frac{\partial \rho_{e,k}}{\partial P_e}\right|_{h_{e,k}}\right)\dot{P}_e + \left(\left.\frac{\partial \rho_{e,k}}{\partial h_{e,k}}\right|_{P_e}\right)\dot{h}_{e,k}\right]V_{e,k} \quad (2.37)$$

$$\dot{E}_{w,k} = \left(C_p \rho V\right)_w \dot{T}_{w,k} \quad (2.38)$$

Equations 2.35, 2.37 and 2.38 can be extended for all the control regions of the heat exchanger to represent the refrigerant energy, refrigerant mass and tube wall energy respectively. The resulting equations along with Equation 2.25 and 2.29 can be combined and simplified into $(2n+1)$ nonlinear differential equations and reorganized

into a matrix form given by Equation 2.39 where x is the state vector. The state vector x, input vector u and the output vector y are given in Equations 2.40, 2.41 and 2.42 respectively. The elements of matrices $Z(x,u)$ and $f(x,u)$ are given in Equations 2.43 through 2.59.

$$Z(x,u)\cdot \dot{x} = f(x,u) \tag{2.39}$$

$$x = \begin{bmatrix} P_e & h_{e,1} & \dots & h_{e,k} & \dots & h_{e,n} & T_{w,1} & \dots & T_{w,k} & \dots & T_{w,n} \end{bmatrix}^T \tag{2.40}$$

$$u = \begin{bmatrix} \dot{m}_{in} & \dot{m}_{out} & h_{in} & T_{a,in} & \dot{m}_{air} \end{bmatrix}^T \tag{2.41}$$

$$y = \begin{bmatrix} P_e & h_{out} & T_{w,1} & \cdots & T_{w,k} & \cdots & T_{w,n} & T_{a,out} & T_{r,out} & m_{e,1} \cdots & m_{e,k} & \cdots & m_{e,n} \end{bmatrix}^T \tag{2.42}$$

$$Z(x,u) = \begin{bmatrix} Z_{11} & Z_{12} & 0 \\ Z_{21} & Z_{22} & 0 \\ 0 & 0 & Z_{33} \end{bmatrix}_{(2n+1)X(2n+1)} \tag{2.43}$$

$$Z_{11} = \begin{bmatrix} Z_{11}^1 \\ \vdots \\ Z_{11}^k \\ \vdots \\ Z_{11}^n \end{bmatrix}_{nX1} \tag{2.44}$$

$$Z_{11}^1 = V_{e,1} \frac{\partial \rho_{e,1}}{\partial P_e}\bigg|_{h_{e,1}} \left(h_{e,1} - h_1\right) - V_{e,1} \tag{2.45}$$

$$Z_{11}^{k} = V_{e,k}\left.\frac{\partial \rho_{e,k}}{\partial P_e}\right|_{h_{e,k}} \left(h_{e,k} - h_k\right) - V_{e,k} + \left(h_{e,k} - h_k\right)\left(V_{e,1}\left.\frac{\partial \rho_{e,1}}{\partial P_e}\right|_{h_{e,1}} + \cdots + V_{e,k-1}\left.\frac{\partial \rho_{e,k-1}}{\partial P_e}\right|_{h_{e,k-1}} \right) \quad (2.46)$$

$$Z_{11}^{n} = V_{e,n}\left.\frac{\partial \rho_{e,n}}{\partial P_e}\right|_{h_{e,n}} \left(h_{e,n} - h_{out}\right) - V_{e,n} + \left(h_{e,n} - h_{out}\right)\left(V_{e,1}\left.\frac{\partial \rho_{e,1}}{\partial P_e}\right|_{h_{e,1}} + \cdots + V_{e,n-1}\left.\frac{\partial \rho_{e,n-1}}{\partial P_e}\right|_{h_{e,n-1}} \right) \quad (2.47)$$

$$Z_{12} = \begin{bmatrix} Z_{12}^{11} & 0 & \cdots & 0 & 0 \\ \vdots & & & & \vdots \\ Z_{12}^{k1} & \cdots & Z_{12}^{k(k-1)} & Z_{12}^{kk} & 0 \\ \vdots & & \ddots & \ddots & \vdots \\ Z_{12}^{n1} & \cdots & & Z_{12}^{n(n-1)} & Z_{12}^{nn} \end{bmatrix}_{nXn} \quad (2.48)$$

$$Z_{12}^{11} = V_{e,1}\left.\frac{\partial \rho_{e,1}}{\partial P_e}\right|_{h_{e,1}} \left(h_{e,1} - h_1\right) + V_{e,1}\rho_{e,1} \quad (2.49)$$

$$Z_{12}^{k1} = \left(h_{k-1} - h_k\right) V_{e,1}\left.\frac{\partial \rho_{e,1}}{\partial h_{e,1}}\right|_{P_e} \quad (2.50)$$

$$Z_{12}^{k(k-1)} = \left(h_{k-1} - h_k\right) V_{e,k-1}\left.\frac{\partial \rho_{e,k-1}}{\partial h_{e,k-1}}\right|_{P_e} \quad (2.51)$$

$$Z_{12}^{kk} = \left(h_{e,k} - h_k\right) V_{e,k}\left.\frac{\partial \rho_{e,k}}{\partial h_{e,k}}\right|_{P_e} + V_{e,k}\rho_{e,k} \quad (2.52)$$

$$Z_{12}^{n1} = (h_{n-1} - h_n) V_{e,1} \left. \frac{\partial \rho_{e,1}}{\partial h_{e,1}} \right|_{P_e} \tag{2.53}$$

$$Z_{12}^{n(n-1)} = (h_{n-1} - h_n) V_{e,n-1} \left. \frac{\partial \rho_{e,n-1}}{\partial h_{e,n-1}} \right|_{P_e} \tag{2.54}$$

$$Z_{12}^{nn} = (h_{e,n} - h_n) V_{e,n} \left. \frac{\partial \rho_{e,n}}{\partial h_{e,n}} \right|_{P_e} + V_{e,n} \rho_{e,n} \tag{2.55}$$

$$Z_{21} = \left[\left. V_{e,1} \frac{\partial \rho_{e,1}}{\partial P_e} \right|_{h_{e,1}} + \cdots + \left. V_{e,n} \frac{\partial \rho_{e,n}}{\partial P_e} \right|_{h_{e,n}} \right]_{1X1} \tag{2.56}$$

$$Z_{22} = \left[\left. V_{e,1} \frac{\partial \rho_{e,1}}{\partial h_{e,1}} \right|_{P_e} \quad \cdots \quad \left. V_{e,n} \frac{\partial \rho_{e,n}}{\partial h_{e,n}} \right|_{P_e} \right]_{1Xn} \tag{2.57}$$

$$Z_{33} = diag\left\{ \left[\left(C_p \rho V \right)_{w,1} \quad \cdots \quad \left(C_p \rho V \right)_{w,n} \right] \right\} \tag{2.58}$$

$$f(x,u) = \begin{bmatrix} \dot{m}_{in}(h_{in} - h_1) + \alpha_{i,1} A_{i,1} (T_{w,1} - T_{r,1}) \\ \vdots \\ \dot{m}_{in}(h_{k-1} - h_k) + \alpha_{i,k} A_{i,k} (T_{w,k} - T_{r,k}) \\ \vdots \\ \dot{m}_{in}(h_{n-1} - h_{out}) + \alpha_{i,n} A_{i,n} (T_{w,n} - T_{r,n}) \\ \dot{m}_{in} - \dot{m}_{out} \\ \alpha_{i,1} A_{i,1} (T_{r,1} - T_{w,1}) + \alpha_o A_{o,1} (T_{a,1} - T_{w,1}) \\ \vdots \\ \alpha_{i,k} A_{i,k} (T_{r,k} - T_{w,k}) + \alpha_o A_{o,k} (T_{a,k} - T_{w,k}) \\ \vdots \\ \alpha_{i,n} A_{i,n} (T_{r,n} - T_{w,n}) + \alpha_o A_{o,n} (T_{a,n} - T_{w,n}) \end{bmatrix}_{(2n+1)X1} \tag{2.59}$$

As discussed in Chapter 1, void fraction is the ratio of vapor volume to the total volume in the region being considered. It is used to describe characteristics of two-phase flow. The void fraction of k^{th} control region is given by Equation 2.60 where x_k is the quality (ratio of vapor mass to total mass of the refrigerant) of the region and S is the slip ratio (ratio of vapor velocity to liquid velocity). ρ_g and ρ_f are the saturated vapor density and saturated liquid density of the fluid at the evaporator pressure respectively. Thus, void fraction is a function of quality and pressure, say $f_1(x_k, P_e)$. Quality of the fluid in the k^{th} control region is given by Equation 2.61 which is a function of average enthalpy, $h_{e,k}$ and evaporator pressure, P_e. h_g and h_f are the saturated vapor enthalpy and saturated liquid enthalpy of the fluid at the evaporator pressure respectively. It can be assumed that $x_k = f_2(h_{e,k}, P_e)$. Now, the density of the k^{th} control region is given by Equation 2.62 and can be assumed as a function of void fraction and evaporator pressure as $\rho_{e,k} = f_3(\gamma_k, P_e)$. The partial derivative of density with respect to evaporator pressure and with respect to average enthalpy is given in Equations 2.63 and 2.64 respectively. Other derivatives required for calculating Equations 2.63 and 2.64 are given in Equations 2.65 through 2.72.

$$\gamma_k = \frac{\rho_f x_k}{\rho_f x_k + \rho_g (1 - x_k) S} = f_1(x_k, P_e) \qquad (2.60)$$

$$x_k = \frac{h_{e,k} - h_f}{h_g - h_f} = f_2(h_{e,k}, P_e) \qquad (2.61)$$

$$\rho_{e,k} = \rho_f \gamma_k + \rho_g (1-\gamma_k) = f_3(\gamma_k, P_e) \tag{2.62}$$

$$\frac{\partial \rho_{e,k}}{\partial P_e} = \frac{\partial f_3}{\partial P_e} + \frac{\partial f_3}{\partial \gamma_k}\frac{\partial \gamma_k}{\partial P_e} \tag{2.63}$$

$$\frac{\partial \rho_{e,k}}{\partial h_{e,k}} = \frac{\partial f_3}{\partial \gamma_k}\frac{\partial \gamma_k}{\partial h_{e,k}} \tag{2.64}$$

$$\frac{\partial f_3}{\partial P_e} = \gamma_k \left(\frac{d\rho_g}{dP_e} - \frac{d\rho_f}{dP_e} \right) \tag{2.65}$$

$$\frac{\partial f_3}{\partial \gamma_k} = \left(\rho_g - \rho_f \right) \tag{2.66}$$

$$\frac{\partial \gamma_k}{\partial P_e} = \frac{\partial f_1}{\partial P_e} + \frac{\partial f_1}{\partial x_k}\frac{\partial x_k}{\partial P_e} \tag{2.67}$$

$$\frac{\partial \gamma_k}{\partial h_{e,k}} = \frac{\partial f_1}{\partial x_k}\frac{\partial x_k}{\partial h_{e,k}} \tag{2.68}$$

$$\frac{\partial f_1}{\partial P_e} = \frac{\left(\rho_f x_k + \rho_g (1-x_k)S\right) x_k \dfrac{\partial \rho_f}{\partial P_e} - \rho_f x_k \left(\dfrac{\partial \rho_f}{\partial P_e} x_k + \dfrac{\partial \rho_g}{\partial P_e}(1-x_k)S \right)}{\left(\rho_f x_k + \rho_g (1-x_k)S\right)^2} \tag{2.69}$$

$$\frac{\partial f_1}{\partial x_k} = \frac{\left(\rho_f x_k + \rho_g (1-x_k)S\right)\rho_f - \rho_f x_k \left(\rho_f - \rho_g S\right)}{\left(\rho_f x_k + \rho_g (1-x_k)S\right)^2} \tag{2.70}$$

$$\frac{\partial x_k}{\partial P_e} = \frac{1}{\left(h_g - h_f\right)}\left[-\frac{dh_f}{dP_e} \right] + \left(h_{e,k} - h_f\right)\frac{1}{\left(h_g - h_f\right)^2}\left[\frac{dh_f}{dP_e} - \frac{dh_g}{dP_e} \right] \tag{2.71}$$

$$\frac{\partial x_k}{\partial h_{e,k}} = \frac{1}{h_g - h_f} \qquad (2.72)$$

As mentioned earlier, the state of the fluid in a control region can be determined on the basis of the outlet enthalpy of that region. If the fluid is in two-phase, we calculate the partial derivative of density with respect to evaporator pressure and enthalpy given in Equations 2.63 and 2.64 respectively. If the fluid is in single-phase, we can use the property tables to determine the partial derivative of density with respect to evaporator pressure and enthalpy.

2.4 Finite Control Volume Condenser Model

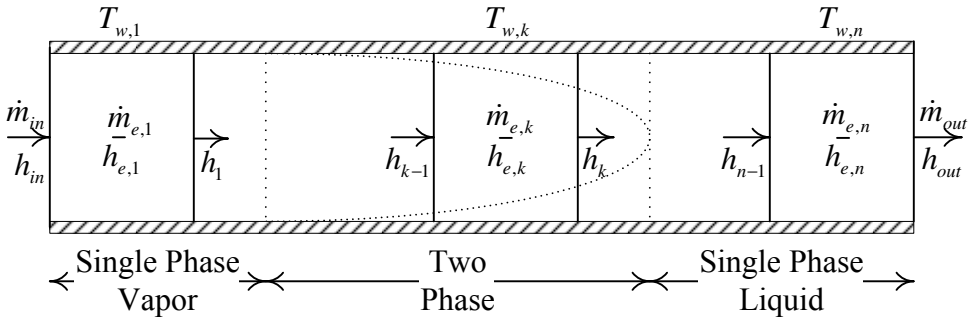

Figure 2.3: FCV Condenser Model Diagram

Usually, the fluid entering the condenser is single-phase super-heated vapor and the fluid exiting the condenser is single-phase super-cooled liquid as shown in Figure 2.3. Thus, the condenser broadly consists of three regions: superheated region, two-phase region and a super-cooled region. For developing the finite control volume (FCV)

approach, we begin with discretizing the condenser model into n control volumes. As mentioned earlier, the outlet enthalpy of the fluid in a control region determines the state of the fluid in that region. If the outlet enthalpy of the fluid in a region is greater than the vapor saturation enthalpy (at the condenser pressure), the state of the fluid in that region is single-phase superheated vapor. If the outlet enthalpy of the fluid in a region is less than or equal to the vapor saturation enthalpy and greater than or equal to the liquid saturation enthalpy, the state of the fluid in that region is two-phase. If the outlet enthalpy of the fluid in a region is less than the liquid saturation enthalpy (at the condenser pressure), the state of the fluid in that region is single-phase super-cooled liquid. The governing equations for the condenser model are the same as those for the evaporator model as described in Section 2.3. Equation 2.39 gives the $(2n+1)$ nonlinear differential equations for the condenser model where x is the state vector. The partial derivatives of density required are calculated using Equations 2.63 and 2.64 if the state of the fluid is two-phase. Property tables are used to determine the partial derivatives of density if the state of the refrigerant is singe phase.

CHAPTER 3

MODEL LINEARIZATION

The finite control volume model developed for the heat exchangers in the previous chapter is highly nonlinear. For analysis and model reduction purposes, a linear model is required. Also, for parameter tuning purposes, we need to selectively reduce the FCV model for comparison with models developed using moving boundary approach. This chapter outlines the procedure for obtaining linearized models from the nonlinear models. Two different linearized models have been discussed in this chapter. For obtaining the first model, it has been assumed that the average enthalpy of the refrigerant in a control region is the mean of the enthalpy of the refrigerant at the inlet and outlet of the region. The prediction of system dynamics using this model is not accurate. The transients in the models maybe induced due to several reasons like a change in compressor speed and so on. The average enthalpy of each control region is dependent on the inlet and outlet enthalpies of that region. Also, the outlet enthalpy of one control region is the inlet enthalpy of the subsequent control region. Thus, there is a strict mathematical relationship between the average enthalpies of all the control regions. So, even the slightest change in the input enthalpy of the system propagates through all the control regions in a single time step, which may not be the reality. The second model assumes that the average enthalpy of the refrigerant in a control region is the enthalpy of the refrigerant at the outlet of that region.

The first section of this chapter outlines the general linearization procedure. The next two sections describe the linearization of the FCV models derived in Chapter 2. The models have been linearized using the mean of inlet and outlet enthalpies as average enthalpy of a control region as well as assuming the average enthalpy of a control region as the outlet enthalpy of that region.

3.1 General Linearization Procedure

This procedure follows a standard linearization procedure, where the partial derivatives of the nonlinear functions with respect to the states and inputs are calculated neglecting the 2nd and higher order terms [19]. The FCV heat exchanger models have a unique form as given in Equation 3.1.

$$Z(x,u)\cdot \dot{x} = f(x,u) \tag{3.1}$$

$$\begin{aligned} \dot{x} &= Z(x,u)^{-1} f(x,u) \\ &= h(x,u) \end{aligned} \tag{3.2}$$

Using the assumption $x = x_o + \delta x$, a local linearization of this, neglecting higher order terms, would be Equation 3.3, and with the substitution $\delta x = x - x_o$, becomes Equation 3.4.

$$\delta \dot{x} = \left[\left. \frac{\partial h}{\partial x} \right|_{x_0,u_0} \right] \delta x + \left[\left. \frac{\partial h}{\partial u} \right|_{x_0,u_0} \right] \delta u \tag{3.3}$$

$$\dot{x} = \left[\left.\frac{\partial h}{\partial x}\right|_{x_0,u_0}\right](x - x_o) + \left[\left.\frac{\partial h}{\partial u}\right|_{x_0,u_0}\right](u - u_o) \tag{3.4}$$

Expanding the first term of Equation 3.4, results in Equation 3.5. Likewise, expanding the second term results in Equation 3.6. This is of the familiar form $\dot{x} = Ax + Bu$ (Equation 3.7). This form will be denoted as Equation 3.8, or in the standard form as Equation 3.9 using the substitutions in Equation 3.10.

$$\begin{aligned}\left[\left.\frac{\partial h}{\partial x}\right|_{x_0,u_0}\right] &= \left[Z\big|_{x_0,u_0}\right]^{-1}\left[\left.\frac{\partial f}{\partial x}\right|_{x_0,u_0}\right] - \left[Z\big|_{x_0,u_0}\right]^{-2}\left[\left.\frac{\partial Z}{\partial x}\right|_{x_0,u_0}\right]\underbrace{\left[f\big|_{x_0,u_0}\right]}_{0} \\ &= \left[Z\big|_{x_0,u_0}\right]^{-1}\left[\left.\frac{\partial f}{\partial x}\right|_{x_0,u_0}\right]\end{aligned} \tag{3.5}$$

$$\left[\left.\frac{\partial h}{\partial u}\right|_{x_0,u_0}\right] = \left[Z\big|_{x_0,u_0}\right]^{-1}\left[\left.\frac{\partial f}{\partial u}\right|_{x_0,u_0}\right] \tag{3.6}$$

$$\dot{x} = \left[Z\big|_{x_0,u_0}\right]^{-1}\underbrace{\left[\left.\frac{\partial f}{\partial x}\right|_{x_0,u_0}\right]}_{F_x}(x - x_o) + \left[Z\big|_{x_0,u_0}\right]^{-1}\underbrace{\left[\left.\frac{\partial f}{\partial u}\right|_{x_0,u_0}\right]}_{F_u}(u - u_o) \tag{3.7}$$

$$\dot{x} = Z^{-1}F_x\delta x + Z^{-1}F_u\delta u \tag{3.8}$$

$$\dot{x} = A\delta x + B\delta u \tag{3.9}$$

$$\begin{aligned}A &= Z^{-1}F_x \\ B &= Z^{-1}F_u\end{aligned} \tag{3.10}$$

The nonlinear output equations are denoted as Equation 3.11. The linearized version is then given as Equation 3.12, or in the standard form as Equation 3.13, using the substitutions in Equation 3.14.

$$y = g(x,u) \tag{3.11}$$

$$\delta y = G_x \delta x + G_u \delta u \tag{3.12}$$

$$\delta y = C \delta x + D \delta u \tag{3.13}$$

$$\begin{aligned} C &= G_x \\ D &= G_u \end{aligned} \tag{3.14}$$

3.2 FCV Evaporator/Condenser Model (using average properties)

As discussed earlier, both the evaporator and the condenser can be modeled as $Z(x,u)\cdot \dot{x} = f(x,u)$. The states are given in Equation 3.17 and the function $f(x,u)$ is defined in Equation 3.15. The model outputs are given as nonlinear function of states and inputs in Equation 3.16. The inputs to the model are defined in Equation 3.18.

$$f(x,u)=\begin{bmatrix} \dot{m}_{in}\left(h_{in}-h_1\right)+\alpha_{i,1}A_{i,1}\left(T_{w,1}-T_{r,1}\right) \\ \vdots \\ \dot{m}_{in}\left(h_{k-1}-h_k\right)+\alpha_{i,k}A_{i,k}\left(T_{w,k}-T_{r,k}\right) \\ \vdots \\ \dot{m}_{in}\left(h_{n-1}-h_{out}\right)+\alpha_{i,n}A_{i,n}\left(T_{w,n}-T_{r,n}\right) \\ \dot{m}_{in}-\dot{m}_{out} \\ \alpha_{i,1}A_{i,1}\left(T_{r,1}-T_{w,1}\right)+\alpha_{o}A_{o,1}\left(T_{a,1}-T_{w,1}\right) \\ \vdots \\ \alpha_{i,k}A_{i,k}\left(T_{r,k}-T_{w,k}\right)+\alpha_{o}A_{o,k}\left(T_{a,k}-T_{w,k}\right) \\ \vdots \\ \alpha_{i,n}A_{i,n}\left(T_{r,n}-T_{w,n}\right)+\alpha_{o}A_{o,n}\left(T_{a,n}-T_{w,n}\right) \end{bmatrix} \tag{3.15}$$

$$y=g(x,u)=\begin{bmatrix} P_e \\ h_{out} \\ T_{w,1} \\ \vdots \\ T_{w,k} \\ \vdots \\ T_{w,n} \\ T_{a,out} \\ T_{r,out} \\ m_{e,1} \\ \vdots \\ m_{e,k} \\ \vdots \\ m_{e,n} \end{bmatrix}=\begin{bmatrix} P_e \\ 2\begin{pmatrix} h_{e,n}-h_{e,n-1}+\cdots+(-1)^{n-k}h_{e,k} \\ +\cdots+(-1)^{n-1}h_{e,1} \end{pmatrix}+(-1)^n h_{in} \\ T_{w,1} \\ \vdots \\ T_{w,k} \\ \vdots \\ T_{w,n} \\ \frac{1}{n}\sum_{k=1}^{n}\left\{\left(T_{ao,k}-T_{a,in}\right)\right\}+T_{a,in} \\ T\left(P_e,h_{out}\right) \\ \rho_{e,1}\cdot V_{e,1} \\ \vdots \\ \rho_{e,k}\cdot V_{e,k} \\ \vdots \\ \rho_{e,n}\cdot V_{e,n} \end{bmatrix} \tag{3.16}$$

$$x=\begin{bmatrix} P_e & h_{e,1} & \dots & h_{e,k} & \dots & h_{e,n} & T_{w,1} & \dots & T_{w,k} & \dots & T_{w,n} \end{bmatrix}^T \tag{3.17}$$

$$u=\begin{bmatrix} \dot{m}_{in} & \dot{m}_{out} & h_{in} & T_{a,in} & \dot{m}_{air} \end{bmatrix}^T \tag{3.18}$$

The energy balance for the secondary fluid given a heat exchanger with n regions is given in Equation 3.19 where $T_{ao,k}$ is the outlet temperature of secondary fluid in the k^{th} control region. The average temperature of secondary fluid is assumed as a weighted average of inlet temperature and outlet temperature of the secondary fluid in the region being considered given in Equation 3.20. μ is the coefficient between 0 and 1 used for calculating the weighted average of temperature. Solving for the average temperature of secondary fluid, $T_{a,k}$ in the k^{th} control region is given by Equation 3.21. It can also be deduced that the overall outlet temperature of secondary fluid, $T_{a,out}$ is related with the outlet temperature of secondary fluid of each control region by Equation 3.22. Thus, the overall outlet temperature of secondary fluid can be calculated as given in Equation 3.23.

$$\dot{m}_{air} C_{p,air} (T_{a,in} - T_{ao,k}) = \alpha_{o,k} A_{o,k} (T_{a,k} - T_{w,k}) \quad (3.19)$$

$$T_{a,k} = \mu T_{a,in} + (1-\mu) T_{ao,k} \quad (3.20)$$

$$T_{a,k} = \frac{\left(\frac{T_{a,in}}{1-\mu}\right)\left(\frac{\dot{m}_{air} C_{p,air}}{\alpha_{o,k} A_{o,k}}\right) + T_{w,k}}{\left(\frac{1}{1-\mu}\right)\left(\frac{\dot{m}_{air} C_{p,air}}{\alpha_{o,k} A_{o,k}}\right) + 1} \quad (3.21)$$

$$\dot{m}_{air} C_{p,air} (T_{a,out} - T_{a,in}) = \sum_{k=1}^{n} \left\{ \frac{\dot{m}_{air}}{n} C_{p,air} \left(T_{ao,k} - T_{a,in}\right) \right\} \quad (3.22)$$

$$T_{a,out} = \frac{1}{n}\sum_{k=1}^{n}\left(T_{ao,k}\right) \quad (3.23)$$

For linearization, the partial derivatives of average temperature of secondary fluid are required. The partial derivatives of average temperature for the k^{th} control region are given in Equations 3.24 – 3.26. The secondary fluid side heat transfer coefficient is a function of mass flow rate of secondary fluid. Thus, the partial derivative of heat transfer coefficient can be calculated by calculating the slope of the heat transfer correlation at the initial equilibrium point.

$$\frac{\partial T_{a,k}}{\partial \dot{m}_{air}} = \frac{1}{\left(\left(\frac{1}{1-\mu}\right)\left(\frac{\dot{m}_{air}C_{p,air}}{\alpha_{o,k}A_{o,k}}\right)+1\right)^2}\left(\frac{C_{p,air}}{(1-\mu)\alpha_{o,k}A_{o,k}}\right)\left(1-\frac{\dot{m}_{air}}{\alpha_{o,k}}\frac{\partial \alpha_{o,k}}{\partial \dot{m}_{air}}\right)(T_{a,in}-T_{w,k}) \quad (3.24)$$

$$\frac{\partial T_{a,k}}{\partial T_{a,in}} = \frac{\dot{m}_{air}C_{p,air}}{(\dot{m}_{air}C_{p,air}+(1-\mu)\alpha_{o,k}A_{o,k})} \quad (3.25)$$

$$\frac{\partial T_{a,k}}{\partial T_{w,k}} = \frac{(1-\mu)\alpha_{o,k}A_{o,k}}{(\dot{m}_{air}C_{p,air}+(1-\mu)\alpha_{o,k}A_{o,k})} \quad (3.26)$$

The correlations mentioned in Equations 3.27 – 3.28 are also used. The refrigerant side heat transfer coefficient is a function of mass flow rate of refrigerant mass, heat exchanger pressure and enthalpy of the refrigerant. Thus, the partial derivatives of heat transfer coefficient can be calculated by calculating the slope of the heat transfer correlation at the initial equilibrium point.

$$h_j = 2\left(h_{e,j} - h_{e,j-1} + \cdots + (-1)^{j-k} h_{e,k} + \cdots + (-1)^{j-1} h_{e,1}\right) + (-1)^j h_{in} \qquad (3.27)$$

$$h_{j-1} - h_j = -2h_{e,j} + 4\left(h_{e,j-1} + \cdots + (-1)^{j-k-1} h_{e,k} + \cdots + (-1)^{j-2} h_{e,1}\right) + (-1)^{j-1} 2h_{in} \quad (3.28)$$

The partial derivatives of the functions $f(x,u)$ and $g(x,u)$ with respect to the states and inputs are defined in Equations 3.29 – 3.32 The matrix elements have been defined in Equations 3.33 – 3.60.

$$\frac{\partial f}{\partial x} = F_x = \begin{bmatrix} F_{x11} & F_{x12} & F_{x13} \\ 0 & 0 & 0 \\ F_{x31} & F_{x32} & F_{x33} \end{bmatrix}_{(2n+1)X(2n+1)} \qquad (3.29)$$

$$\frac{\partial f}{\partial u} = F_u = \begin{bmatrix} F_{u11} & 0 & F_{u13} & 0 & 0 \\ 1 & -1 & 0 & 0 & 0 \\ F_{u31} & 0 & 0 & F_{u34} & F_{u35} \end{bmatrix}_{(2n+1)X5} \qquad (3.30)$$

$$\frac{\partial g}{\partial x} = G_x = \begin{bmatrix} 1 & 0^{1Xn} & 0^{1Xn} \\ 0 & g_{x,22} & 0^{1Xn} \\ 0^{nX1} & 0^{nXn} & I^n \\ 0 & 0^{1Xn} & g_{x,43} \\ g_{x,51} & g_{x,52} & 0^{1Xn} \\ g_{x,61} & g_{x,62} & 0^{nXn} \end{bmatrix}_{(2n+4)X(2n+1)} \qquad (3.31)$$

$$\frac{\partial g}{\partial u} = G_u = \begin{bmatrix} 0 & 0 & 0 & 0 & 0 \\ 0 & 0 & g_{u,23} & 0 & 0 \\ 0^{nX1} & 0^{nX1} & 0^{nX1} & 0^{nX1} & 0^{nX1} \\ 0 & 0 & 0 & g_{u,44} & g_{u,45} \\ 0 & 0 & g_{u,53} & 0 & 0 \\ 0^{nX1} & 0^{nX1} & 0^{nX1} & 0^{nX1} & 0^{nX1} \end{bmatrix}_{(2n+4)X5} \qquad (3.32)$$

$$F_{x11} = \begin{bmatrix} -\alpha_{i,1} A_{i,1} \left.\frac{\partial T_{r,1}}{\partial P_e}\right|_{h_{e,1}} + \left.\frac{\partial \alpha_{i,1}}{\partial P_e}\right|_{h_{e,1},\dot{m}_{in}} A_{i,1}\left(T_{w,1} - T_{r,1}\right) \\ \vdots \\ -\alpha_{i,k} A_{i,k} \left.\frac{\partial T_{r,k}}{\partial P_e}\right|_{h_{e,k}} + \left.\frac{\partial \alpha_{i,k}}{\partial P_e}\right|_{h_{e,k},\dot{m}_{in}} A_{i,k}\left(T_{w,k} - T_{r,k}\right) \\ \vdots \\ -\alpha_{i,n} A_{i,n} \left.\frac{\partial T_{r,n}}{\partial P_e}\right|_{h_{e,n}} + \left.\frac{\partial \alpha_{i,n}}{\partial P_e}\right|_{h_{e,n},\dot{m}_{in}} A_{i,n}\left(T_{w,n} - T_{r,n}\right) \end{bmatrix}_{nX1} \tag{3.33}$$

$$F_{x12} = \begin{bmatrix} F_{x12}^{11} & 0 & \cdots & & 0 \\ \vdots & \ddots & & & \vdots \\ F_{x12}^{k1} & \cdots & F_{x12}^{k(k-1)} & F_{x12}^{kk} & 0 \\ \vdots & & \ddots & \ddots & \vdots \\ F_{x12}^{n1} & \cdots & & F_{x12}^{n(n-1)} & F_{x12}^{nn} \end{bmatrix}_{nXn} \tag{3.34}$$

$$F_{x12}^{11} = -2\dot{m}_{in} - \alpha_{i,1} A_{i,1} \left.\frac{\partial T_{r,1}}{\partial h_{e,1}}\right|_{P_e} \tag{3.35}$$

$$F_{x12}^{k1} = (-1)^k 4\dot{m}_{in} \tag{3.36}$$

$$F_{x12}^{k(k-1)} = (-1)^{k+j-1} 4\dot{m}_{in} \tag{3.37}$$

$$F_{x12}^{kk} = -2\dot{m}_{in} - \alpha_{i,k} A_{i,k} \left.\frac{\partial T_{r,k}}{\partial h_{e,k}}\right|_{P_e} \tag{3.38}$$

$$F_{x12}^{n1} = (-1)^n 4\dot{m}_{in} \tag{3.39}$$

$$F_{x12}^{n(n-1)} = (-1)^{n+j-1} 4\dot{m}_{in} \tag{3.40}$$

$$F_{x12}^{nn} = -2\dot{m}_{in} - \alpha_{i,n} A_{i,n} \left.\frac{\partial T_{r,n}}{\partial h_{e,n}}\right|_{P_e} \tag{3.41}$$

$$F_{x13} = diag\left\{\begin{bmatrix}\alpha_{i,1}A_{i,1} & \dots & \alpha_{i,k}A_{i,k} & \dots & \alpha_{i,n}A_{i,n}\end{bmatrix}\right\} \tag{3.42}$$

$$F_{x31} = \begin{bmatrix} \alpha_{i,1}A_{i,1}\left.\frac{\partial T_{r,1}}{\partial P_e}\right|_{h_{e,1}} + \left.\frac{\partial \alpha_{i,1}}{\partial P_e}\right|_{h_{e,1},\dot{m}_{in}} A_{i,1}\left(T_{r,1} - T_{w,1}\right) \\ \vdots \\ \alpha_{i,k}A_{i,k}\left.\frac{\partial T_{r,k}}{\partial P_e}\right|_{h_{e,k}} + \left.\frac{\partial \alpha_{i,k}}{\partial P_e}\right|_{h_{e,k},\dot{m}_{in}} A_{i,k}\left(T_{r,k} - T_{w,k}\right) \\ \vdots \\ \alpha_{i,n}A_{i,n}\left.\frac{\partial T_{r,n}}{\partial P_e}\right|_{h_{e,n}} + \left.\frac{\partial \alpha_{i,n}}{\partial P_e}\right|_{h_{e,n},\dot{m}_{in}} A_{i,n}\left(T_{r,n} - T_{w,n}\right) \end{bmatrix}_{nX1} \tag{3.43}$$

$$F_{x32} = diag\left\{\begin{bmatrix} \alpha_{i,1}A_{i,1}\left.\frac{\partial T_{r,1}}{\partial h_{e,1}}\right|_{P_e} - \left.\frac{\partial \alpha_{i,1}}{\partial h_{e,1}}\right|_{P_e,\dot{m}_{in}} A_{i,1}\left(T_{r,1} - T_{w,1}\right) \\ \vdots \\ \alpha_{i,k}A_{i,k}\left.\frac{\partial T_{r,k}}{\partial h_{e,k}}\right|_{P_e} - \left.\frac{\partial \alpha_{i,k}}{\partial h_{e,k}}\right|_{P_e,\dot{m}_{in}} A_{i,k}\left(T_{r,k} - T_{w,k}\right) \\ \vdots \\ \alpha_{i,n}A_{i,n}\left.\frac{\partial T_{r,n}}{\partial h_{e,n}}\right|_{P_e} - \left.\frac{\partial \alpha_{i,n}}{\partial h_{e,n}}\right|_{P_e,\dot{m}_{in}} A_{i,n}\left(T_{r,n} - T_{w,n}\right) \end{bmatrix}\right\} \tag{3.44}$$

$$F_{x33} = diag\left\{\begin{bmatrix} -\alpha_{i,1}A_{i,1} + \alpha_{o,1}A_{o,1}\left(\frac{\partial T_{a,1}}{\partial T_{w,1}} - 1\right) \\ \vdots \\ -\alpha_{i,k}A_{i,k} + \alpha_{o,k}A_{o,k}\left(\frac{\partial T_{a,k}}{\partial T_{w,k}} - 1\right) \\ \vdots \\ -\alpha_{i,n}A_{i,n} + \alpha_{o,n}A_{o,n}\left(\frac{\partial T_{a,n}}{\partial T_{w,n}} - 1\right) \end{bmatrix}\right\} \tag{3.45}$$

$$F_{u11}=\begin{bmatrix} h_{in}-h_1+\left.\dfrac{\partial\alpha_{i,1}}{\partial\dot{m}_{in}}\right|_{P_e,h_{e,1}} A_{i,1}\left(T_{w,1}-T_{r,1}\right) \\ \vdots \\ h_{k-1}-h_k+\left.\dfrac{\partial\alpha_{i,k}}{\partial\dot{m}_{in}}\right|_{P_e,h_{e,k}} A_{i,k}\left(T_{w,k}-T_{r,k}\right) \\ \vdots \\ h_{n-1}-h_{out}+\left.\dfrac{\partial\alpha_{i,n}}{\partial\dot{m}_{in}}\right|_{P_e,h_{e,n}} A_{i,n}\left(T_{w,n}-T_{r,n}\right) \end{bmatrix}_{nX1} \qquad (3.46)$$

$$F_{u13}=\begin{bmatrix} 2\dot{m}_{in} \\ \vdots \\ (-1)^{(k-1)}2\dot{m}_{in} \\ \vdots \\ (-1)^{(n-1)}2\dot{m}_{in} \end{bmatrix}_{nX1} \qquad (3.47)$$

$$F_{u31}=\begin{bmatrix} \left.\dfrac{\partial\alpha_{i,1}}{\partial\dot{m}_{in}}\right|_{P_e,h_{e,1}} A_{i,1}\left(T_{r,1}-T_{w,1}\right) \\ \vdots \\ \left.\dfrac{\partial\alpha_{i,k}}{\partial\dot{m}_{in}}\right|_{P_e,h_{e,k}} A_{i,k}\left(T_{r,k}-T_{w,k}\right) \\ \vdots \\ \left.\dfrac{\partial\alpha_{i,n}}{\partial\dot{m}_{in}}\right|_{P_e,h_{e,n}} A_{i,n}\left(T_{r,n}-T_{w,n}\right) \end{bmatrix}_{nX1} \qquad (3.48)$$

$$F_{u34}=\begin{bmatrix} \alpha_{o,1}A_{o,1}\dfrac{\partial T_{a,1}}{\partial T_{a,in}} \\ \vdots \\ \alpha_{o,k}A_{o,k}\dfrac{\partial T_{a,k}}{\partial T_{a,in}} \\ \vdots \\ \alpha_{o,n}A_{o,n}\dfrac{\partial T_{a,n}}{\partial T_{a,in}} \end{bmatrix}_{nX1} \qquad (3.49)$$

$$F_{u35} = \begin{bmatrix} \dfrac{\partial \alpha_{o,1}}{\partial \dot{m}_{air}} A_{o,1}(T_{a,1} - T_{w,1}) + \alpha_{o,1} A_{o,1} \dfrac{\partial T_{a,1}}{\partial \dot{m}_{air}} \\ \vdots \\ \dfrac{\partial \alpha_{o,k}}{\partial \dot{m}_{air}} A_{o,k}(T_{a,k} - T_{w,k}) + \alpha_{o,k} A_{o,k} \dfrac{\partial T_{a,k}}{\partial \dot{m}_{air}} \\ \vdots \\ \dfrac{\partial \alpha_{o,n}}{\partial \dot{m}_{air}} A_{o,n}(T_{a,n} - T_{w,n}) + \alpha_{o,n} A_{o,n} \dfrac{\partial T_{a,n}}{\partial \dot{m}_{air}} \end{bmatrix}_{nX1} \quad (3.50)$$

$$g_{x,22} = \begin{bmatrix} (-1)^{n-1}2 & \cdots & (-1)^{n-k}2 & \cdots & -2 & 2 \end{bmatrix}_{1Xn} \quad (3.51)$$

$$g_{x,43} = \begin{bmatrix} \dfrac{1}{n(1-\mu)} \dfrac{\partial T_{a,1}}{\partial T_{w,1}} & \cdots & \dfrac{1}{n(1-\mu)} \dfrac{\partial T_{a,k}}{\partial T_{w,k}} & \cdots & \dfrac{1}{n(1-\mu)} \dfrac{\partial T_{a,n}}{\partial T_{w,n}} \end{bmatrix}_{1Xn} \quad (3.52)$$

$$g_{x,51} = \left. \frac{\partial T_{r,out}}{\partial P_e} \right|_{h_{out}} \quad (3.53)$$

$$g_{x,52} = \begin{bmatrix} (-1)^{n-1}2\left(\left. \dfrac{\partial T_{r,out}}{\partial h_{out}} \right|_{P_e} \right) & \cdots & (-1)^{n-k}2\left(\left. \dfrac{\partial T_{r,out}}{\partial h_{out}} \right|_{P_e} \right) & \cdots & 2\left(\left. \dfrac{\partial T_{r,out}}{\partial h_{out}} \right|_{P_e} \right) \end{bmatrix}_{1Xn} \quad (3.54)$$

$$g_{x,61} = \begin{bmatrix} V_{e,1} \left. \dfrac{\partial \rho_{e,1}}{\partial P_e} \right|_{h_{e,1}} \\ \vdots \\ V_{e,k} \left. \dfrac{\partial \rho_{e,k}}{\partial P_e} \right|_{h_{e,k}} \\ \vdots \\ V_{e,n} \left. \dfrac{\partial \rho_{e,n}}{\partial P_e} \right|_{h_{e,n}} \end{bmatrix}_{nX1} \quad (3.55)$$

$$g_{x,62} = diag\left\{\left[V_{e,1}\left.\frac{\partial \rho_{e,1}}{\partial h_{e,1}}\right|_{P_e} \quad \cdots \quad V_{e,k}\left.\frac{\partial \rho_{e,k}}{\partial h_{e,k}}\right|_{P_e} \quad \cdots \quad V_{e,n}\left.\frac{\partial \rho_{e,n}}{\partial h_{e,n}}\right|_{P_e} \right]\right\} \qquad (3.56)$$

$$g_{u,23} = (-1)^n \qquad (3.57)$$

$$g_{u,44} = \frac{1}{n(1-\mu)}\left(\frac{\partial T_{a,1}}{\partial T_{a,in}} + \ldots + \frac{\partial T_{a,k}}{\partial T_{a,in}} + \ldots + \frac{\partial T_{a,n}}{\partial T_{a,in}} \right) - \frac{1}{(1-\mu)} + 1 \qquad (3.58)$$

$$g_{u,45} = \frac{1}{n(1-\mu)}\left(\frac{\partial T_{a,1}}{\partial \dot{m}_{air}} + \ldots + \frac{\partial T_{a,k}}{\partial \dot{m}_{air}} + \ldots + \frac{\partial T_{a,n}}{\partial \dot{m}_{air}} \right) \qquad (3.59)$$

$$g_{u,53} = (-1)^n \left.\frac{\partial T_{r,out}}{\partial h_{out}}\right|_{P_e} \qquad (3.60)$$

This model is not capable of capturing the system outputs due to induced transients such as a change in the valve opening or a change in the compressor speed. Even the slightest change in the input enthalpy instantaneously affects the output enthalpy of the refrigerant as they are tightly coupled together due to a strict mathematical relationship. The inlet and outlet enthalpies of the system are related through the average enthalpies of all the control regions as given by Equation 3.27.

3.3 FCV Evaporator/Condenser Model (using properties at outlet)

As discussed earlier, both the evaporator and the condenser can be modeled as $Z(x,u)\cdot \dot{x} = f(x,u)$. The states are given in Equation 3.63 and the function $f(x,u)$ is

defined in Equation 3.61. The model outputs are given as nonlinear function of states and inputs in Equation 3.62. The inputs to the model are defined in Equation 3.64.

$$f(x,u)=\begin{bmatrix} \dot{m}_{in}(h_{in}-h_1)+\alpha_{i,1}A_{i,1}(T_{w,1}-T_{r,1}) \\ \vdots \\ \dot{m}_{in}(h_{k-1}-h_k)+\alpha_{i,k}A_{i,k}(T_{w,k}-T_{r,k}) \\ \vdots \\ \dot{m}_{in}(h_{n-1}-h_{out})+\alpha_{i,n}A_{i,n}(T_{w,n}-T_{r,n}) \\ \dot{m}_{in}-\dot{m}_{out} \\ \alpha_{i,1}A_{i,1}(T_{r,1}-T_{w,1})+\alpha_o A_{o,1}(T_{a,1}-T_{w,1}) \\ \vdots \\ \alpha_{i,k}A_{i,k}(T_{r,k}-T_{w,k})+\alpha_o A_{o,k}(T_{a,k}-T_{w,k}) \\ \vdots \\ \alpha_{i,n}A_{i,n}(T_{r,n}-T_{w,n})+\alpha_o A_{o,n}(T_{a,n}-T_{w,n}) \end{bmatrix} \tag{3.61}$$

$$y=g(x,u)=\begin{bmatrix} P_e \\ h_{out} \\ T_{w,1} \\ \vdots \\ T_{w,k} \\ \vdots \\ T_{w,n} \\ T_{a,out} \\ T_{r,out} \\ m_{e,1} \\ \vdots \\ m_{e,k} \\ \vdots \\ m_{e,n} \end{bmatrix}=\begin{bmatrix} P_e \\ h_{e,n} \\ T_{w,1} \\ \vdots \\ T_{w,k} \\ \vdots \\ T_{w,n} \\ \frac{1}{n}\sum_{k=1}^{n}\{(T_{ao,k}-T_{a,in})\}+T_{a,in} \\ T(P_e,h_{out}) \\ \rho_{e,1}\cdot V_{e,1} \\ \vdots \\ \rho_{e,k}\cdot V_{e,k} \\ \vdots \\ \rho_{e,n}\cdot V_{e,n} \end{bmatrix} \tag{3.62}$$

$$x=\begin{bmatrix} P_e & h_{e,1} & \dots & h_{e,k} & \dots & h_{e,n} & T_{w,1} & \dots & T_{w,k} & \dots & T_{w,n} \end{bmatrix}^T \tag{3.63}$$

$$u = \begin{bmatrix} \dot{m}_{in} & \dot{m}_{out} & h_{in} & T_{a,in} & \dot{m}_{air} \end{bmatrix}^T \quad (3.64)$$

The energy balance for the secondary fluid given a heat exchanger with n regions is given in Equation 3.65 where $T_{ao,k}$ is the outlet temperature of secondary fluid in the k^{th} control region. The average temperature of secondary fluid is assumed as a weighted average of inlet temperature and outlet temperature of the secondary fluid in the region being considered given in Equation 3.66. μ is the coefficient between 0 and 1 used for calculating the weighted average of temperature. Solving for the average temperature of secondary fluid, $T_{a,k}$ in the k^{th} control region is given by Equation 3.67. It can also be deduced that the overall outlet temperature of secondary fluid, $T_{a,out}$ is related with the outlet temperature of secondary fluid of each control region by Equation 3.68. Thus, the overall outlet temperature of secondary fluid can be calculated as given in Equation 3.69.

$$\dot{m}_{air} C_{p,air} (T_{a,in} - T_{ao,k}) = \alpha_{o,k} A_{o,k} (T_{a,k} - T_{w,k}) \quad (3.65)$$

$$T_{a,k} = \mu T_{a,in} + (1-\mu) T_{ao,k} \quad (3.66)$$

$$T_{a,k} = \frac{\left(\frac{T_{a,in}}{1-\mu}\right)\left(\frac{\dot{m}_{air} C_{p,air}}{\alpha_{o,k} A_{o,k}}\right) + T_{w,k}}{\left(\frac{1}{1-\mu}\right)\left(\frac{\dot{m}_{air} C_{p,air}}{\alpha_{o,k} A_{o,k}}\right) + 1} \quad (3.67)$$

$$\dot{m}_{air} C_{p,air} (T_{a,out} - T_{a,in}) = \sum_{k=1}^{n} \left\{ \frac{\dot{m}_{air}}{n} C_{p,air} \left(T_{ao,k} - T_{a,in} \right) \right\} \quad (3.68)$$

$$T_{a,out} = \frac{1}{n} \sum_{k=1}^{n} \left(T_{ao,k} \right) \quad (3.69)$$

For linearization, the partial derivatives of average temperature of secondary fluid are required. The partial derivatives of average temperature for the k^{th} control region are given in Equations 3.70 – 3.72. The secondary fluid side heat transfer coefficient is a function of mass flow rate of secondary fluid. Thus, the partial derivative of heat transfer coefficient can be calculated by calculating the slope of the heat transfer correlation at the initial equilibrium point.

$$\frac{\partial T_{a,k}}{\partial \dot{m}_{air}} = \frac{1}{\left(\left(\frac{1}{1-\mu} \right) \left(\frac{\dot{m}_{air} C_{p,air}}{\alpha_{o,k} A_{o,k}} \right) + 1 \right)^2} \left(\frac{C_{p,air}}{(1-\mu)\alpha_{o,k} A_{o,k}} \right) \left(1 - \frac{\dot{m}_{air}}{\alpha_{o,k}} \frac{\partial \alpha_{o,k}}{\partial \dot{m}_{air}} \right) (T_{a,in} - T_{w,k}) \quad (3.70)$$

$$\frac{\partial T_{a,k}}{\partial T_{a,in}} = \frac{\dot{m}_{air} C_{p,air}}{(\dot{m}_{air} C_{p,air} + (1-\mu)\alpha_{o,k} A_{o,k})} \quad (3.71)$$

$$\frac{\partial T_{a,k}}{\partial T_{w,k}} = \frac{(1-\mu)\alpha_{o,k} A_{o,k}}{(\dot{m}_{air} C_{p,air} + (1-\mu)\alpha_{o,k} A_{o,k})} \quad (3.72)$$

The refrigerant side heat transfer coefficient is a function of mass flow rate of refrigerant mass, heat exchanger pressure and enthalpy of the refrigerant. Thus, the partial derivatives of heat transfer coefficient can be calculated by calculating the slope

of the heat transfer correlation at the initial equilibrium point. The partial derivatives of the functions $f(x,u)$ and $g(x,u)$ with respect to the states and inputs are defined in Equations 3.73 – 3.76 The matrix elements have been defined in Equations 3.77 – 3.100.

$$\frac{\partial f}{\partial x} = F_x = \begin{bmatrix} F_{x11} & F_{x12} & F_{x13} \\ 0 & 0 & 0 \\ F_{x31} & F_{x32} & F_{x33} \end{bmatrix}_{(2n+1)X(2n+1)} \tag{3.73}$$

$$\frac{\partial f}{\partial u} = F_u = \begin{bmatrix} F_{u11} & 0 & F_{u13} & 0 & 0 \\ 1 & -1 & 0 & 0 & 0 \\ F_{u31} & 0 & 0 & F_{u34} & F_{u35} \end{bmatrix}_{(2n+1)X5} \tag{3.74}$$

$$\frac{\partial g}{\partial x} = G_x = \begin{bmatrix} 1 & 0^{1Xn} & 0^{1Xn} \\ 0 & g_{x,22} & 0^{1Xn} \\ 0^{nX1} & 0^{nXn} & I^n \\ 0 & 0^{1Xn} & g_{x,43} \\ g_{x,51} & g_{x,52} & 0^{1Xn} \\ g_{x,61} & g_{x,62} & 0^{nXn} \end{bmatrix}_{(2n+4)X(2n+1)} \tag{3.75}$$

$$\frac{\partial g}{\partial u} = G_u = \begin{bmatrix} 0 & 0 & 0 & 0 & 0 \\ 0 & 0 & g_{u,23} & 0 & 0 \\ 0^{nX1} & 0^{nX1} & 0^{nX1} & 0^{nX1} & 0^{nX1} \\ 0 & 0 & 0 & g_{u,44} & g_{u,45} \\ 0 & 0 & g_{u,53} & 0 & 0 \\ 0^{nX1} & 0^{nX1} & 0^{nX1} & 0^{nX1} & 0^{nX1} \end{bmatrix}_{(2n+4)X5} \tag{3.76}$$

$$F_{x11}=\begin{bmatrix} -\alpha_{i,1}A_{i,1}\left.\frac{\partial T_{r,1}}{\partial P_e}\right|_{h_{e,1}}+\left.\frac{\partial \alpha_{i,1}}{\partial P_e}\right|_{h_{e,1},\dot{m}_{in}} A_{i,1}\left(T_{w,1}-T_{r,1}\right) \\ \vdots \\ -\alpha_{i,k}A_{i,k}\left.\frac{\partial T_{r,k}}{\partial P_e}\right|_{h_{e,k}}+\left.\frac{\partial \alpha_{i,k}}{\partial P_e}\right|_{h_{e,k},\dot{m}_{in}} A_{i,k}\left(T_{w,k}-T_{r,k}\right) \\ \vdots \\ -\alpha_{i,n}A_{i,n}\left.\frac{\partial T_{r,n}}{\partial P_e}\right|_{h_{e,n}}+\left.\frac{\partial \alpha_{i,n}}{\partial P_e}\right|_{h_{e,n},\dot{m}_{in}} A_{i,n}\left(T_{w,n}-T_{r,n}\right) \end{bmatrix}_{nX1} \quad (3.77)$$

$$F_{x12}=\begin{bmatrix} F_{x12}^{11} & 0 & \cdots & 0 & \cdots & & 0 \\ & & \ddots & \ddots & & & \vdots \\ 0 & \cdots & 0 & F_{x12}^{k(k-1)} & F_{x12}^{kk} & 0 & 0 \\ & & & & \ddots & \ddots & \vdots \\ 0 & & \cdots & & 0 & F_{x12}^{n(n-1)} & F_{x12}^{nn} \end{bmatrix}_{nXn} \quad (3.78)$$

$$F_{x12}^{11}=-\dot{m}_{in}-\alpha_{i,1}A_{i,1}\left.\frac{\partial T_{r,1}}{\partial h_{e,1}}\right|_{P_e}-\left.\frac{\partial \alpha_{i,1}}{\partial h_{e,1}}\right|_{P_e,\dot{m}_{in}} A_{i,1}\left(T_{r,1}-T_{w,1}\right) \quad (3.79)$$

$$F_{x12}^{k(k-1)}=\dot{m}_{in} \quad (3.80)$$

$$F_{x12}^{kk}=-\dot{m}_{in}-\alpha_{i,k}A_{i,k}\left.\frac{\partial T_{r,k}}{\partial h_{e,k}}\right|_{P_e}-\left.\frac{\partial \alpha_{i,k}}{\partial h_{e,k}}\right|_{P_e,\dot{m}_{in}} A_{i,k}\left(T_{r,k}-T_{w,k}\right) \quad (3.81)$$

$$F_{x12}^{n(n-1)}=\dot{m}_{in} \quad (3.82)$$

$$F_{x12}^{nn}=-\dot{m}_{in}-\alpha_{i,n}A_{i,n}\left.\frac{\partial T_{r,n}}{\partial h_{e,n}}\right|_{P_e}-\left.\frac{\partial \alpha_{i,n}}{\partial h_{e,n}}\right|_{P_e,\dot{m}_{in}} A_{i,n}\left(T_{r,n}-T_{w,n}\right) \quad (3.83)$$

$$F_{x13}=diag\left\{\begin{bmatrix}\alpha_{i,1}A_{i,1} & \ldots & \alpha_{i,k}A_{i,k} & \ldots & \alpha_{i,n}A_{i,n}\end{bmatrix}\right\} \quad (3.84)$$

$$F_{x31} = \begin{bmatrix} \alpha_{i,1}A_{i,1}\left.\frac{\partial T_{r,1}}{\partial P_e}\right|_{h_{e,1}} + \left.\frac{\partial \alpha_{i,1}}{\partial P_e}\right|_{h_{e,1},\dot{m}_{in}} A_{i,1}\left(T_{r,1} - T_{w,1}\right) \\ \vdots \\ \alpha_{i,k}A_{i,k}\left.\frac{\partial T_{r,k}}{\partial P_e}\right|_{h_{e,k}} + \left.\frac{\partial \alpha_{i,k}}{\partial P_e}\right|_{h_{e,k},\dot{m}_{in}} A_{i,k}\left(T_{r,k} - T_{w,k}\right) \\ \vdots \\ \alpha_{i,n}A_{i,n}\left.\frac{\partial T_{r,n}}{\partial P_e}\right|_{h_{e,n}} + \left.\frac{\partial \alpha_{i,n}}{\partial P_e}\right|_{h_{e,n},\dot{m}_{in}} A_{i,n}\left(T_{r,n} - T_{w,n}\right) \end{bmatrix}_{nX1} \quad (3.85)$$

$$F_{x32} = diag\left\{\begin{bmatrix} \alpha_{i,1}A_{i,1}\left.\frac{\partial T_{r,1}}{\partial h_{e,1}}\right|_{P_e} - \left.\frac{\partial \alpha_{i,1}}{\partial h_{e,1}}\right|_{P_e,\dot{m}_{in}} A_{i,1}\left(T_{r,1} - T_{w,1}\right) \\ \vdots \\ \alpha_{i,k}A_{i,k}\left.\frac{\partial T_{r,k}}{\partial h_{e,k}}\right|_{P_e} - \left.\frac{\partial \alpha_{i,k}}{\partial h_{e,k}}\right|_{P_e,\dot{m}_{in}} A_{i,k}\left(T_{r,k} - T_{w,k}\right) \\ \vdots \\ \alpha_{i,n}A_{i,n}\left.\frac{\partial T_{r,n}}{\partial h_{e,n}}\right|_{P_e} - \left.\frac{\partial \alpha_{i,n}}{\partial h_{e,n}}\right|_{P_e,\dot{m}_{in}} A_{i,n}\left(T_{r,n} - T_{w,n}\right) \end{bmatrix}\right\} \quad (3.86)$$

$$F_{x33} = diag\left\{\begin{bmatrix} -\alpha_{i,1}A_{i,1} + \alpha_{o,1}A_{o,1}\left(\frac{\partial T_{a,1}}{\partial T_{w,1}} - 1\right) \\ \vdots \\ -\alpha_{i,k}A_{i,k} + \alpha_{o,k}A_{o,k}\left(\frac{\partial T_{a,k}}{\partial T_{w,k}} - 1\right) \\ \vdots \\ -\alpha_{i,n}A_{i,n} + \alpha_{o,n}A_{o,n}\left(\frac{\partial T_{a,n}}{\partial T_{w,n}} - 1\right) \end{bmatrix}\right\} \quad (3.87)$$

$$F_{u11}=\begin{bmatrix} h_{in}-h_1+\left.\dfrac{\partial\alpha_{i,1}}{\partial\dot{m}_{in}}\right|_{P_e,h_{e,1}} A_{i,1}\left(T_{w,1}-T_{r,1}\right) \\ \vdots \\ h_{k-1}-h_k+\left.\dfrac{\partial\alpha_{i,k}}{\partial\dot{m}_{in}}\right|_{P_e,h_{e,k}} A_{i,k}\left(T_{w,k}-T_{r,k}\right) \\ \vdots \\ h_{n-1}-h_{out}+\left.\dfrac{\partial\alpha_{i,n}}{\partial\dot{m}_{in}}\right|_{P_e,h_{e,n}} A_{i,n}\left(T_{w,n}-T_{r,n}\right) \end{bmatrix}_{nX1} \tag{3.88}$$

$$F_{u13}=\begin{bmatrix} \dot{m}_{in} \\ 0 \\ \vdots \\ \vdots \\ 0 \end{bmatrix}_{nX1} \tag{3.89}$$

$$F_{u31}=\begin{bmatrix} \left.\dfrac{\partial\alpha_{i,1}}{\partial\dot{m}_{in}}\right|_{P_e,h_{e,1}} A_{i,1}\left(T_{r,1}-T_{w,1}\right) \\ \vdots \\ \left.\dfrac{\partial\alpha_{i,k}}{\partial\dot{m}_{in}}\right|_{P_e,h_{e,k}} A_{i,k}\left(T_{r,k}-T_{w,k}\right) \\ \vdots \\ \left.\dfrac{\partial\alpha_{i,n}}{\partial\dot{m}_{in}}\right|_{P_e,h_{e,n}} A_{i,n}\left(T_{r,n}-T_{w,n}\right) \end{bmatrix}_{nX1} \tag{3.90}$$

$$F_{u34}=\begin{bmatrix} \alpha_{o,1}A_{o,1}\dfrac{\partial T_{a,1}}{\partial T_{a,in}} \\ \vdots \\ \alpha_{o,k}A_{o,k}\dfrac{\partial T_{a,k}}{\partial T_{a,in}} \\ \vdots \\ \alpha_{o,n}A_{o,n}\dfrac{\partial T_{a,n}}{\partial T_{a,in}} \end{bmatrix}_{nX1} \tag{3.91}$$

$$F_{u35} = \begin{bmatrix} \dfrac{\partial \alpha_{o,1}}{\partial \dot{m}_{air}} A_{o,1}(T_{a,1} - T_{w,1}) + \alpha_{o,1} A_{o,1} \dfrac{\partial T_{a,1}}{\partial \dot{m}_{air}} \\ \vdots \\ \dfrac{\partial \alpha_{o,k}}{\partial \dot{m}_{air}} A_{o,k}(T_{a,k} - T_{w,k}) + \alpha_{o,k} A_{o,k} \dfrac{\partial T_{a,k}}{\partial \dot{m}_{air}} \\ \vdots \\ \dfrac{\partial \alpha_{o,n}}{\partial \dot{m}_{air}} A_{o,n}(T_{a,n} - T_{w,n}) + \alpha_{o,n} A_{o,n} \dfrac{\partial T_{a,n}}{\partial \dot{m}_{air}} \end{bmatrix}_{nX1} \quad (3.92)$$

$$g_{x,22} = \begin{bmatrix} 0 & \cdots & 0 & 1 \end{bmatrix}_{1Xn} \quad (3.93)$$

$$g_{x,43} = \begin{bmatrix} \dfrac{1}{n(1-\mu)} \dfrac{\partial T_{a,1}}{\partial T_{w,1}} & \cdots & \dfrac{1}{n(1-\mu)} \dfrac{\partial T_{a,k}}{\partial T_{w,k}} & \cdots & \dfrac{1}{n(1-\mu)} \dfrac{\partial T_{a,n}}{\partial T_{w,n}} \end{bmatrix}_{1Xn} \quad (3.94)$$

$$g_{x,51} = \left. \frac{\partial T_{r,out}}{\partial P_e} \right|_{h_{out}} \quad (3.95)$$

$$g_{x,52} = \begin{bmatrix} 0 & \cdots & 0 & \left(\left. \dfrac{\partial T_{r,out}}{\partial h_{out}} \right|_{P_e} \right) \end{bmatrix}_{1Xn} \quad (3.96)$$

$$g_{x,61} = \begin{bmatrix} V_{e,1} \left. \dfrac{\partial \rho_{e,1}}{\partial P_e} \right|_{h_{e,1}} \\ \vdots \\ V_{e,k} \left. \dfrac{\partial \rho_{e,k}}{\partial P_e} \right|_{h_{e,k}} \\ \vdots \\ V_{e,n} \left. \dfrac{\partial \rho_{e,n}}{\partial P_e} \right|_{h_{e,n}} \end{bmatrix}_{nX1} \quad (3.97)$$

$$g_{x,62} = diag\left\{\left[V_{e,1}\left.\frac{\partial \rho_{e,1}}{\partial h_{e,1}}\right|_{P_e} \quad \cdots \quad V_{e,k}\left.\frac{\partial \rho_{e,k}}{\partial h_{e,k}}\right|_{P_e} \quad \cdots \quad V_{e,n}\left.\frac{\partial \rho_{e,n}}{\partial h_{e,n}}\right|_{P_e} \right]\right\} \qquad (3.98)$$

$$g_{u,44} = \frac{1}{n(1-\mu)}\left(\frac{\partial T_{a,1}}{\partial T_{a,in}} + \ldots + \frac{\partial T_{a,k}}{\partial T_{a,in}} + \ldots + \frac{\partial T_{a,n}}{\partial T_{a,in}}\right) - \frac{1}{(1-\mu)} + 1 \qquad (3.99)$$

$$g_{u,45} = \frac{1}{n(1-\mu)}\left(\frac{\partial T_{a,1}}{\partial \dot{m}_{air}} + \ldots + \frac{\partial T_{a,k}}{\partial \dot{m}_{air}} + \ldots + \frac{\partial T_{a,n}}{\partial \dot{m}_{air}}\right) \qquad (3.100)$$

CHAPTER 4

EXPERIMENTAL SETUP

This chapter discusses the experimental equipment and the testing procedure for generating and acquiring the data. The results are used for validating the nonlinear as well as linearized models discussed in Chapters 2 and 3. The validation procedure has been addressed in Chapter 6.

4.1 Test Facility

4.1.1 System Description

The test facility is located at the Thermo-Fluids Control Laboratory at Texas A&M University at College Station, TX. The experimental system has been designed to emulate heat exchange in a vapor compression cycle. The system components have been fabricated to drive R134a (1,1,1,2 - Tetrafluoroethane) as the refrigerant and water as the secondary fluid. Diagrams of the experimental system for the primary loop and the secondary loop have been depicted in Figure 4.1 and Figure 4.2 respectively.

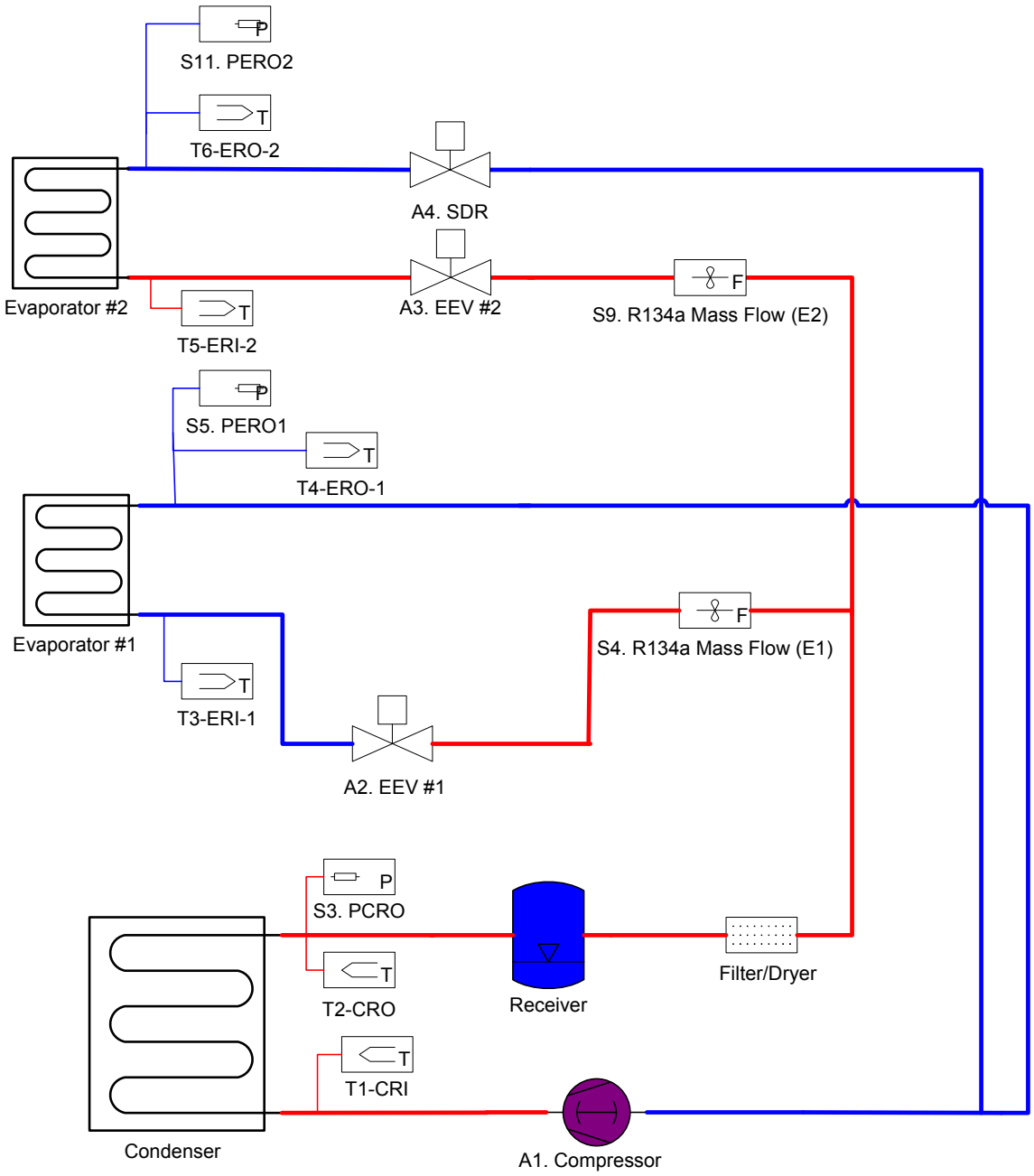

Figure 4.1: Experimental System Schematic for the Primary Loop

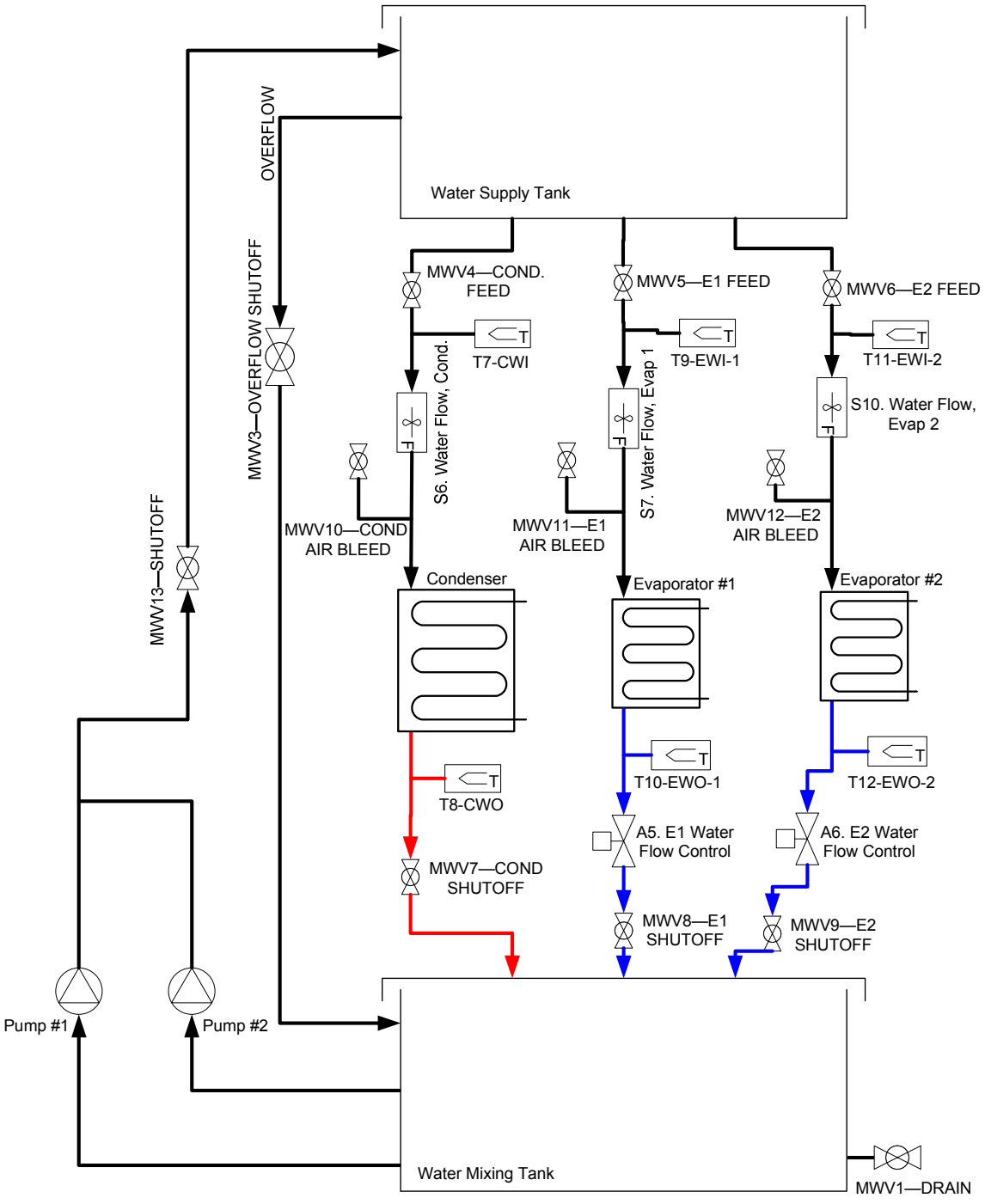

Figure 4.2: Experimental System Schematic for the Secondary Loop

In Figure 4.1, beginning at the compressor (Figure 4.3), the pressurized fluid (typically vapor) flows into the condenser. The condenser consists of a copper tube coiled around a plastic core such that water can flow between the coil and the core. It has been enclosed in a PVC pipe with openings for inlet and outlet of water as shown in Figure 4.4. The refrigerant rejects heat to water inside the condenser. The condensed fluid flows into the receiver shown in Figure 4.5. The receiver consists of a pressure vessel such that only liquid refrigerant is withdrawn from it. The fluid is then made to pass through a filter dryer shown in Figure 4.6 to make sure there are no remaining vapors. To ensure proper functioning of the expansion valve only liquid refrigerant should enter the valve. Trapped vapor in the valve opening will reduce the true area available for fluid flow.

Figure 4.3: Compressor

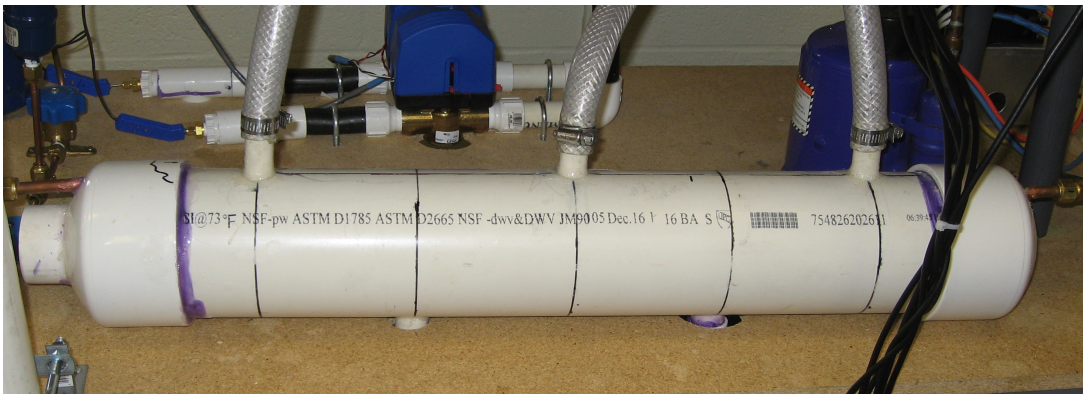

Figure 4.4: Condenser

Figure 4.5: Receiver

Figure 4.6: Filter Dryer

The system contains two evaporators. The fluid flow lines are split into two before the fluid enters the electronic expansion valves (EEV) as shown in Figure 4.**7**. One EEV is placed in both lines before the fluid enters an evaporator in each line. The refrigerant absorbs heat inside an evaporator. Each evaporator consists of a straight copper tube enclosed in a PVC pipe with openings for inlet and outlet of water as shown in Figure 4.8. The fluid from one of the evaporators passes through another valve. The fluid (typically superheated vapor) exiting the two evaporators is intermixed as the fluid flow lines combine before entering the compressor and thus, completing the loop. By shutting one of the valves completely, the system can be operated utilizing only one evaporator.

Figure 4.7: Electronic Expansion Valve

Figure 4.8: Evaporators

The secondary fluid (water) is fed into the heat exchangers using gravity. As shown in Figure 4.2, a water supply tank is placed above the whole system. The water flows through all the heat exchangers outside the copper tube and inside the PVC pipes before it is collected in a common mixing tank at the bottom of the system. The water flow through the different heat exchangers can be regulated using the manual flow valves placed in each pipeline. The water collected in the mixing tank is pumped up into the water supply tank. There is an overflow line from the supply tank to the mixing tank in case the discharge from the pumps is greater than the water withdrawn from the supply tank. Table 4.1 lists the physical parameters of the system. The parameters have either been measured or calculated based on information provided by the manufacturer. A photograph of the complete setup is shown in Figure 4.9.

Table 4.1 Experimental System Parameters

Evaporator	
Mass [kg]	0.408
Specific Heat of Copper [$kJkg^{-1}K^{-1}$]	0.385
External Surface Area [m^2]	0.04
Internal Surface Area [m^2]	0.032
Cross-Sectional Area [m^2]	8.39e-5
Frontal Area [m^2]	0.013
Length [m]	1
Diameter [m]	0.01
Condenser	
Mass [kg]	1.493
Specific Heat of Copper [$kJkg^{-1}K^{-1}$]	0.385
External Surface Area [m^2]	0.25
Internal Surface Area [m^2]	0.207
Cross-Sectional Area [m^2]	4.87e-5
Frontal Area [m^2]	0.052
Length [m]	8.36
Diameter [m]	0.008
Compressor	
Volume [m^3]	3.04e-5
Receiver	
Volume [m^3]	0.001

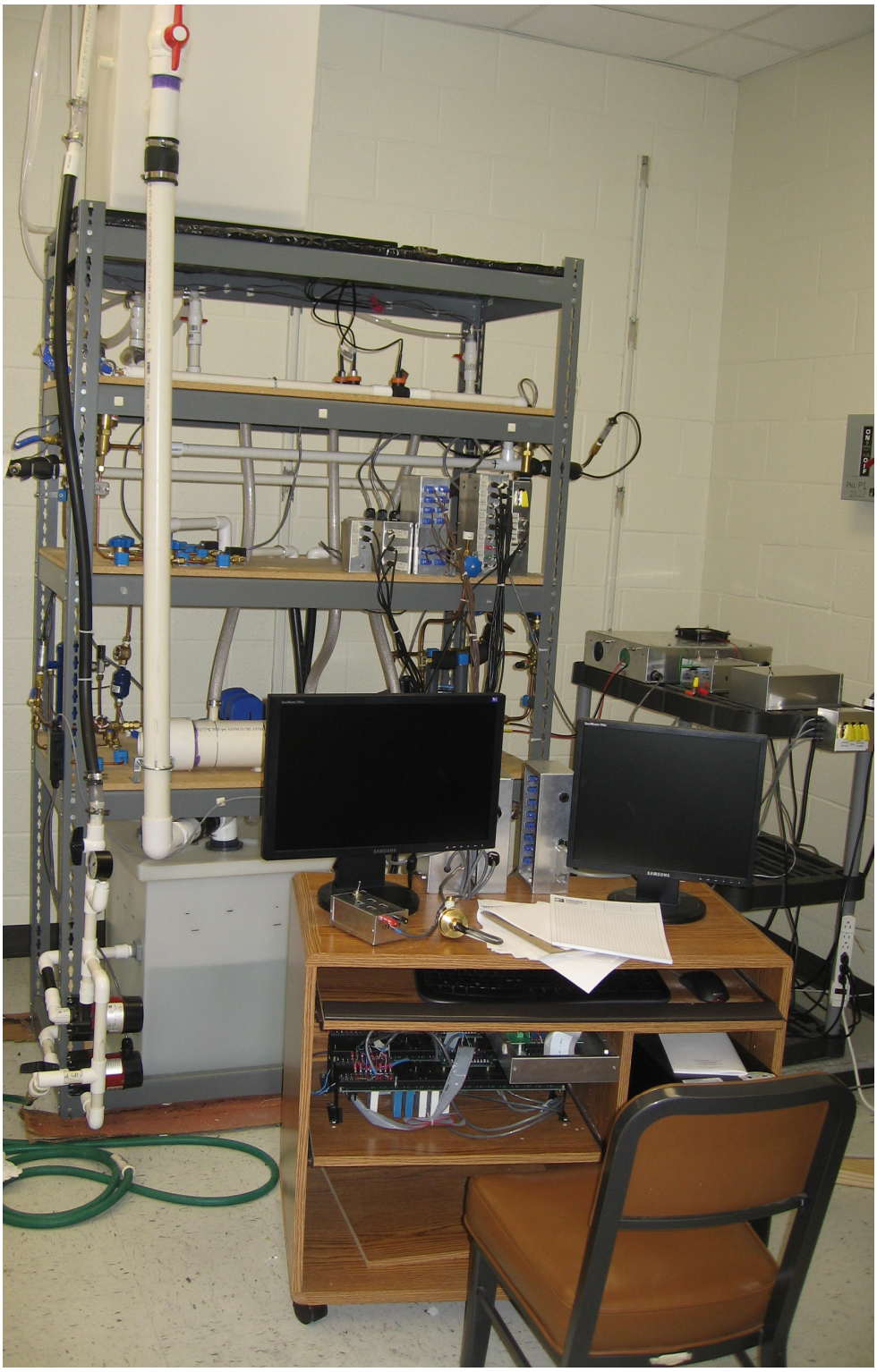

Figure 4.9: Complete Experimental Setup

4.1.2 Sensors and Actuators

This section discusses the important sensors and actuators used in the experimental system. Different thermocouples, pressure transducers and mass flow meters have been used along the fluid flow paths as depicted in Figure 4.1 and Figure 4.2.

The pressure transducers used for refrigerant measurements were manufactured by Cole-Parmer® (part 07356 - 04). They have a range of 0 – 300 psig with an accuracy of ±0.4%. Thermocouples used for temperature measurements have a range of -270 °C to 400 °C. They were manufactured by Omega® (part GTMQSS-062U-6). The thermocouples have an accuracy of ±1 °C. The mass flow sensor for measuring the mass flow rate of the refrigerant was manufactured by Mc Millan® (Model 102 Liquid Flo-Sensor) which has a range of 50 – 500 mL/min with an accuracy of ±3%. The mass flow sensor for measuring the mass flow rate of water was manufactured by KOBOLD Instruments Inc.® (Model DRS-0350 K0000) which has a range of 2 – 50 l/min with an accuracy of ±1.5%. Photographs of the sensors are shown in Figure 4.10 – Figure 4.13.

A scroll compressor manufactured by MasterFlux® (part Sierra 03-0982Y3) was used. The speed range of the compressor is from 1800 – 6500 RPM. It has been shown in Figure 4.1. Electronic expansion valves manufactured by Sporlan® (part SEI 0.5) as shown in Figure 4.**7** were used. The operation of the valve is through a stepper motor consisting of 6386 steps. The valves can be safely operated up to 620 psig in an

operating temperature range between -45 °C to 60 °C. The flow rate of water flowing in the system could also be regulated using flow control valve Erie® (part AP23A000) but it was kept constant during the experiments.

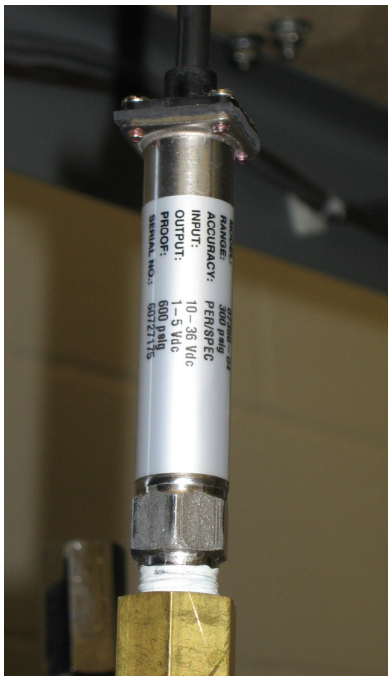

Figure 4.10: Pressure Gauge

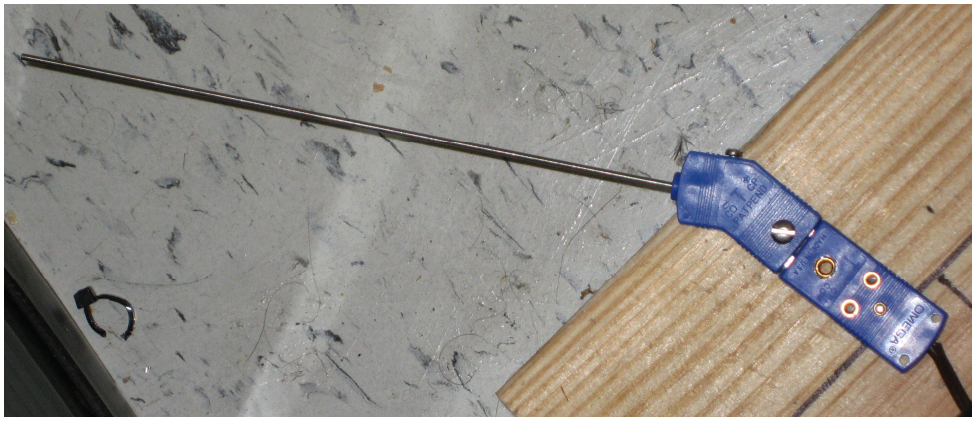

Figure 4.11: Thermocouple

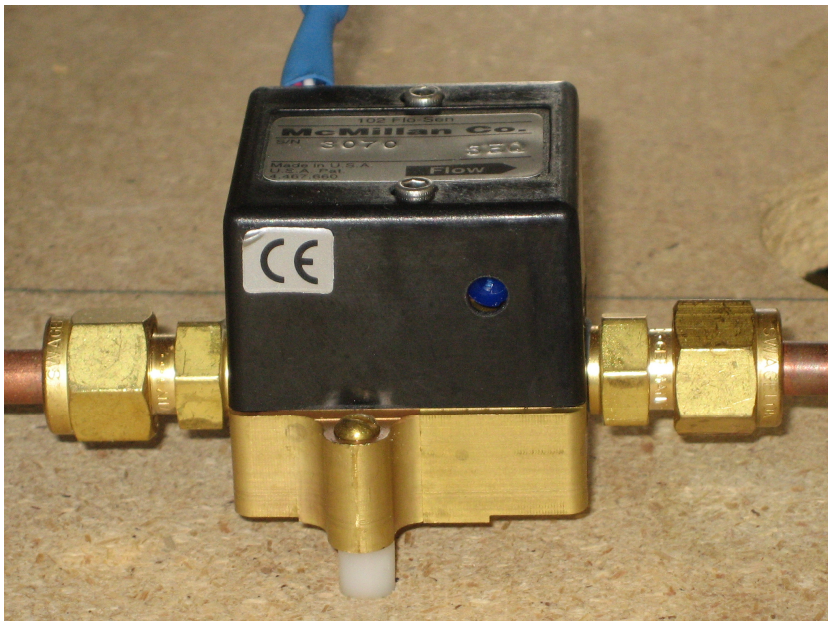

Figure 4.12: Mass Flow Sensor for Refrigerant

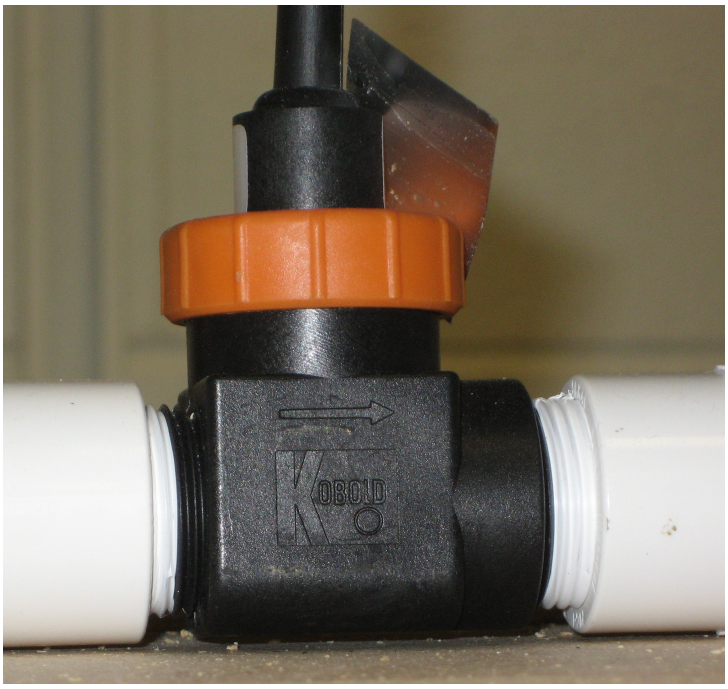

Figure 4.13: Mass Flow Sensor for Secondary Fluid (water)

Chapter 5

SIMULATION SOFTWARE: THERMOSYS™ ACADEMIC

This chapter describes a set of simulation tools developed for the purposes of model validation, analysis, and controller design. This library was developed for use with MatLab® and its associated simulation program Simulink®. At the time of publication of this document, this software was entitled "Thermosys™ Academic".

5.1 Introduction to Thermosys Academic

Creation of Thermosys Academic was initiated to provide a graphic drag-and-drop interface for the user to utilize the mathematical modeling of vapor compression components. The user can utilize the toolbox to predict the steady state as well as dynamic behavior of a real complex system. The user is required to connect the inputs and outputs to each component appropriately to represent the system. The toolbox also provides a platform to validate new models as it can be used to compare the simulated outputs with experimental data. The first version of this software was called Thermosys Toolbox. Further details regarding the first version of the toolbox can be found in [5,22,23].

Thermosys Academic has been designed with an open architecture where a user can customize the existing components according to his preferences or add new ones. The framework of the software has been designed in MatLab while Simulink is used to

solve the dynamics associated with the models. A basic skeleton of the static and dynamic models has been created in Simulink. The models can be appropriately renamed, using the Graphical User Interface (GUI), to provide the functioning of the required component. The names of the components available in the Thermosys library conform to a pre-defined naming convention, as discussed in subsequent sections.

5.2 Thermosys under New Setup

Due to some fundamental problems that were associated with the original design of the Thermosys toolbox, it was decided to shift to the new Thermosys™ Academic. By using the Thermosys under the new setup, it is much easier to customize the existing models available in the Thermosys library as well as add new models to the library. The basic structure of the Thermosys components has been described in this section.

5.2.1 Thermosys Academic Simulink Blocks

Several tools required to simulate the proper functioning of a vapor compression system are available in the Thermosys library. The tools can be accessed using the Simulink Library browser under Thermosys as shown in Figure 5.1. The tools are organized into two directories: Components and Fluid Properties. Three types of components are available in Thermosys: Dynamic model, Static model and Static model with transport delay. Any of these components can be dragged in a Simulink model to

simulate the functioning of the appropriate component. These are generic blocks and can morph into the appropriate component as chosen by the user, to simulate the real component. The models of different components are categorized into one of the three types based on its nature. All the variations of evaporator, condenser and compressor models are dynamics models, for example evaporator with receiver model. The expansion valve is a static model while all the pipe models are static models with transport delay. The user needs to rename the appropriate generic blocks into component models which are required. An exhaustive list of available components can be found at [4]. The next section discusses the dynamic model block. The other two static model blocks are used in the same manner as the dynamic model block.

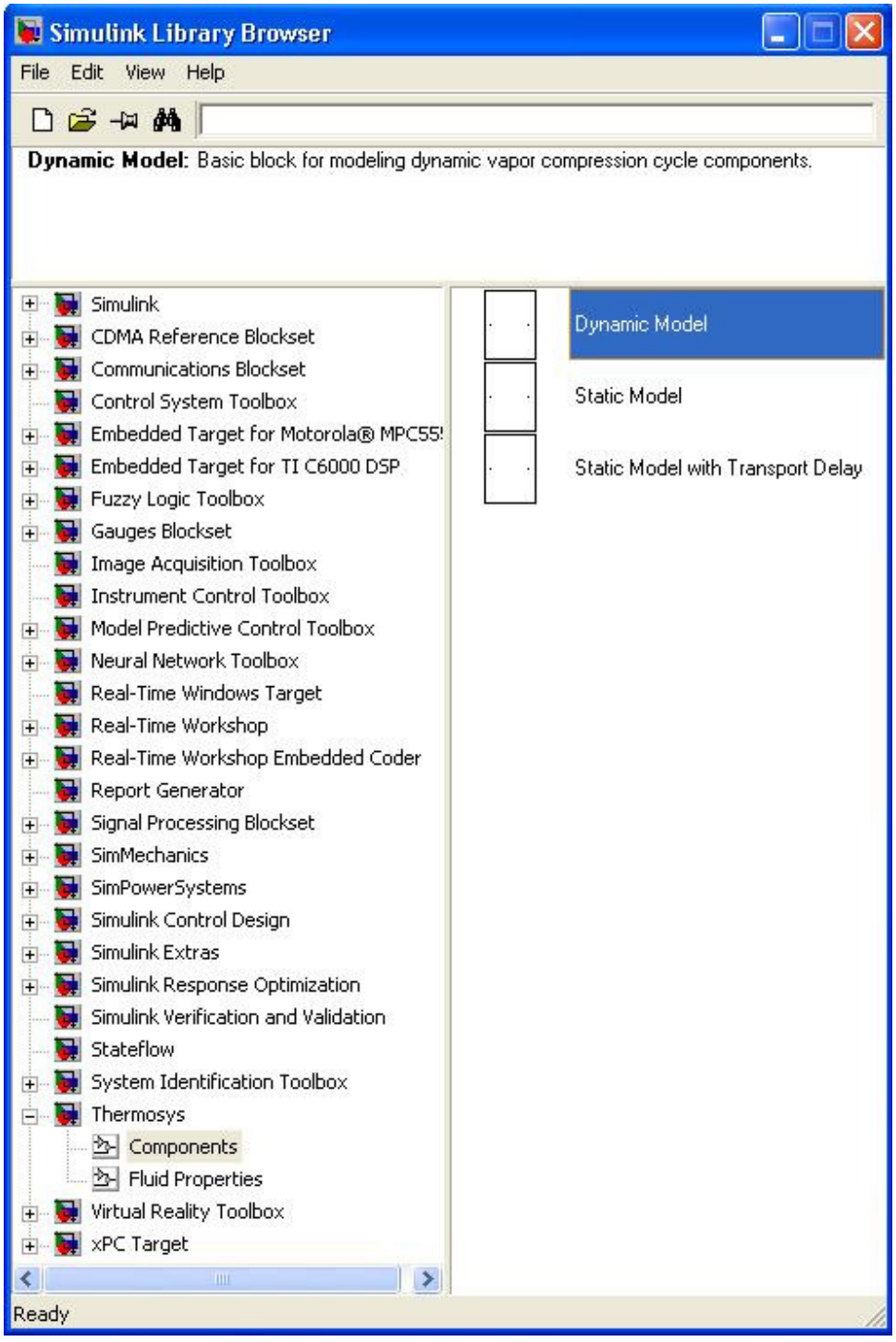

Figure 5.1: Simulink Library Browser

5.2.1.1 Dynamic Model Block

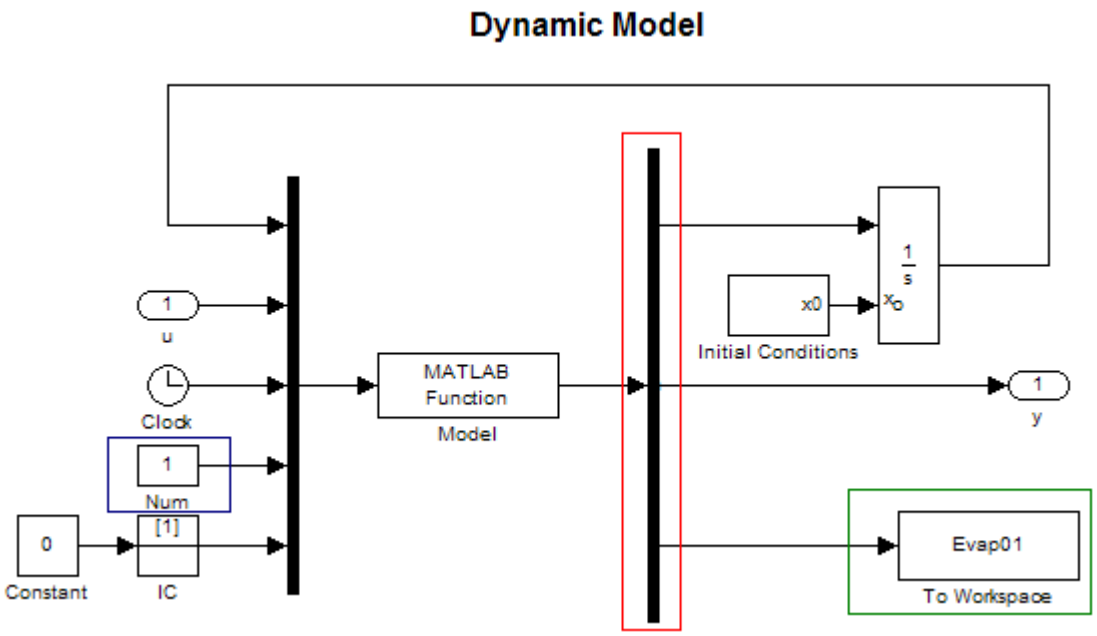

Figure 5.2: Basic dynamic model layout for Thermosys Academic

As mentioned previously, the dynamic model block in the Thermosys Academic library is utilized for simulating a dynamic component such as an evaporator, condenser etc. The user is required to specify the Base Function Name and the Component Number for the dynamic model block using a GUI which has been discussed in subsequent sections. To access the Simulink block diagram of the dynamic model block the user can right click on the block and select the Look Under Mask option. This will open up the Simulink diagram shown in Figure 5.2. The primary dynamic model function to simulate the component is placed in the function block titled Model by the GUI. The Base Function Name followed by the Component Number is used to rename the To

Workspace block (outlined in green in Figure 5.2). The Component Number field is written in the block titled Num (outlined in blue in Figure 5.2). Another function (following the predefined naming structure discussed in the following section) is called to set the input and output dimensions of the demux block (outlined in red in Figure 5.2).

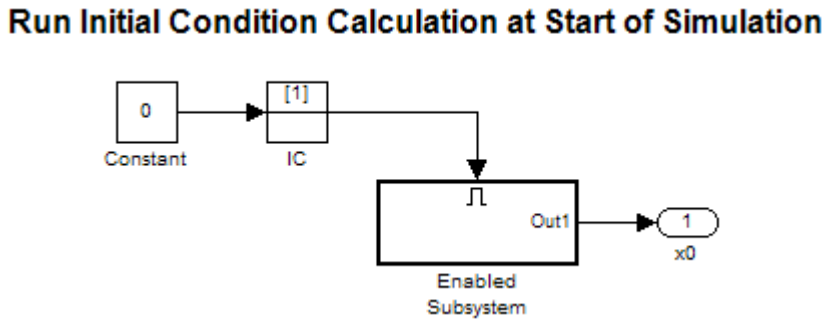

Figure 5.3: Initial Conditions Subsystem

At the start of the simulation, the initial conditions to the integrator block are provided by the Initial Conditions subsystem as shown in Figure 5.2. Double clicking on this Initial Conditions subsystem, opens up the Simulink diagram shown in Figure 5.3. This subsystem is enabled only at the first time step of the simulation. Double clicking the Enabled Subsystem block in Figure 5.3, opens up the Simulink diagram depicted in Figure 5.4. The GUI writes an appropriate function name to the X0 block in Figure 5.4 using the Base Function Name provided by the user. This function name also follows the predefined naming structure. This function outputs the initial conditions for the component which had been created before the start of the simulation using the Initial Conditions Creator for the component.

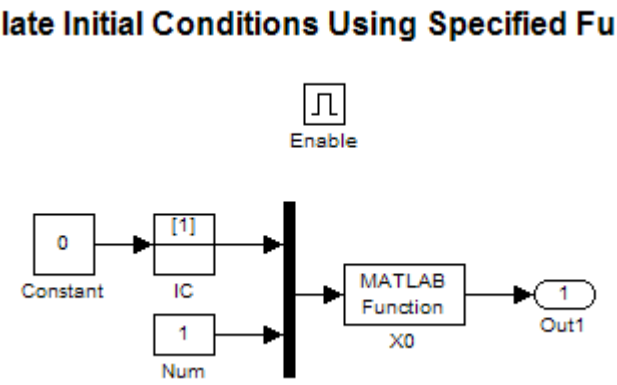

Figure 5.4: The Enabled Subsystem used to calculate the initial conditions

5.2.3 Component Naming Convention

For each of the dynamic components available in Thermosys Academic, there are five associated m-files (MatLab function files) with that component. The predefined naming structure for each associated m-file is shown in Table 5.1. An example for an evaporator (Base Function Name: Evap) is also shown. The first m-file is the primary model file which is required to simulate the dynamics associated with the component. It is called at each time step during the simulation and is placed in the function block titled Model in Figure 5.2. The second m-file is required to set up the inputs and outputs of the demux block shown in Figure 5.2. It is called by the GUI each time the dynamic model is renamed. The third m-file is called only at the first time step of the simulation. It is placed in the XO block in Figure 5.4. It provides the initial conditions to the integrator block shown in Figure 5.2 through the Enable Subsystem block shown in Figure 5.3. The fourth file is called at the end of the simulation and is known as the Record Function.

The simulation may come to an end or may be terminated by the user. At the stop of the simulation, the Stop Function associated with the To Workspace block shown in Figure 5.2 is invoked which in turn invokes the Record function associated with the component. The Stop Function can be accessed by right clicking the To Workspace block, selecting Block Properties and then selecting Callbacks tab. It has been shown in Figure 5.5. The Record function for a component reorganizes the individual outputs from that component and stores them in a structure called Simulated_Outputs. Within this structure the outputs from all the different components are organized under their own formatted name ([component][component_number]). The last m-file is known as the Initial Conditions Creator (or IC Creator). It is run before the start of the simulation after the global structures have been created. Global structures are discussed in the next section. The IC Creator helps create the initial conditions for the component using the operating conditions and physical parameters specified by the user in the global structures. It contains different solution methods to create the initial conditions for the component. If no solution method is specified by the user, the first method will be used as default. Description of the available solution methods for creating the initial conditions for the component can be read by typing help [component]IC_Creator on the MatLab command prompt. All the files are required for the functioning of the component in the Thermosys toolbox. For static components, all the files except [component]IC.m are required.

Table 5.1: Component Naming Structure

S. No.	Naming Structure	Example
1	[component].m	Evap.m
2	[component]Dim.m	EvapDim.m
3	[component]IC.m	EvapIC.m
4	[component]Rec.m	EvapRec.m
5	[component]IC_Creator.m	EvapIC_Creator.m

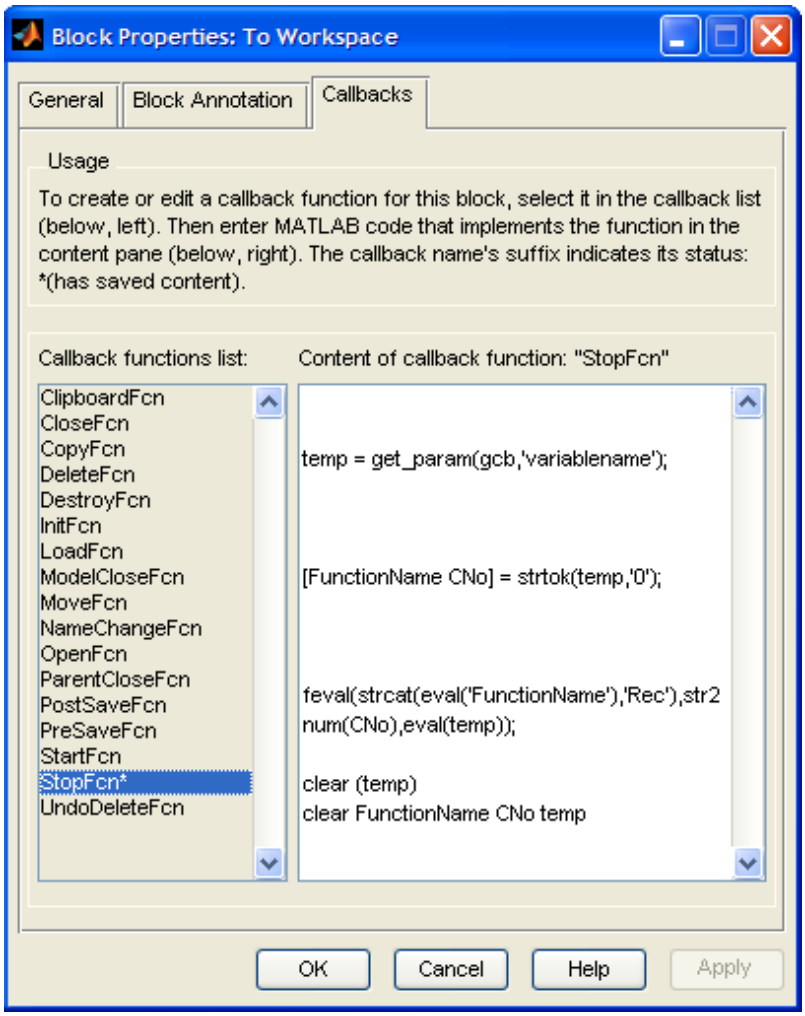

Figure 5.5: Stop Function for To Workspace Block

5.2.4 Global Structures

Thermosys Academic uses global parameter structures to perform a variety of tasks in the modeling process. These structures are accessed by the various MatLab function blocks via the associated m-file. The two basic structures that the user must load manually into the MatLab workspace are named Physical_Parameters and Operating_Conditions. These two structures provide the component models with the necessary heat exchanger geometry and initial simulation operating conditions required to calculate the initial conditions. The global parameter structures need to be created using the naming convention where the Base Function Name concatenated with the Component Number is the primary subheading in the global parameter structure.

A third structure, named Initial_Conditions, is created by invoking the [component]IC_Creator m-file mentioned earlier. The IC Creator for each component is required to be run prior to the start of the simulation. A fourth structure called Simulated_Outputs, is created automatically at the stop of the simulation. Simulated_Outputs contains the outputs generated by all the individual components at each time step.

5.2.5 Fluid Property Tables

Fluid properties are calculated using tables or subroutines. The tables use interpolation based on predefined tables, whereas the subroutines iteratively solve

empirical equations of state for the selected fluid. The Thermosys Toolbox currently contains thermo-physical properties and data for five different refrigerants: R134a, R744 (CO2), R22, R404a and R410a.

1-D and 2-D look-up tables were generated in EES (Engineering Equation Solver) and saved as comma-delimited files (csv). A MatLab m-file loads the comma-delimited files and stores the data in matrix form. Partial derivatives of thermodynamic functions are also evaluated and stored as matrices. The tables can be used to calculate thermodynamic properties by using the interpolation routines included with MatLab/Simulink®. The Thermosys Toolbox contains pre-programmed Simulink 1-D and 2-D interpolation blocks for fluid property calculation. These are independent of the type of fluid. The properties of the fluid loaded in the MatLab workspace are used.

5.2.6 Heat Transfer Correlations

The heat exchanger components use correlations to calculate the necessary heat transfer coefficients. However, because of the unlimited number and variety of such correlations, it is impossible to include even a fraction of those desired. Some of the more important correlations have been included in Thermosys Academic as subroutines. Other options have also been included such as to specify a constant value, a user-defined correlation, or to calculate the value from entered data. Under the new setup, the subroutines are called at each time step and the heat transfer coefficient values are updated.

5.3 Software Usage

5.3.1 Customization of Existing Components

This section describes how the existing components available in Thermosys Academic can be put to use to simulate a vapor compression cycle. First, the skeletal structure of the system that needs to be simulated is created. During the simulation, Simulink calls the appropriate functions for simulating the dynamics of the individual components in the system. Prior to the start of the simulation, standard global parameter structures need to be created as mentioned in prior sections. MatLab reads the data from the global structures during the simulation. Three global structures are required. The first structure has been called Physical_Parameters. The physical parameters related to the individual components are specified in this structure. Operating conditions for the system are defined in Operating_Conditions structure. A third structure, called the Initial_Conditions, specifying the initial conditions of the system is also required. The initial conditions of the system can either be specified directly in the Initial Conditions structure or can be created using the initial conditions creator available in the Thermosys library for each component used in the system. It is recommended that the user use the available subroutines to setup the initial conditions structure.

Double clicking a component brings up the GUI shown in Figure 5.6, associated with that component. The user is required to specify the standard name of the component in the field titled Base Function Name. In the field titled Component Number, the user is

required to put in the component number in which its corresponding parameters are stored in the global structures. Then, the user needs to press the button titled Apply. This will show the parameters of that component stored in the global parameter structures in the corresponding fields on the GUI. Then the user presses the button titled “OK” to save the changes in the model. This process is repeated one by one for all the components. Once this initial process to setup the simulation has been completed, the user specifies configuration parameters for the simulation in Simulink and starts the simulation. As soon as the simulation completes, or is terminated, the outputs of all the individual components are automatically stored in the MatLab workspace in a structure titled Simulated_Outputs. The outputs are available for the user to access, analyze and/or save them, if required.

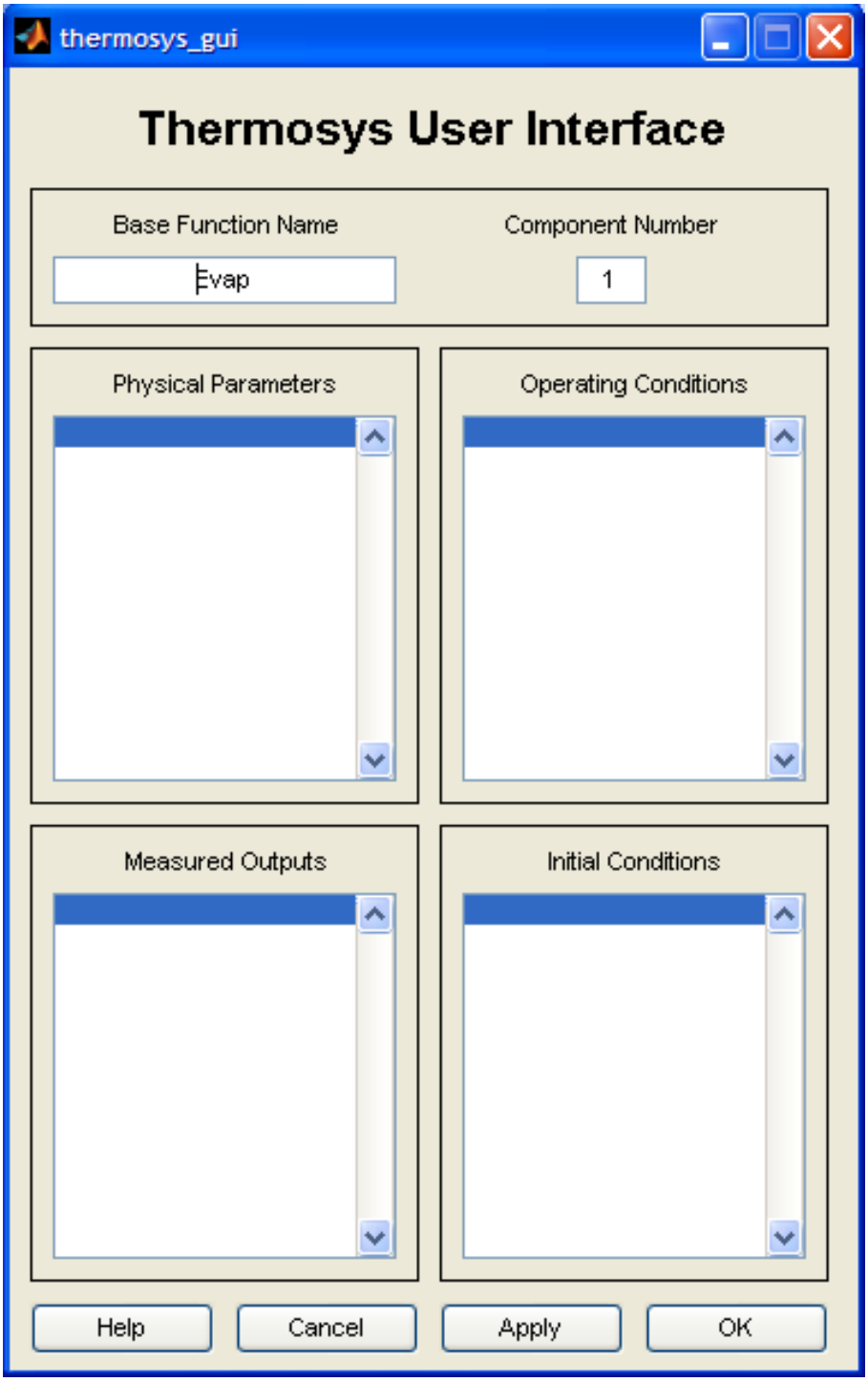

Figure 5.6: GUI for Dynamic/Static Block

5.3.1.1 Step-by-Step Process to Setup the Simulation

The following steps summarize the process to setup a simulation under Thermosys to predict a system response:

- Drag different components from the Thermosys toolbox in the Simulink workspace.

- Create the physical parameters and operating conditions for each of the components to be used in the global structures called Physical_Parameters and Operating_Conditions.

- Create the initial conditions for each of the components by executing their initial conditions creator subroutine. This will automatically create the global structure, Initial_Conditions that is required for the simulation.

- Specify the Base Function Name and Component Number of each of the dynamic or static components by using their associated GUI. Double clicking on the component brings up its associated GUI.

- Make appropriate connections between the different components provide each of them their desired inputs.

- Setup the configuration parameters for the simulation such as step size, ODE solver etc. in Simulink and run the simulation

- Access/analyze and save the generated outputs using the structure Simulated_Outputs from the MatLab workspace. This structure is automatically created after the simulation is terminated or it reaches the end.

5.3.2 Adding New Components to Thermosys Academic

This section is of use for advanced users of Thermosys Academic who would be interested in enhancing the capabilities of the software by adding new dynamic or static components to the Thermosys library. The user needs to create four or five m-files (shown in Table 5.1) depending on whether the component is a static or a dynamic model. The user needs to use a Base Function Name which does not exist in the Thermosys library. The user needs to create all the five m-files described earlier as per the predefined naming convention. The files can be created using the m-files of any of the existing components as a benchmark. If a static model is being created, it is not required to create the [component]IC.m file.

5.3.1.1 Step-by-Step Process to Add a New Component

The following steps summarize the process to add a new component to Thermosys Academic:

- Choose a Base Function Name which does not exist in the Thermosys library.

- Create the primary model file, [component].m which contains the code to simulate the dynamics of the new component

- Create the [component]Dim.m file to appropriate fix the inputs and outputs of the demux block shown in Figure 5.2. This can be done by noting the outputs and states of the new component from the primary model file as well as the relevant outputs that need to be recorded for analysis and future access.

- Create the [component]Rec.m file as discussed earlier. This file will reorganize the component outputs and integrate them to the global structure, Simulated_Outputs at the end of the simulation.

- Create the [component]IC_Creator.m file for creating the global structure, Initial_Conditons. These conditions are required to be sent to the integrator block seen in Figure 5.2.

- If a dynamic model for the new component is being created, then write another file [component]IC.m. This file sends the initial conditions of the component from the Initial_Conditions structure to the integrator block (Figure 5.2) through the Enabled Subsystem (Figure 5.3).

5.4 Simulink Model Limitations

The primary method for fluid property calculation has limitations. First, the calculated result is only as accurate as the mesh used to create the interpolation table (Figure 5.7). Second, when evaluating properties near the critical point, incorrect results are more likely. A good example of this can be seen when plotting specific heat near the critical point (Figure 5.8). There is a sudden drop in the specific heat as there is a change in the state of the fluid. This increases the gradient of specific heat to infinity near the critical point.

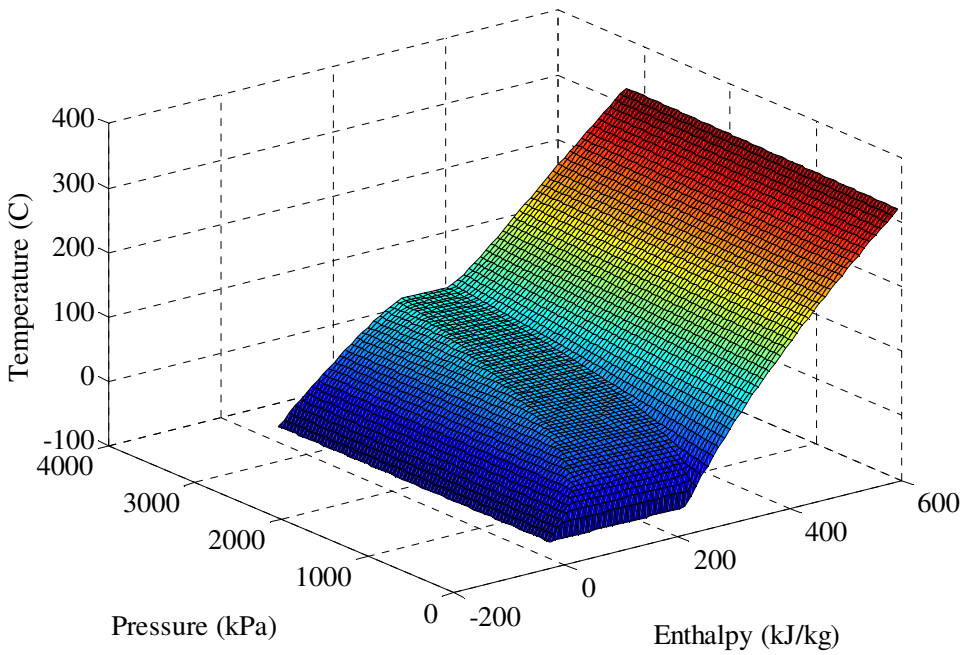

Figure 5.7: Sample Interpolation Table: Temperature as a Function of Pressure and Enthalpy for R134a

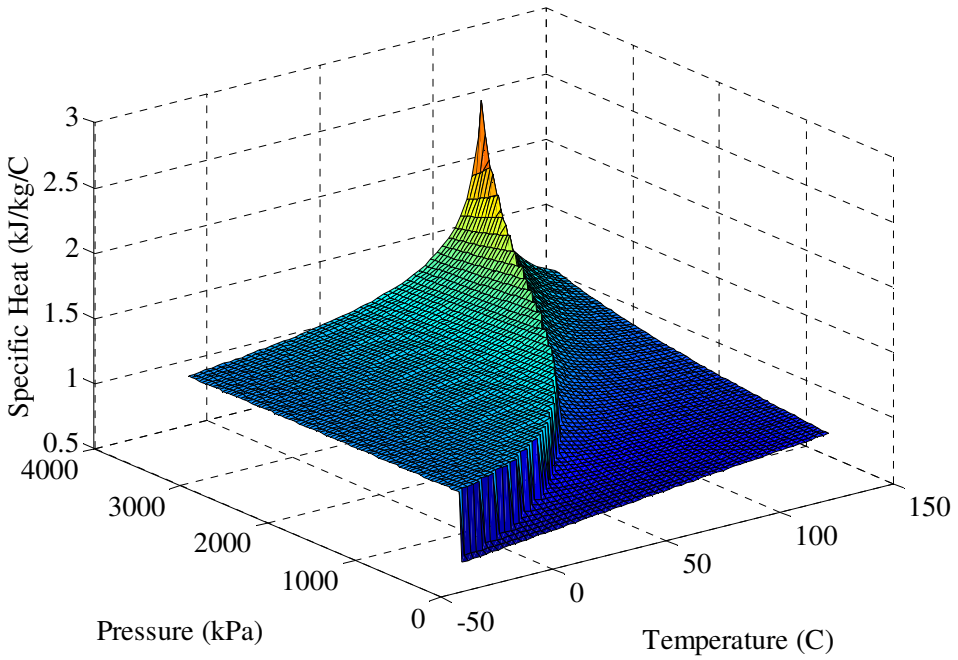

Figure 5.8: Sample Interpolation Table: Specific Heat as a Function of Pressure and Temperature for R134a

5.5 Future Additions

Efforts to improve the library are continuous. Planned additions to the library include addition of FCV models of heat exchangers with pressure drop, separation of liquid side and vapor side property tables to prevent inaccurate calculations near the critical point as well as greater variety of component models.

CHAPTER 6

MODEL VALIDATION

While it is never possible to verify that a theory is true however many observations appear to confirm it, it is possible to falsify a theory if just one observation contradicts it. This means that scientific theories are testable though not provable and so the demarcation criterion is whether or not the theory is falsifiable [21]. To test that the modeling approach outlined in this report appropriately predicts the dynamic behavior of vapor compression cycles, simulation results were compared with experimental data obtained. A detailed description of the model validation approach is given in [22,23]. Relevant information from these publications is replicated with permission in this section for convenience.

The model validation procedure includes the verification of both the prediction of steady state data as well as the ability of the model to capture the transients of the system. The first section outlines the general validation procedure, and includes a description of the various parameters used in the simulation. The next section presents the comparisons between simulated and experimental data followed by observations.

6.1 Validation Procedure

The parameters for each of the individual components are grouped in three categories: measurable, empirical, and tunable. The measurable parameters are physical

characteristics of the component such as lengths, masses, diameters, etc. For each of the component, these were measured or calculated based on data provided by the manufacturer. The empirical parameters are efficiencies or other empirically determined relationships. Usually, the tunable parameters cannot be measured easily, but are known to be within a certain range of values and are assumed to follow commonly accepted parameter correlations.

Thus, the first step of model verification will be determining the measurable and empirical parameters. Then the tunable parameters are adjusted within reasonable bounds so that the simulated dynamics approximate the experimentally recorded dynamics.

6.1.1 Physical Parameters

6.1.1.1 Evaporator and Condenser

Hydraulic Diameter – For different types of heat exchangers (plate, tube, micro-channel, etc.) this value is calculated differently. Suggestions for calculating this value for the different types of heat exchangers are available in the literature, and are heat exchanger dependent. The diameter for the different heat exchangers used in the experimental system was measured.

Fluid Flow Length – This value is defined as the length that the fluid travels from the entrance to the exit of the heat exchanger. All possible fluid flow paths are assumed to have the same length. Many heat exchangers use a series of tubes or plates arranged in a serpentine manner for fluid flow. Often these tubes or plates will join at a "header" and the fluid is redistributed before entering the next "pass" or series of or tubes or plates. The fluid flow length of the heat exchangers used in the experimental system was measured.

Cross-sectional Area – This value can be calculated using the hydraulic diameter. For most heat exchangers the cross-sectional area is not constant. The number of tubes or plates per pass generally increases as the fluid evaporates or decreases as the fluid condensates, thus changing the cross-sectional area. For the purposes of modeling, a constant cross-sectional area in a control region is assumed. If the cross-sectional area is calculated from the hydraulic diameter, then it does not take into account headers, distributors, etc.

Internal Volume – This value can either be calculated as the product of cross-sectional area and fluid flow length or be measured experimentally. The former does not account for headers, entrance pipes, etc. and is considered to be the lower bound. The latter includes all these "extra" volumes and is considered to be the upper bound. Thus this parameter can be tuned within these bounds.

Internal Surface Area – This parameter is calculated from the hydraulic diameter of the heat exchanger.

External Surface Area – This parameter is either calculated from the known fin geometry, or obtained from the manufacturer. The heat exchangers used in the experimental setup do not have any fins and thus, the external surface area is calculated using the outside diameter of the tube.

Mass – This parameter is easily obtained from the manufacturer or measured. Because the header pipes do not play a critical role in heat transfer, the mass of these may be included or neglected. The mass of the heat exchangers used in the experimental system was measured.

Specific Heat – The value of this parameter can be determined using one of the heat transfer correlations available in the literature.

6.1.1.2 Compressor

Volume – The volume of the compressor is generally available from the manufacturer.

6.1.1.3 Expansion Valve

Area of Opening – This value is usually available from the manufacturer.

6.1.1.4 Receiver

Volume – This value is usually available from the manufacturer.

6.1.2 Empirical Parameters

6.1.2.1 Evaporator and Condenser

Mean Void Fraction – Many correlations are available as outlined in Chapter 1. For these simulations, a general slip ratio correlation is assumed.

6.1.2.2 Compressor

Isentropic Efficiency – This value can be estimated using experimental steady state data, or obtained from the manufacturer.

Volumetric Efficiency – This value can be estimated using experimental steady state data, or obtained from the manufacturer.

Rate Limit – Actual compressors are rate-limited in their ability to change speed. This value can be measured from data.

6.1.2.3 Expansion Valve

Control Input Relationship – The control input is related to the valve opening assuming a linear relationship. The empirical parameters for this equation can be determined using experimental data.

Discharge Coefficient – This value can be estimated using experimental steady state data, or obtained from the manufacturer.

Rate Limit – Actual expansion valves are rate-limited in their ability to change the valve opening. This value can be measured from data.

6.1.3 Tunable Parameters

6.1.3.1 Evaporator

Void Fraction Slip Ratio – Slip ratio is defined as the ratio of the velocities of the vapor and liquid phases in a two-phase flow. The generally accepted bounds on this parameter are given by the homogeneous correlation and the Zivi correlation. The homogeneous correlation assumes a slip ratio of unity, $S = 1$, and the Zivi correlation gives the slip ratio as $\left(\rho_f / \rho_g\right)^{1/3}$. Thus, the slip ratio can be varied between these bounds.

Heat Transfer Coefficients – These values are estimated along the course of the simulation using an empirical correlation chosen by the user. For these simulations, the Gnielinski correlation [11] and Wattlet correlation [27] were used for single-phase and two-phase heat transfer coefficients on refrigerant side respectively. The Colburn Factor correlation was used for heat transfer coefficient on the secondary fluid side.

6.2 Simulated and Experimental Results

The final choice of parameters used for simulation for model validation is given in Table 6.1. The initial value of cross-sectional area was estimated based on hydraulic diameter. Due to a faster transient response of pressure, it was concluded that the effective volume of the control regions was underestimated. The upper bound of effective volume of the heat exchanger was calculated as the sum of the volume of the heat exchanger and the volume of entrance and exit pipes. The chosen effective cross-sectional area is a value within these bounds. The value of slip ratio was chosen according to the Zivi correlation. The empirical relationships of mass flow through the compressor and the valve were developed using steady state data. The two-phase flow heat transfer coefficient was estimated at each time step using the Wattlet correlation while that for single-phase flow was estimated using Gnielinski correlation. The Colburn Factor correlation was used for heat transfer coefficient on the secondary fluid side.

Table 6.1 Experimental System Parameters

Component	Parameter	Units	Value	Comment
Evaporator	Mass	[kg]	0.49	Measured
	Specific Heat	[$kJkg^{-1}K^{-1}$]	0.385	Copper
	Surface Area (external)	[m^2]	0.04	Calculated from external diameter
	Surface Area (internal)	[m^2]	0.032	Calculated from hydraulic diameter
	Cross-sectional Area	[m^2]	1.26e-4	Tuned for internal volume
	Frontal Area	[m^2]	0.013	Calculated
	Length	[m]	1	Measured
	Diameter	[m]	0.01	Measured
	Slip Ratio	[-]	5	Tuned parameter
Condenser	Mass	[kg]	1.79	Measured
	Specific Heat	[$kJkg^{-1}K^{-1}$]	0.385	Copper
	Surface Area (external)	[m^2]	0.25	Calculated from external diameter
	Surface Area (internal)	[m^2]	0.207	Calculated from hydraulic diameter
	Cross-sectional Area	[m^2]	7.31e-5	Tuned for internal volume
	Frontal Area	[m^2]	0.052	Calculated
	Length	[m]	8.36	Measured
	Diameter	[m]	0.08	Measured
	Slip Ratio	[-]	5	Tuned parameter
Compressor	Volume	[m^3]	3.04e-5	Calculated
	Empirical Parameter: η_v	[-]	1.006	Calculated from data
	Empirical Parameter: η_a	[-]	0.8911	Calculated from data
	Rate Limit	[rpm/s]	250	Calculated from data
Expansion Valve	Empirical Parameter: K_v	[-]	1.0293	Calculated from Data
	Rate Limit	[steps/s]	200	From Manufacturer

For model validation, data is collected for transients induced in the system at steady state due to change in compressor speed. Both the nonlinear as well as linearized models are compared with experimental data. The outputs of interest evaporator pressure, evaporator superheat and evaporator water exit temperature are compared.

Figure 6. 1 – Figure 6.4 show model outputs for changes in compressor speed. For all the model outputs, there is a general agreement, but also notable discrepancies. For evaporator pressure, the model agrees in the speed of the response but there is a slight aberration in the steady state gain. For evaporator superheat, the general shape of the transient is correct, but the speed of the response and steady state magnitudes are incorrect. The fluid property calculation has limitations which is one of the reasons for inaccurate prediction of steady state magnitude. The evaporator water exit temperature appears to match well with data.

The FCV model was also examined for dependency on the selected number of regions. As expected, the predicted transients increased in accuracy for increasing levels of discretization, with the simulation results virtually indistinguishable at higher discretization levels. Figure 6.6 shows the response of the evaporator pressure of a simple straight tube evaporator for a step change in expansion valve opening (Figure 6.5), for FCV models with 2, 8, 12 and 15 control volumes. While relatively few regions were required for this deliberately simple geometry, higher levels of discretization would be appropriate for more realistic heat exchanger configurations.

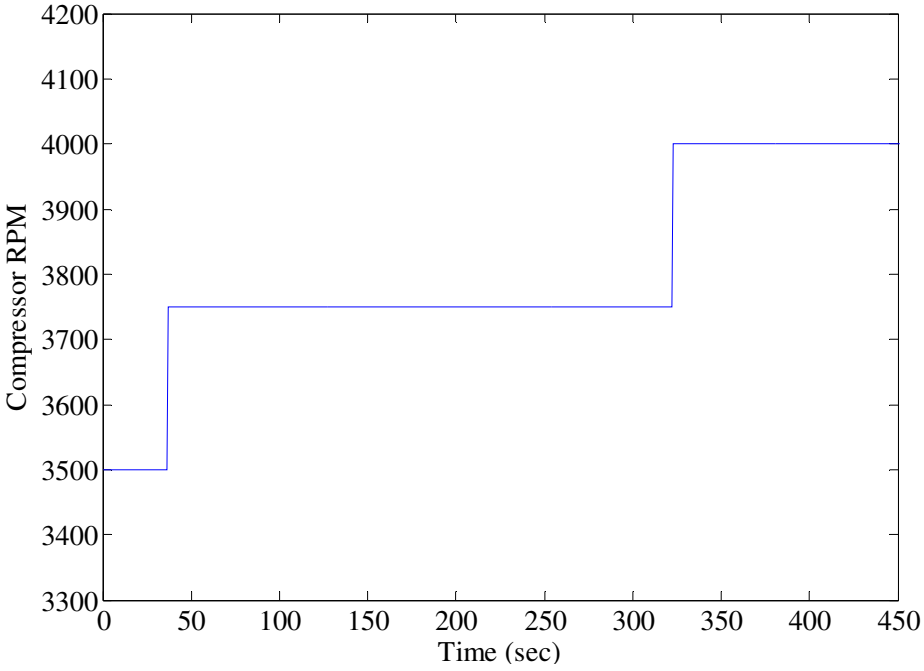

Figure 6. 1: Model Validation: Compressor RPM

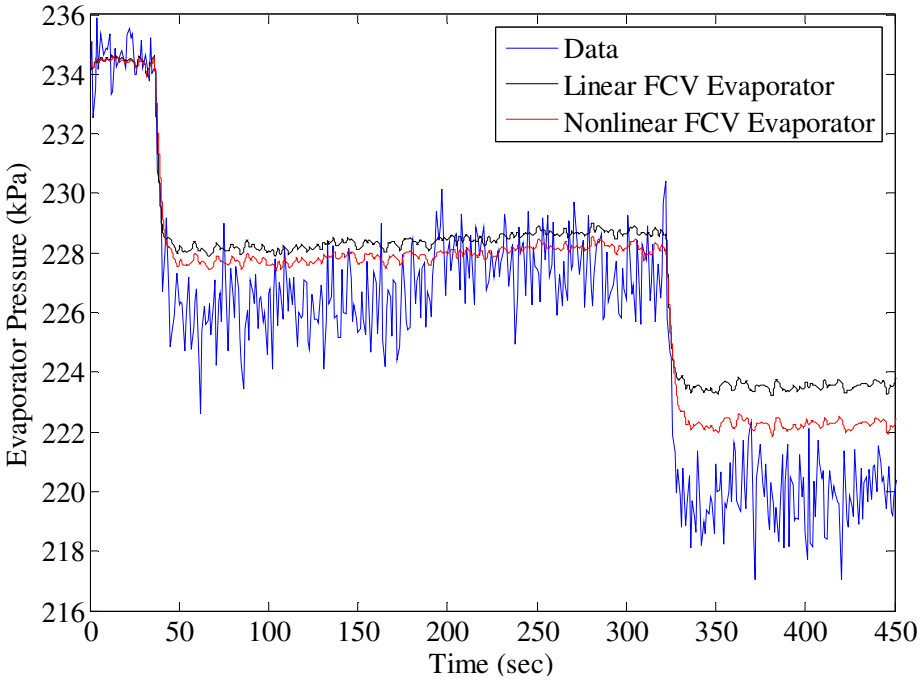

Figure 6. 2: Model Validation: Evaporator Pressure

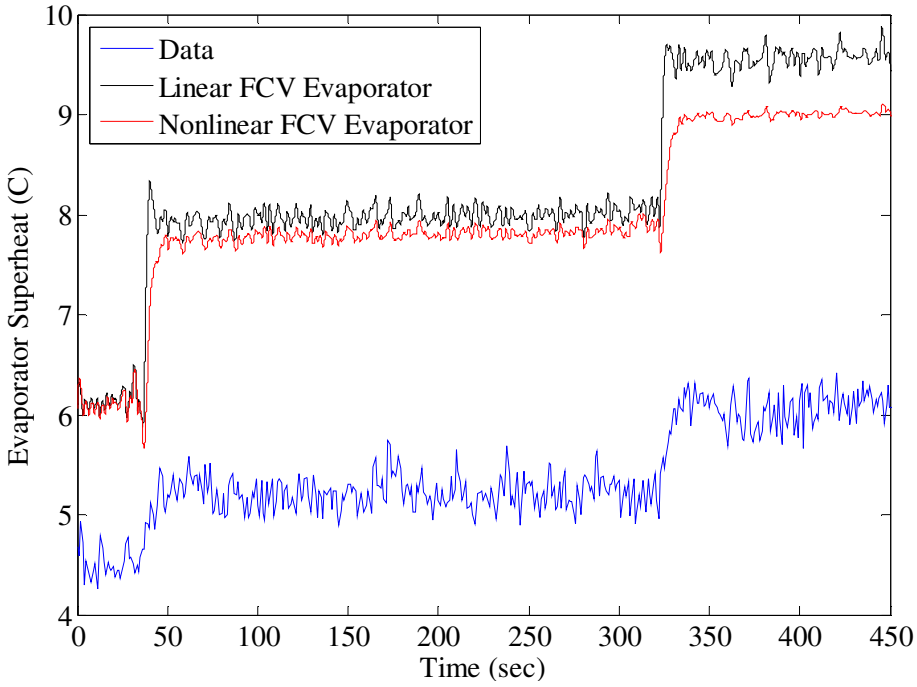

Figure 6.3: Model Validation: Evaporator Superheat

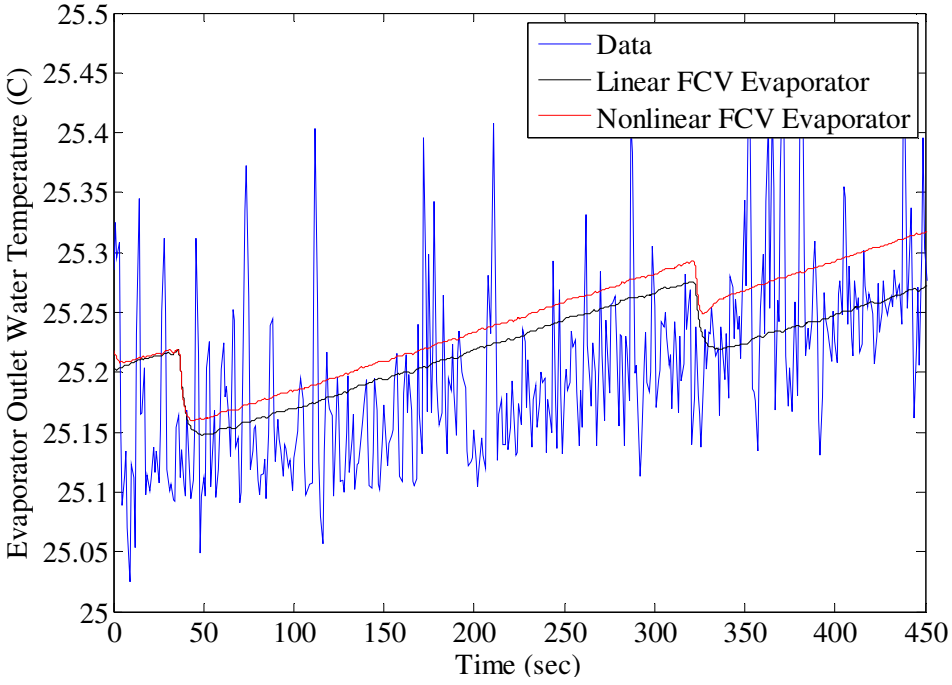

Figure 6.4: Model Validation: Evaporator Water Outlet temperature

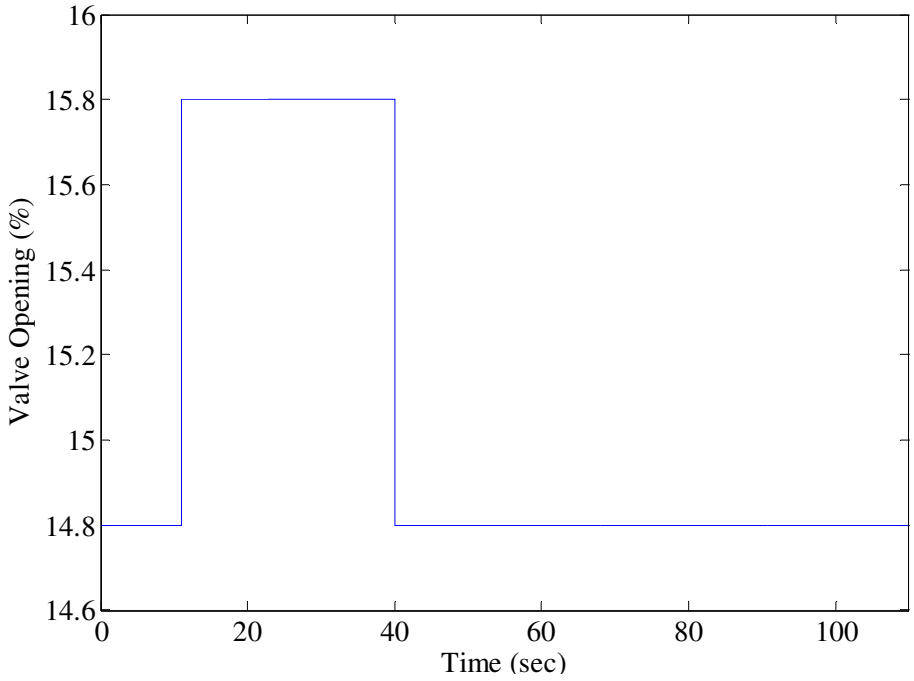

Figure 6.5: Valve Opening

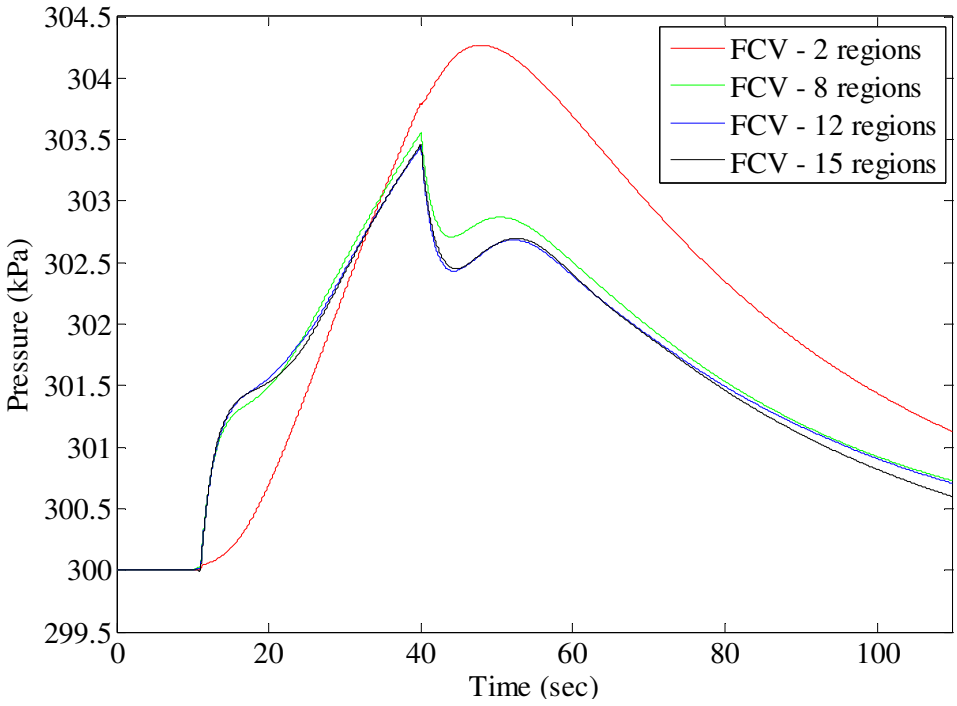

Figure 6.6: Evaporator Pressure

Chapter 7

REDUCED ORDER MODELING

The order of the FCV models depends upon the discretization of the heat exchanger. The order of the model is $(2n+1)$ where n is the number of control volume regions. The model will better capture the transients with greater number of control volume regions. But, increasing the control regions will also add to the complexity of the models. The linearized FCV models presented in Chapter 3 can be easily numerically reduced by applying any of the well known model reduction techniques. The reduced models thus obtained lose the significance of the states of the system. This chapter discusses model reduction techniques using balanced truncation and balanced residualization. Next, a method to numerically reduce the FCV models to obtain low order models is presented such that the physical significance of the states is retained.

7.1 Numerical Model Reduction

Several model reduction techniques are available in text and literature [6,25]. Antoulas et al. [6] have provided with an excellent survey of model reduction techniques for large scale systems. Let us assume that a state space system is defined by Equation 7.1. where x, y and u are a vector of states, outputs and inputs and A, B, C and D are matrices. Suppose some of the states of the system are insignificant as compared to others and the system needs to be reduced such that those states are not represented. The

system can thus be rearranged such that we present the vector of states to be removed, x_2 at the bottom of the system as shown in Equation 7.2. Let us assume that the reduced system is represented by Equation 7.3.

$$\begin{aligned} \dot{x} &= Ax + Bu \\ y &= Cx + Du \end{aligned} \tag{7.1}$$

$$\begin{aligned} \begin{bmatrix} \dot{x}_1 \\ \dot{x}_2 \end{bmatrix} &= \begin{bmatrix} A_{11} & A_{12} \\ A_{21} & A_{22} \end{bmatrix} \begin{bmatrix} x_1 \\ x_2 \end{bmatrix} + \begin{bmatrix} B_1 \\ B_2 \end{bmatrix} u \\ y &= \begin{bmatrix} C_1 \\ C_2 \end{bmatrix} \begin{bmatrix} x_1 \\ x_2 \end{bmatrix} + Du \end{aligned} \tag{7.2}$$

$$\begin{aligned} \dot{\hat{x}} &= \hat{A}x + \hat{B}u \\ \hat{y} &= \hat{C}x + \hat{D}u \end{aligned} \tag{7.3}$$

For balanced truncation model reduction, it is simply assumed that $x_2 = 0$ and $\dot{x}_2 = 0$. Then, the matrices of the state space system reduced by balanced truncation are given by Equation 7.4. For balanced residualization model reduction, it is assumed that $\dot{x}_2 = 0$ which implies that $A_{21}x_1 + A_{22}x_2 + B_2u = 0$. The matrices of the system reduced by balanced residualization are given by Equation 7.5.

$$\begin{aligned} \hat{A} &= A_{11} \\ \hat{B} &= B_1 \\ \hat{C} &= C_1 \\ \hat{D} &= D \end{aligned} \tag{7.4}$$

$$\begin{aligned}\hat{A} &= A_{11} - A_{12}A_{22}^{-1}A_{21} \\ \hat{B} &= B_1 - A_{12}A_{22}^{-1}B_2 \\ \hat{C} &= C_1 - C_2A_{22}^{-1}A_{21} \\ \hat{D} &= D - C_2A_{22}^{-1}B_2\end{aligned} \tag{7.5}$$

7.2 Procedure for Obtaining Reduced Order Models

The state space systems of the FCV models discussed in Chapter 3 can be represented in the standard state space form given in Equation 7.1. Using the matrix $Z(x,u)$ defined in Equation 2.43 as a state transformation matrix, a linearized system representation given in Equation 7.6 is obtained with the states corresponding to the refrigerant energy, refrigerant mass, and heat exchanger wall energy as given in Equation 7.7.

$$\begin{aligned}A'' &= F_x Z^{-1} \\ B'' &= F_u \\ C'' &= G_x Z^{-1} \\ D'' &= G_u\end{aligned} \tag{7.6}$$

$$\bar{x} = \begin{bmatrix} U_1 & \dots & U_n & m_{total} & E_{w,1} & \dots & E_{w,n} \end{bmatrix}^T \tag{7.7}$$

Noting that the conservation of mass equation is a pure integration the resulting state space representation is given by Equation 7.8. This system can also be simply represented by Equation 7.9. Another system of equations is made such that it has the same states and all the states as outputs as given in Equation 7.10. Making a balanced

realization of this system and using balance truncation, we can obtain a numerically reduced 3rd order system represented by Equation 7.11.

$$\begin{bmatrix} \dot{\overline{U}} \\ \dot{m}_{total} \\ \dot{\overline{E}}_w \end{bmatrix} = \begin{bmatrix} A_{UU} & A_{Um} & A_{UE} \\ 0 & 0 & 0 \\ A_{EU} & A_{Em} & A_{EE} \end{bmatrix} \begin{bmatrix} \overline{U} \\ m_{total} \\ \overline{E}_w \end{bmatrix} + \begin{bmatrix} B_U \\ B_m \\ B_E \end{bmatrix} u$$
$$y_o = \begin{bmatrix} C_U & C_m & C_E \end{bmatrix} \begin{bmatrix} \overline{U} \\ m_{total} \\ \overline{E}_w \end{bmatrix} + [D]u \qquad (7.8)$$

$$\dot{\bar{x}} = A_o \bar{x} + B_o u$$
$$y_o = C_o \bar{x} + D_o u \qquad (7.9)$$

$$\dot{\bar{x}} = A_o \bar{x} + B_o u$$
$$\tilde{y}_o = [I]\bar{x} \qquad (7.10)$$

$$\dot{x}_r = A_r x_r + B_r u$$
$$\tilde{y}_o = C_r x_r \qquad (7.11)$$

Then, a transformation matrix T (given in Equation 7.13) is defined to obtain average states for refrigerant energy and heat exchanger wall energy. The average states are given in Equation 7.12. We will obtain the reduced order system in terms of the average states. Using Equations 7.10 – 7.12, we can calculate x_{avg} as given in Equation 7.14. Assuming $P = TC_r$, and applying similarity transformation to Equation 7.11 and using Equations 7.9 – 7.11, we can obtain the system given in Equation 7.15. This is a reduced order linear system having $\begin{bmatrix} \overline{U}_{avg} & m_{total} & \overline{E}_{w,avg} \end{bmatrix}^T$ as states and the original

outputs as the outputs of the system. Alternatively, the system can also be represented as given in Equation 7.16. This is a 3rd order system having states which have a physical significance. Again, since the conservation of mass is a pure integration, the matrix $\hat{A}_r$ can be represented as given in Equation 7.17.

$$x_{avg} = \begin{bmatrix} \overline{U}_{avg} \\ m_{total} \\ \overline{E}_{w,avg} \end{bmatrix} = T\overline{x} \tag{7.12}$$

$$T = \begin{bmatrix} 1^{1Xn} & 0 & 0^{1Xn} \\ 0^{1Xn} & 1 & 0^{1Xn} \\ 0^{1Xn} & 0 & 1^{1Xn} \end{bmatrix} \tag{7.13}$$

$$x_{avg} = TC_r x_r \tag{7.14}$$

$$\begin{aligned} \dot{x}_{avg} &= \left(PA_r P^{-1}\right)x_{avg} + \left(PB_r\right)u \\ y_o &= \left(C_o C_r P^{-1}\right)x_{avg} + D_o u \end{aligned} \tag{7.15}$$

$$\begin{aligned} \dot{x}_{avg} &= \hat{A}_r \begin{bmatrix} \overline{U}_{avg} \\ m_{total} \\ \overline{E}_{w,avg} \end{bmatrix} + \hat{B}_r u \\ y_o &= \hat{C}_r \begin{bmatrix} \overline{U}_{avg} \\ m_{total} \\ \overline{E}_{w,avg} \end{bmatrix} + \hat{D}_r u \end{aligned} \tag{7.16}$$

$$\hat{A}_r = \begin{bmatrix} A_{11} & A_{12} & A_{13} \\ 0 & 0 & 0 \\ A_{31} & A_{32} & A_{33} \end{bmatrix} \tag{7.17}$$

Thus, by using this process, the matrix elements of the reduced order system can be identified. Moreover, this process of FCV high order model generation, linearization and model reduction and transformation can be automated. By repeating this process over the range of operating conditions, numerical maps for the matrix elements of low order models can be generated. Figure 7.1 - Figure 7.6 show the variation of different elements of the $\hat{A}_r$ with superheat and evaporator pressure. These maps were generated by reducing 41st order FCV models to 3rd order models. Similar maps for matrix elements of $\hat{B}_r$, $\hat{C}_r$ and $\hat{D}_r$ were also generated. The bode response of evaporator pressure and superheat with respect to mass flow rate of air and refrigerant mass flow rate at inlet for full order system has been compared with that of reduced order system in Figure 7.7 and Figure 7.8.

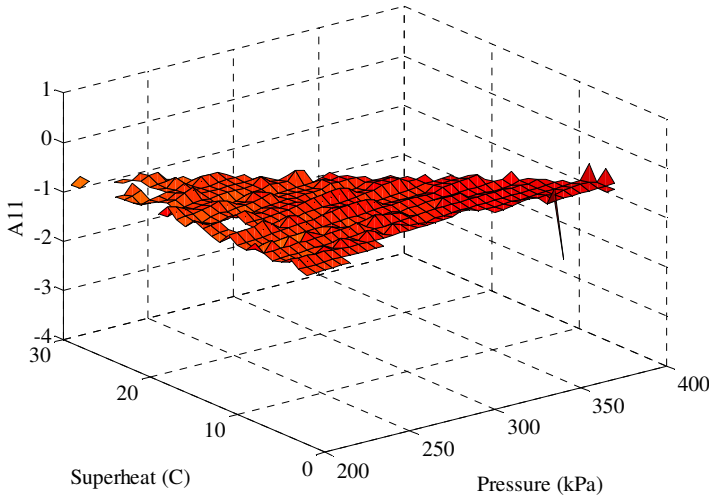

Figure 7.1: Variation of A_{11} with Superheat and Pressure

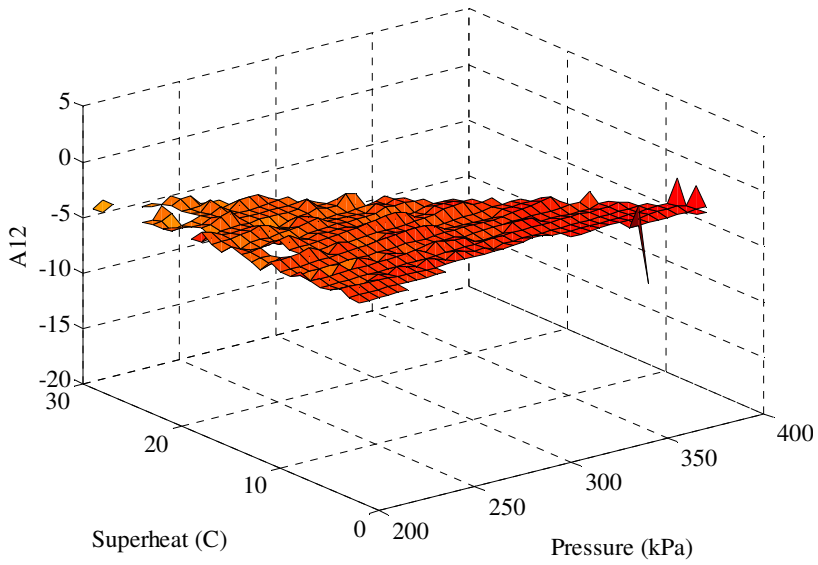

Figure 7.2: Variation of A_{12} with Superheat and Pressure

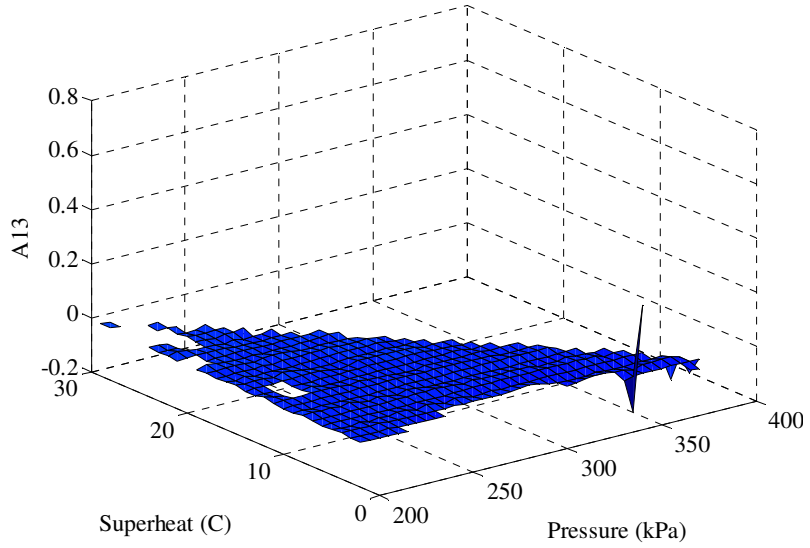

Figure 7.3: Variation of A_{13} with Superheat and Pressure

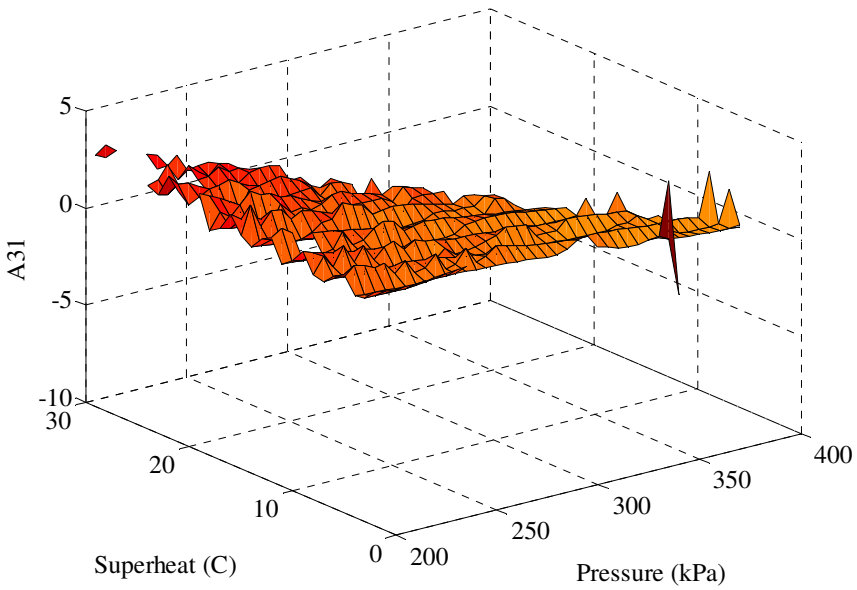

Figure 7.4: Variation of A_{31} with Superheat and Pressure

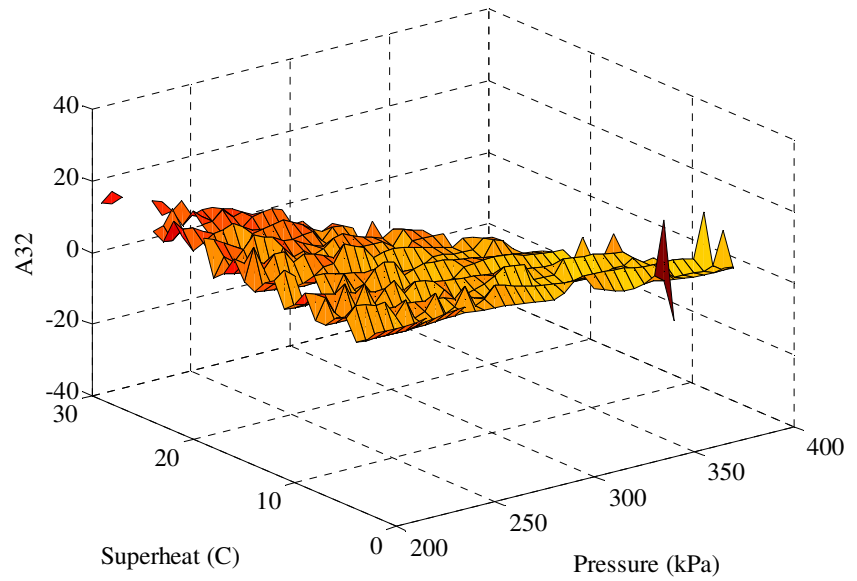

Figure 7.5: Variation of A_{32} with Superheat and Pressure

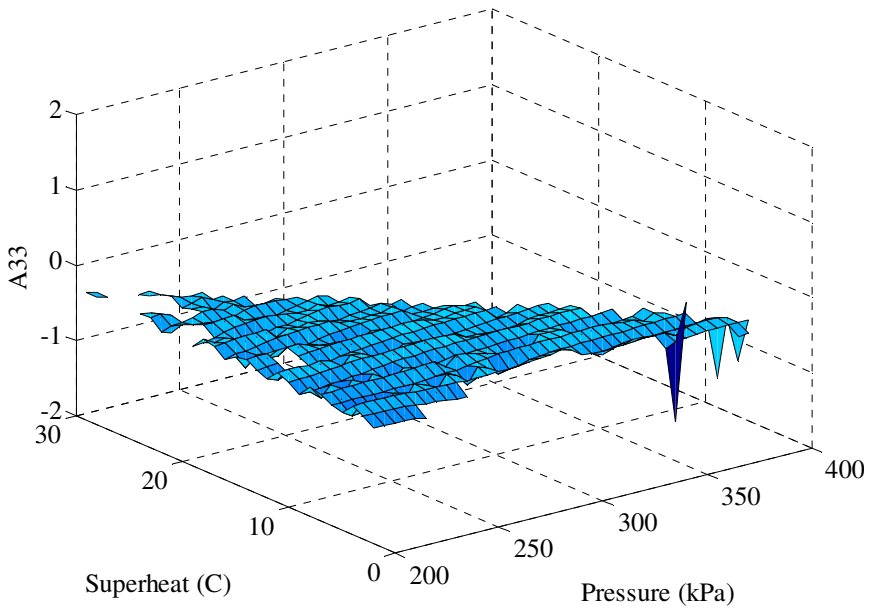

Figure 7.6: Variation of A_{33} with Superheat and Pressure

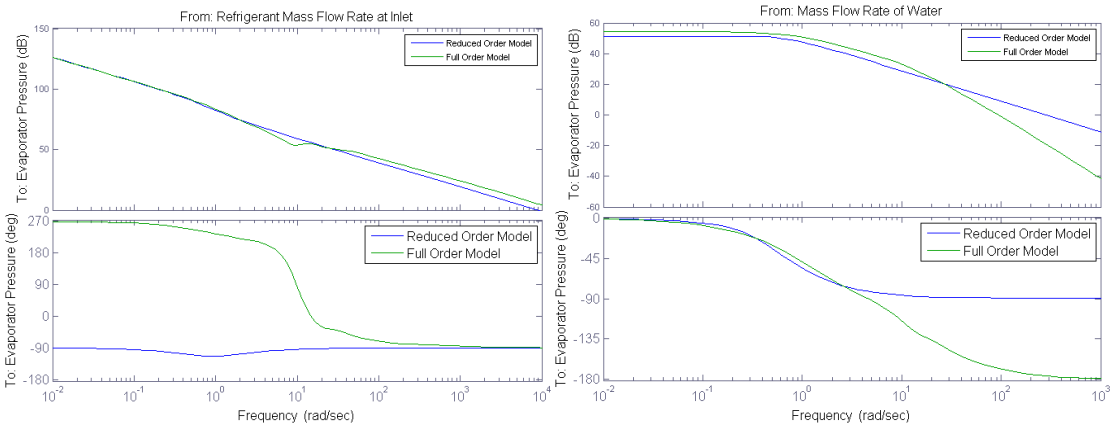

Figure 7.7: Bode Plot: Pressure

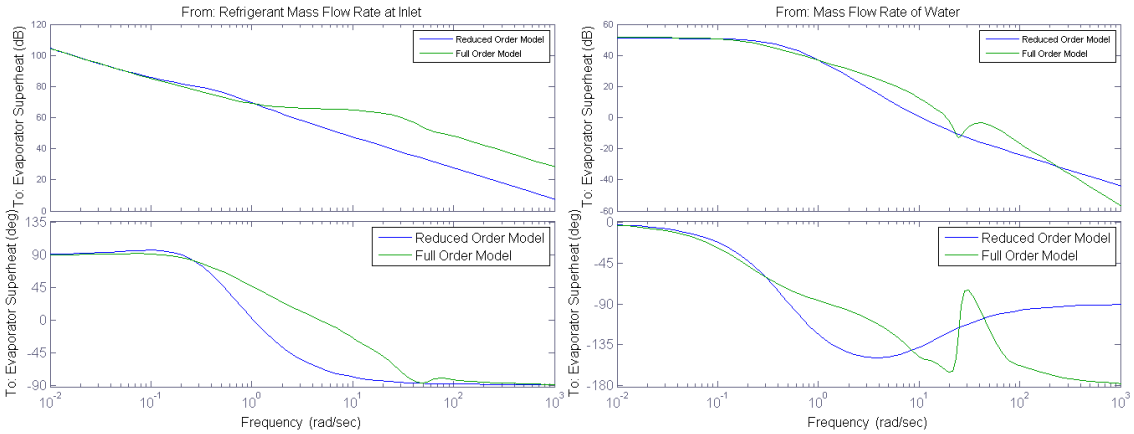

Figure 7.8: Bode Plot: Superheat

Chapter 8

CONCLUSIONS AND FUTURE WORK

8.1 Summary of Results

This research makes several key contributions to the study of vapor compression system dynamics. First, the existing lumped parameter moving boundary approach has been presented, which provides a simple method to obtain low order models. Second, a finite control volume approach is presented, avoiding the standard system of DAEs, and creating a set of nonlinear ODEs. This framework allows inclusion of parametric details omitted by the simpler models. Third, the resulting models are validated against experimental data. Finally, an approach to model reduction procedure to obtain low order models using the high order FCV models has been introduced. The reduced order models are obtained such that the physical significance of the system states is retained. The approach is extended to create numerical maps for the matrix elements of the reduced order models.

8.2 Future Work

This research has many aspects that have yet to be explored. The modeling approach presented in this report has been validated against limited data. The approach

should be validated against data collected for other disturbances such as those due to change in valve opening, change in temperature of secondary fluid etc.

It has been suggested that the parameter tuning approach can be extended to create numerical maps for reduced order models using the higher order FCV models. Such maps should be created for the entire range of operating conditions of a simple heat exchanger and their efficacy should be validated against experimental data.

It has been mentioned in Chapter 5 that the fluid property tables have discontinuities near the critical point as the fluid changes state. The calculation of fluid properties can be improved by separating the property tables for different states of the fluid.

Also, this approach has been validated for simple vapor compression cycle consisting of a single compressor, condenser, valve and evaporator. It can be easily extended to more complex multi-component vapor compression systems containing more than one evaporator, condenser etc.

REFERENCES

[1] "Energy Information Administration: International Energy Outlook 2007," http://www.eia.doe.gov/oiaf/ieo/world.html, 2007

[2] "Environmental Indicators: Climate Change," http://unstats.un.org/unsd/environment/air_co2_emissions.htm, 2007

[3] "Oil falls after striking record $90 a barrel," http://www.reuters.com/article/hotStocksNews/idUSSP10407020071019, 2007

[4] "Thermosys," http://www1.mengr.tamu.edu/TFCL/thermosys.htm, 2007

[5] "Thermosys," http://mr-roboto.me.uiuc.edu/thermosys/index.htm, 2007

[6] Antoulas, A.C., Sorensen, D.C. and Gugercin S., "A survey of model reduction methods for large-scale systems," *Contemporary Mathematics,* vol. 280, pp. 193-219, 2001

[7] Bendapudi, S. and Braun, J. E., "A Review of Literature on Dynamic Models of Vapor Compression Equipment," ASHRAE Report #4036-5, May 2002

[8] Bendapudi, S., "Development and Evaluation of Modeling Approaches for Transients in Centrifugal Chillers," *Thesis,* Purdue University, Aug 2004

[9] Chen, Chi-Tsong, "Linear System Theory and Design," New York: Oxford University Press, 1999

[10] Drew, D.A., "Mathematical Modeling of Two-Phase Flow," *Annual Review of Fluid Mechanics,* vol. 15, pp. 261-291, 1983

[11] Gnielinski, V., "New Equations for Heat and Mass Transfer in Turbulent Pipe and Channel Flow," *International Chemical Engineering,* vol. 16, pp. 359-368, 1976

[12] Grald, E. W. and MacArthur, J. W., "A Moving boundary Formulation for Modeling Time-Dependent Two-Phase Flows," *International Journal of Heat & Fluid Flow,* vol. 13, no. 3, pp. 266-272, Sep 1992

[13] Gruhle, W.–D. and Isermann, R., "Modeling and Control of a Refrigerant Evaporator," *Journal of Dynamic Systems, Measurement and control-Transactions of the ASME,* vol. 107, no. 4, pp. 235-240, Dec 1985

[14] He, X.-D., Liu, S., and Asada, H. H., "Modeling of Vapor Compression Cycles for Multivariable Feedback Control of HVAC Systems," *Journal of Dynamic Systems Measurement & Control-Transactions of the ASME,* vol. 119, no. 2, pp. 183-191, Jun, 1997

[15] He, X.-D., "Dynamic Modeling and Multivariable Control of Vapor Compression Cycles in Air Conditioning Systems," *Thesis,* Massachusetts Institute of Technology, Feb 1996

[16] MacArthur, J. W. and Grald, E. W., "Prediction of Cyclic Heat Pump Performance with a Fully Distributed Model and a Comparison with Experimental Data," *ASHRAE Transactions,* vol. 93, no. 2, pp. 1159-1178, Jun 1987

[17] Mithraratne, P., Wijeysundera, N.E., and Bong, T.Y., "Dynamic Simulation of a Thermostatically Controlled Counter-Flow Evaporator," *International Journal of Refrigeration*, vol. 23, no. 3, pp. 174-189, 2000

[18] Narayanan, S., Srinivas, B., Pushpavanam, S., Bhallamudi, S. Murty, "Non-linear Dynamics of a Two-Phase Flow System in an Evaporator: The Effects of

(i) A Time Varying Pressure Drop (ii) An Axially Varying Heat Flux," *Nuclear Engineering and Design,* vol. 178, pp. 279-294, 1997

[19] Ogata, Katsuhiko, "Modern Control Engineering," Upper Saddle River, New Jersey: Pearson Education, Inc., 2002

[20] Paynter, Henry M. and Takahashi, Yashundo, " A New Method of Evaluating Dynamic Response of Counter-Flow and Parallel-Flow Heat Exchangers," *ASME Diamond Jubilee Semi-annual Meeting,* Boston, MA, Jun 1955

[21] Popper, K., "Conjectures and Refutations: The Growth of Scientific Knowledge," New York: Harper Torchbooks, 1963

[22] Rasmussen, Bryan P., "Control-Oriented Modeling of Transcritical Vapor Compression Systems," *Thesis,* University of Illinois at Urbana-Champaign, 2002

[23] Rasmussen, Bryan P., "Dynamic Modeling and Advanced Control of Air Conditioning and Refrigeration Systems," *Thesis,* University of Illinois at Urbana-Champaign, 2005

[24] Rice, C. K., "Effect of Void Fraction Correlation and Heat Flux Assumption on Refrigerant Charge Inventory Predictions," *ASHRAE Transactions,* vol. 93, no. 1, pp. 341-367, 1987

[25] Skogestad, Sigurd and Postlethwaite, Ian, "Multivariable Feedback Control: Analysis and Design," Hoboken, NJ: John Wiley, 2005

[26] Tummescheit, Hubertus and Eborn, Jonas, "Design of a Thermo-Hydraulic Model Library in Modelica™," *European Simulation Multiconference,* Manchester, UK, 1998

[27] Wattelet, J.P. et al., "Heat transfer flow regimes of refrigerants in a horizontal - tube evaporator," *ACRC TR-55,* University of Illinois at Urbana-Champaign, 1994

[28] Willatzen, M., Pettit, N. B. O. L., and Ploug-Sorensen, L., "A General Dynamic Simulation Model for Evaporators and Condensers in Refrigeration. Part I: Moving Boundary Formulation of Two-Phase Flows with Heat Exchange," *International Journal of Refrigeration,* vol. 21, no. 5, pp. 398-403, Aug, 1998